Title
SOLUTION CHEMISTRY OF CATECHOLATE METAL COMPLEXES

Author
Kappel, M.J.

Publication Date
1983-06-01

Lawrence Berkeley Laboratory
UNIVERSITY OF CALIFORNIA

Materials & Molecular Research Division

SOLUTION CHEMISTRY OF CATECHOLATE METAL COMPLEXES

M.J. Kappel
(Ph.D. Thesis)

June 1983

Prepared for the U.S. Department of Energy under Contract DE-AC03-76SF00098

DISCLAIMER

LBL-16273

SOLUTION CHEMISTRY OF CATECHOLATE METAL COMPLEXES

Mary Jean Kappel
(Ph.D Thesis)

Lawrence Berkeley Laboratory
University of California
Berkeley, California 94720

June 1983

This work was supported by the Director, Office of Energy Research, Office of Basic Energy Sciences, Chemical Sciences Division of the U.S. Department of Energy under Contract Number DE-AC03-76SF00098.

Solution Chemistry of Catecholate Metal Complexes

Mary Jean Kappel

Abstract

The aqueous solution chemistry of a series of synthetic catechoylamide ligands has been studied in view of the potential use of these ligands for chelation therapy in the treatment of Fe(III) overload or for actinide(IV) decorporation.

The first chapter describes design concepts for the ligands and their potential use not only for sequestering Fe(III) and the radiopharmaceuticals ^{67}Ga(III) and ^{111}In(III), but (with slight structural modifications) also in complexing actinide(IV) ions, particularly Pu(IV).

Chapter II is a thermodynamic study of the complexation of biologically significant divalent metal ions with a di-, tri-, and tetracatecholyamide, to evaluate the specificity of the catechoylamide ligands for Fe(III) or Pu(IV). Results indicate that these ligands are specific for metal ions of high charge to ionic radius ratios.

Chapter III describes the stability and protonation behavior of a series of N-substituted catechoylamide complexes of Ga(III) and Fe(III) as determined by potentiometric and spectral titration, and infrared analysis. These ligands show lower affinity for Ga(III) or

Fe(III) than unsubstituted catechoylamides and they remove Fe(III) from diferric transferrin at a slower rate.

The results of the first *in vitro* experiments of complexation of catechoylamide ligands with plutonium are presented in Chapter IV. Electrochemical techniques have allowed the elucidation of the protonation behavior of Pu(IV)- and Pu(III)-catechoylamide complexes. These results are compared to the protonation behavior of catechoylamide complexes of Ce(IV) and Ce(III), frequently used models for Pu(IV) and Pu(III). Above pH 12 it is thought that a Pu(IV)tetrakiscatecholate complex and a Pu(III)triscatecholate complex is formed. At neutral pH, a triscatecholate-Pu(IV) complex appears to be present, indicating that the full denticity of the tetracatecholate is not utilized *in vivo*.

In order to explore some curious results in the *in vivo* chelation by catechoylamides of americium, the complexation of americium was studied by electrochemical and spectroscopic methods. Results indicate that catechoylamide ligands bind Am(III). In addition, lack of evidence of the Am(IV)/(III)-catecholate electrochemical couple indicates that the potential of the free ion Am(IV)/(III) reduction couple is greater than +2.6 volts.

K. N. Raymond

Acknowledgements

I wish to thank Professor Ken Raymond for his support, discussions, and for allowing me the freedom to pursue my own primrose path, errant as it may have been at times. My collaborators in chaos are acknowledged for their friendship and patience; Vince Pecoraro, for getting me started, Geoffrey Wong, Rob Scarrow, Daohong Zhu, Pat Durbin, and Heino Nitsche.

Many other friends have made my Berkeley experience memorable; Tom Tufano, Sue Barclay, Brandan Borgias, Tom Chung, Gwen Raine, Marianne Begemann, Chris Orvig, Steve Rodjers, and Carol Balfe. Each of them deserve a paragraph for their help, but I will thank them all collectively for their kindness and support in my weakest moments.

The people at LBL are acknowledged for their patience in putting up with my neuroses in the past year; most notably, David White, but also, Norm Edelstein, Jerry Bucher, Ken Smith, and John Brennan.

June Smith deserves special thanks for her hours of free counseling. She's right--it's hard to soar like an eagle when you work with a bunch of turkeys.

There once was a girl from St. Paul,
Who thought Pu thermo a ball,
Four years in the lab
Made her pallid and drab
'A right proper suthun gull now, yawl.'

DEDICATED

with abiding affection and gratitude

to those who have shown me the good life,

the art of success in relationships,

the true meaning of family living,

and the love that is essential to it:

To my parents

Jack and Gerry Kappel

To my grandparents

Elmer and Mary Garceau

and

to my own Bob.

Table of Contents

Acknowledgements i

Dedication ii

Table of Contents iii

List of Tables v

List of Figures vi

CHAPTER I - Introduction 1

References 8

Figure Captions 11

Figures 12

CHAPTER II - Selectivity of Sulfonated Polycatechoylamides for Ferric Ion 16

Experimental 18

Results and Discussion 19

Summary 28

References 29

Tables 32

Figure Captions 35

Figures 36

CHAPTER III - Complexation of Ga(III) and Fe(III) by Terminally N-Substituted Catechoylamide Ligands. 42

Experimental 44

Results and Discussion 50

Summary 64

References 66

Tables 68

CHAPTER III (cont)

Figure Captions 73

Figures 75

CHAPTER IV - Complexation of Plutonium and Cerium by Catecholate Ligands 82

Experimental 84

Results and Discussion 90

Summary 104

References 106

Tables 109

Figure Captions 110

Figures 112

CHAPTER V - Complexation of Americium by Catecholate Ligands 126

Experimental 129

Results and Discussion 131

Summary 137

References 138

Tables 140

Figure Captions 142

Figures 143

APPENDIX - Summary of Program BETA 147

References 154

List of Tables

CHAPTER II.

I. Protonation Constants of CAMS ligands 32

II. Stability Constants of Metal-CAMS complexes 33

III. pM Values for Fe(III) and divalent metals 34

CHAPTER III.

I. Protonation Constants of lipophilic CAMS ligands. . 68

IIA. Ferric Complex Protonation Constants. 69

IIB. Gallium Complex Protonation Constants 69

III. Normal Formation Constants and K* Values of Ga(III) and Fe(III)-CAMS complexes. 70

IV. pM Values for Ferric and Gallium Complexes. 71

V. Rate Constants of Removal of Fe(III) from Fe_2Tf . . 72

CHAPTER IV.

I. Potential Shifts of Catecholate-bound Pu and Ce . . 109

CHAPTER V.

I. Reduction Potentials of Catecholate Ligands 140

II. Summary of Am(III) Spectra. 141

List of Figures

1.1 Enterobactin 12

1.2 Synthetic Catechoylamides. 13

1.3 Lipophilic Catechoylamides 14

1.4 Synthetic Tetracatechoylamides 15

2.1 CAMS Ligands 36

2.2 Titration Curves of 4-LICAMS-Metal 37

2.3 Titration Curves of MECAMS-Metal 38

2.4 Titration Curves of 1:1 3,4,3-LICAMS:Metal 39

2.5 Titration Curves of 1:2 3,4,3-LICAMS:Metal 40

2.6 Corelation of pM and Charge/Ionic Radius 41

3.1 Lipophilic CAMS Ligands. 75

3.2 Titration Curves of Lipophilic CAMS-Fe(III). 76

3.3 Visible Spectra of Fe(III)-DiP-3,4-LICAMS 77

3.4 Schwarzenbach Plot of Fe(III)-DiP-3,4-LICAMS 78

3.5 FT IR of Fe(III)-DiP-3,4-LICAMS. 79

3.6 Titration Curves of Lipophilic CAMS-Ga(III). 80

3.7 Visible Spectra of Removal of Fe(III) from Fe_2Tf 81

4.1 Monocatecholates and CAM Ligands 112

4.2 Differential Pulse Schematic 113

4.3 Voltammograms of Pu-catechol 114

4.4 Plot of Ce-catechol Ligand Variation 115

4.5 Plot of Pu-catechol Ligand Variation 116

4.6 Voltammograms of Pu-3,4,3-LICAMS with Time 117

4.7 Voltammograms of Pu-3,4,3-LICAMS with pH 118

List of Figures (cont.)

4.8 Plot of Pu-3,4,3-LICAMS $E_{\frac{1}{2}}$ / pH Variation 119

4.9 Voltammograms of Pu-3,4-LICAMS with pH. 120

4.10 Dependence of Peak Current on pH. 121

4.11 Voltammograms of Ce-3,4,3-LICAMS with pH. 122

4.12 Voltammograms of Pu-3,4,3-LICAMC with pH. 123

4.13 Plot of Pu-3,4,3-LICAMC $E_{\frac{1}{2}}$ / pH Variation 124

4.14 Summary of Pu-catechoylamide Complexation 125

5.1 Plasma Clearance Curves of Am(III). 143

5.2 Voltammograms of Monocatecholates 144

5.3 Voltammograms of 3,4,3-LICAMS and 3,4,3-LICAMC. 145

5.4 Visible Spectra of Free Am(III) and Am(III)-catecholates. . 146

CHAPTER I

Introduction

An appreciation for the role metal ions and their coordinating environments play in essential biological functions forms the basis for the expanding interdisciplinary field of bioinorganic chemistry. Traditional coordination chemistry concepts combined with a variety of physical and analytical methods applied to metalloproteins (transport or storage), metalloporphyrins, and metalloenzymes have elucidated the identity of binding groups and their effects on the reactivity of the metal center. These studies concentrate on normal homeostatic conditions of essential metal ions, not on conditions of metal toxicity.

Virtually every metal is known to be potentially toxic *in vivo*.[1,2] Almost exclusively, chelation therapy has been used to remove the toxic metal-usually with deleterious side-effects.[3] A chelating agent used to sequester a target metal should fulfill several basic criteria: it should be specific for the target metal and not bind biological essential metal ions; it must have the kinetic and

thermodynamic capability of removing the target metal from storage and/or transport proteins; and in itself, the chelating agent should be non-toxic and water soluble.

This thesis concerns itself with the characterization of metal complexes in aqueous solution of Fe(III) and Pu(IV), two potentially toxic metal ions, with a new class of chelating agents, synthetic catechoylamide ligands. Development of the ligand design concepts and synthesis program is summarized in this chapter. Perhaps the most noteworthy aspect of this progect is its integration of classical inorganic coordination chemistry with organic synthesis, physical methods of characterization, and biological evaluation.

The focus of research first centered solely on the coordination chemistry of naturally occurring microbial ferric ion sequestering agents such as enterobactin (Figure 1.1),[4-7] a tricatecholate ligand with catechol (1,2-dihydroxybenzene) linked to a backbone of a triester of l-serine via amide bonds. Upon deprotonation of the six phenolic oxygens of the catechol groups this ligand is capable of binding Fe(III) in an octahedral fashion resulting in an iron complex of unrivaled stability (log K = 52),[8] necessarily so due to the insolubility and consequent inavailability of free Fe(III) at physiological pH. This observation led to the synthesis of new chelating agents for ferric ion utilizing the catecholate dianion as the chelating entity.[9]

From its conception this project had in mind the thousands of victims of β-thalassemia whose condition of acute iron overload due to multiple blood transfusions leads to enlargement of the spleen and

liver, cardiac dysfunction and eventual death.[10,11] The resulting synthetic triCatechoylAMide (CAM) ligands (Figure 1.2) do not resemble enterobactin in the structure of their organic backbones. The hydrolytically unstable triester backbone of enterobactin has been replaced by a cyclic backbone (CYCAM), by a linear triamine backbone with amines separated by three and four methylenes (3,4-LICAM),[12] or by a mesitylene backbone (MECAM) (Figure 1.2).[13] The design of these ligands was based on data obtained from the X-ray structure of simple tris(catecholato) Fe(III) and Cr(III) complexes to provide optimum fit of the catecholate arms of the macrochelate about Fe(III).[7]

In addition to modifying the backbone of enterobactin, substituents such as carboxylate or sulfonate have been added to the catecholate ring to increase water solubility, increase the resistance toward air oxidation of the catechol, and to increase the acidity of the phenolic protons of catechol. These derivatives have been dubbed the CAMS (sulfonated)[14] and the CAMC (carboxylated)[15] ligands (Figure 1.2). Another modification seeks to increase the lipophilicity of the ligand and alter its *in vivo* distribution by appending alkyl substituents to the amide nitrogens (Figure 1.3).[16]

The original impetus toward development of synthetic tricatecholate chelating agents for iron removal has since diversified into a research effort including chelation of other metal ions which resemble Fe(III).[17,18] Ferric ion is a relatively small, nonpolarizable cation the hardness of which causes it to be very insoluble in water ($K_{sp}=10^{-39}$), as alluded to earlier. Thus, nature has developed strong chelating agents such as enterobactin with hard

oxygen anions as the base to sequester Fe(III) and deliver it to the living organism where it is necessary for growth.[19] In mammalian systems this iron is transported in the plus three oxidation state via the protein transferrin and stored as ferric ion in the storage proteins ferritin and hemosiderin.[20] Transferrin contains two iron binding sites with histidine and tyrosine being amoung the ligating groups. The tyrosine residues bind via a hard oxygen anion. In fact, at least four of the atoms ligating Fe(III) are oxygen atoms.[21] A number of toxic metals when introduced to the body are transported by transferrin by binding to one or both sites. This is part of the difficulty in removing these toxic metals since the transferrin binds with particularly high affinity (for Fe(III), $K_f=10^{24}$)[22] and then quickly circulates the ion until it is eliminated or deposited in the liver or bone.[23-25] Consequently, hard metal ions or those possessing high charge to ionic radius ratios similar to Fe(III) are transported by iron biological pathways.

This similarity of metal ions to Fe(III) has been used to some advantage by the administration of ^{67}Ga(III) and ^{111}In(III) as imaging agents for tumors and abscesses. Following injection of the radionuclide, the need for neoplastic cells to acquire larger than normal amounts of Fe(III) for growth also causes deposition and concentration of the imaging agents in these cells with transferrin acting as the shuttle.[20,26-30] The synthetic tricatecholate ligands have been successfully used in mice to reduce the amount of background due to unaccumulated nuclide as well as reducing the exposure to excess nuclide.[18,31]

Expanding the coordinating capabilities of the synthetic tricatechoylamides from six to eight by appending a fourth catecholate arm introduces another realm of ion binding--that of the tetravalent actinides. The prevalence of nuclear fuel sources has increased the risk of exposure to actinide poisoning, in particular exposure to plutonium or uranium; however, development of new complexing agents for decorporation of actinides has been ignored. It was surmised that the catecholate dianion would be a good choice to bind *in vivo* and decorporate Pu(IV), the oxidation state most prevalent in the body, because of this ion's hard acidic characteristics. In this respect Pu(IV) and Fe(III) are similar; both have large charge to ionic radius ratios (4.2 e/Å and 4.6 e/Å, respectively),[32] both have large hydrolysis constants,[33] and plutonium is transported by transferrin *in vivo*.[34-36] Since actinide(IV) ions prefer to be eight-coordinate with bidentate ligands, tetracatecholate ligands were synthesized which were designed to provide optimum geometric preferences of the actinide(IV) ion indicated by data obtained from X-ray structures of unsubstituted catechol with tetravalent cerium, thorium, and uranium $[Na_4M(C_6H_4O_2)_4]$.[37,38] The resulting tetracatecholate ligands (Figure 1.4) have been shown to be effective in sequestering Pu(IV) in dogs and mice.[39,40] In particular; 3,4,3-LICAMC is the most effective *in vivo* sequestering agent for Pu(IV) tested to date and without evidence of toxicity.[15,41]

Of course, the synthetic catechoylamides were designed to be specific for hard metal ions such as Fe(III), Ga(III), In(III), or Pu(IV); but the extent of their specificity for these ions had not

been quantitated. Chapter II presents the stabilities of three synthetic sulfonated catechoylamide ligands with divalent metal ions found in biological systems. In addition to stability constants, the coordination chemistry of these ligands with divalent metals in solution is discussed.[42]

Chapter III is a study of four N-substituted, sulfonated tricatecholate ligands with Fe(III) and Ga(III). Complex stabilities are presented as well as the protonation behavior of the metal complexes. The rates of removal of Fe(III) from transferrin by these ligands is also included and compared to those rates obtained with unsubstituted tricatecholates.

The first _in vitro_ experiments of plutonium with catecholate ligands are presented in Chapter IV. This chapter includes a discussion of protonated Pu(IV)LICAMC and Pu(IV)LICAMS complexes as well as the respective Pu(III) complexes as determined by electrochemical techniques. Some results with Ce(IV) are also included to determine to what extent this metal ion can act as a model for Pu(IV).

As evidenced by the electrochemistry of Pu(IV), Ce(IV),[38] Fe(III),[43] and Ti(IV)[44] in the presence of catechol, the catecholate dianion possesses a remarkable ability to stabilize higher oxidation states of metal ions. _In vivo_ experiments had indicated that the synthetic tetracatecholates 3,4,3-LICAMS and 3,4,3-LICAMC may stabilize Am(IV). The americium(IV) ion is normally an inaccessible oxidation state. (The Am(IV)/Am(III) reduction potential is estimated to be +2.0 to +2.9 V versus NHE.)[45] Chapter V details the results of

the electrochemistry of 3,4,3-LICAMS and 3,4,3-LICAMC with Am(III) utilizing a new electrode, reticulated vitreous carbon. Finally, the oxidation of the catecholate ligands themselves in basic solution as a function of ring substituent are studied by electrochemical techniques.

REFERENCES

1. Luckey, T.D.; Venugopal, B. "Metal Toxicity in Mammals.1" Plenum Press: New York (1977).

2. Friberg, L.; Nordberg, G.; Vouk, V., Eds. "Handbook on the Toxicology of Metals" Elsevier-North Holland: Amsterdam, 1979.

3. Mays, C.W.; Taylor, G.N.; Lloyd, R.D.; Wrenn, M.E., Actinides in Men and Animals (M.E. Wrenn, Ed.) R.D. Press, Radiobiology Division, University of Utah, Salt Lake City, 1981, 351-368.

4. O'Brien, I.G.;Gibson, F., Biochim. Biophys. Acta (1970), 215, 393-402.

5. Pollack, J.R.; Neilands, J.B., Biochem. Biophys. Res. Commun. (1970), 38, 989-992.

6. Isied, S.S.; Kuo, G.; Raymond, K.N., J. Am. Chem. Soc. (1976), 98, 1763.

7. Raymond, K.N.; Isied, S.S.; Brown, L.D.; Fronczek, F.; Nibert, J.H., J. Am. Chem. Soc. (1976), 98, 1767.

8. Harris, W.R.; Carrano, C.J.; Raymond, K.N., J. Am. Chem. Soc. (1979), 101, 2213.

9. Raymond, K.N.; Harris, W.R.; Carrano, C.J.; Weitl, F.L., ACS Symp. Ser. (1980), No. 140, 313-332.

10. Anderson, W.F.; Hiller, M.C., Eds. "Development of Iron Chelators for Clinical Use," Department of Health, Education and Welfare, Publication No. (NIH) 77-994, 1975.

11. Martell, A.E.; Anderson, W.F.; Badman, D.G., Eds. "Development of Iron Chelators for Clinical Use," Proc. second symposium, San Francisco, California, Aug. 1980. Elsevier/North Holland: New York, 1981.

12. Weitl, F.L.; Raymond, K.N., J. Am. Chem. Soc. (1979), 101, 2728-2731.

13. Harris, W.R.; Weitl, F.L.; Raymond, K.N., J. Chem. Soc., Chem. Comm. (1979), 177-178.

14. Weitl, F.L.; Harris, W.R.; Raymond, K.N., J. Med. Chem. (1979), 22, 1281-1283.

15. Weitl, F.L.; Raymond, K.N.; Durbin, P.W., J. Med. Chem. (1981), 24, 203-206.

16. Weitl, F.L.; Raymond, K.N., J. Org. Chem. (1981), 46, 5234-5237.

17. Raymond, K.N.; Smith, W.L. Struct. Bonding (Berlin) (1981), 43, 159-186.

18. Moerlein, S.M.; Welch, M.J.; Raymond, K.N.; Weitl, F.L., J. Nucl. Med. (1981), 22, 710-719.

19. Neilands, J.B., Ed. "Microbial Iron Metabolism," Academic Press: New York, 1974.

20. Crichton, R.R., Ed. "Proteins of Iron Storage and Transport in Biochemistry and Medicine," North-Holland: Amsterdam, 1975.

21. Pecoraro, V.L.; Harris, W.R.; Carrano, C.J.; Raymond, K.N., Biochemistry (1981), 20, 7033-7039.

22. Aasa, R.; Malmstrom, B.G.; Saltman, P.; Vanngard, T., Biochim. Biophys. Acta (1963), 75, 203.

23. Bothwell, T.H.; Finch, C.A., "Iron Metabolism," Little, Brown and Co.: Boston, 1962.

24. Lindenbaum, A.; Rosenthal, M.W., Health Phys. (1972), 22, 597-606.

25. Durbin, P.W., Health Phys. (1962), 8, 665-671.

26. Clausen, J.; Edeling, C.; Fogh, J., Cancer Res. (1974), 34, 1931.

27. Gunasekera, S.W.; King, L.J.; Larender, P.J., Clin. Chim. Acta (1972), 39, 401.

28. Vallabhajosula, S.R.; Harwig, J.F.; Siemsen, J.K.; Wolf, W., J. Nucl. Med. (1980), 21, 650.

29. Aisen, P.; Brown, E.B., Hematology (2nd Ed.) (1977), 14, 31.

30. Welch, M.; Welch, T., "Radiopharmaceuticals;" Subramanian, Rhodes, Cooper, Sodd, Eds.; Society of Nucl. Med.: New York, 1975, 73-79.

31. Moerlein, S.M.; Welch, M.J.; Raymond, K.N., J. Nucl. Med. (1982), 23, 501-506.

32. Shannon, R.D., Acta Crystallogr., Sect. A (1976), A32 (5), 751-767.

33. Martell, A.E.; Smith, R.M., "Critical Stability Constants;" Plenum Press: New York, 1977.

34. Durbin, P.W., Health Phys. (1975), 29, 495-510.

35. Boocock, G.; Danpure, C.J.; Popplewell, D.S.; Taylor, D.M., Radiat. Res. (1970), 42, 381-396.

36. Stover, B.J.; Bruenger, F.W.; Stevens, W., Radiat. Res. (1968), 33, 381-394.

37. Sofen, S.R.; Abu-Dari, K.; Freyberg, D.P.; Raymond, K.N., J. Am. Chem. Soc. (1978), 100, 7882.

38. Sofen, S.R.; Cooper, S.R.; Raymond, K.N., Inorg. Chem. (1979), 18, 1611.

39. Durbin, P.W.; Jones, E.S.; Raymond, K.N.; Weitl, F.L., Radiat. Res. (1980), 81, 170-187.

40. Lloyd, R.D.; Bruenger, F.W.; Atherton, D.R.; Jones, C.W.; Taylor, G.N.; Stevens, W.; Mays, C.W.; Durbin, P.W.; Jeung, N.; Jones, E.S.; Kappel, M.J.; Raymond, K.N.; Weitl, F.L., submitted to Radiat. Res.

41. Durbin, P.W.; Jeung, N.; Jones, E.S.; Weitl, F.L.; Raymond, K.N., submitted to Radiat. Res.

42. Kappel, M.J.; Raymond, K.N., Inorg. Chem. (1982), 21, 3437-3442.

43. Harris, W.R.; Carrano, C.J.; Cooper, S.R.; Sofen, S.R.; Avdeef, A.E.; McArdle, J.V.; Raymond, K.N., J. Am. Chem. Soc. (1979), 101, 6097.

44. Borgias, B.; Cooper, S.R.; Koh, Y.B.; Raymond, K.N., submitted to J. Am. Chem. Soc.

45. Morss, L.R.; Fuger, J., J. Inorg. Nucl. Chem. (1981), 43, 2059.

Figure Captions for Chapter I

Figure 1.1. The structural formula for enterobactin.

Figure 1.2. Synthetic enterobactin analogues.

Figure 1.3. Lipophilic synthetic catecholate ligands.

Figure 1.4. Actinide-specific catecholate sequestering agents.

ENTEROBACTIN

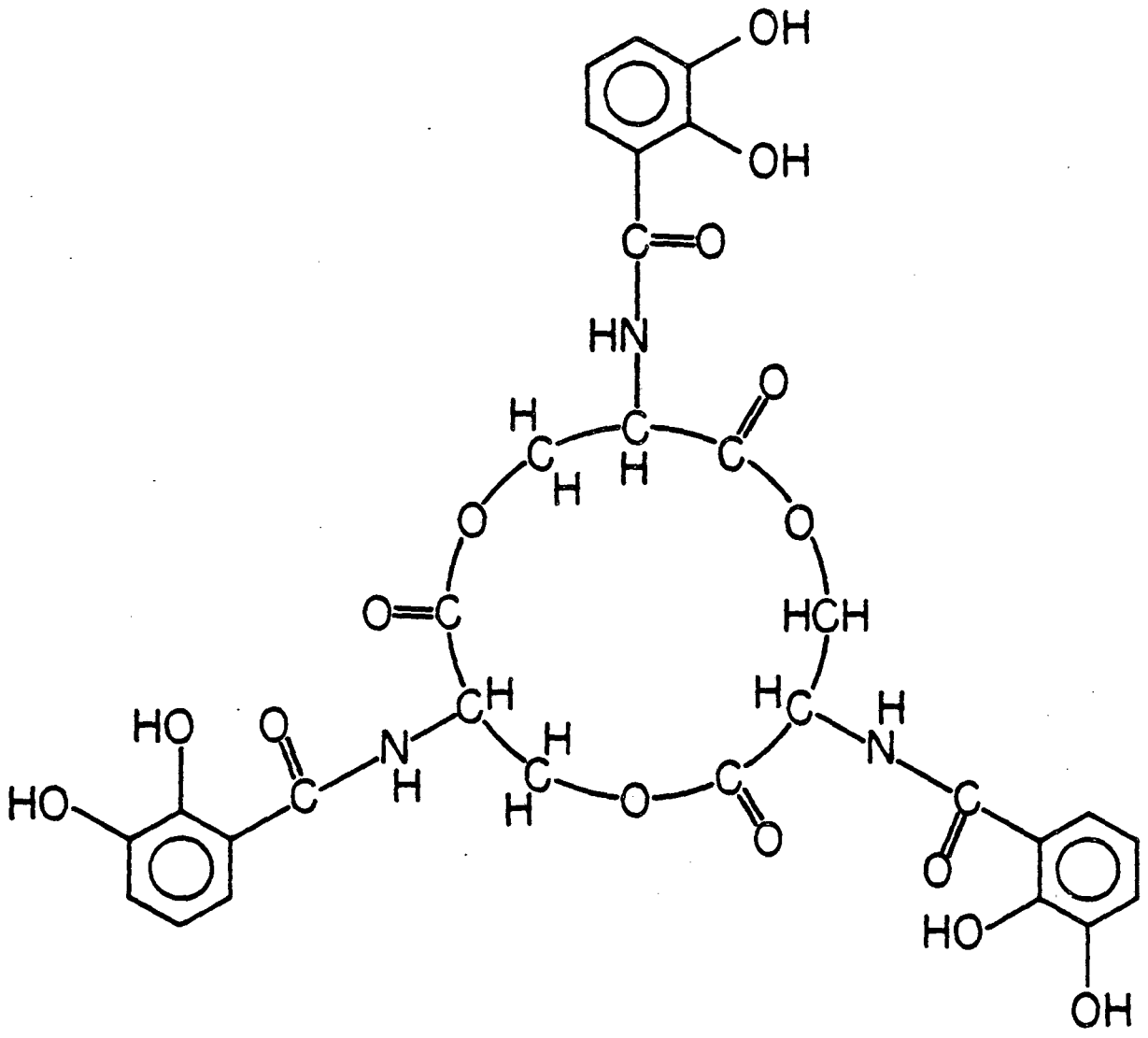

XBL 7610-4903

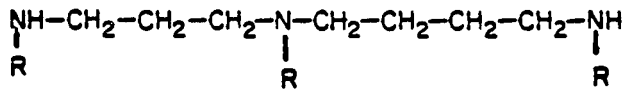

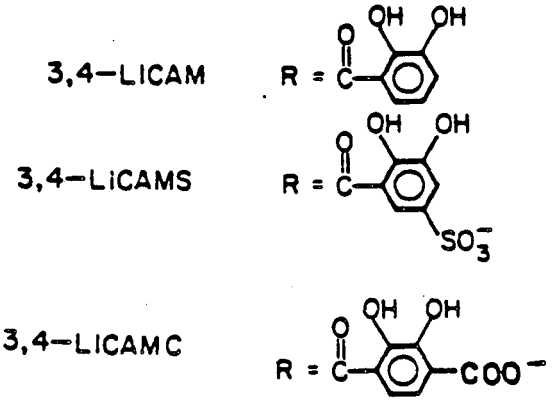
3,4–LICAM
R =
3,4–LICAMS
R =
SO3−
3,4–LICAMC
R =
COO−

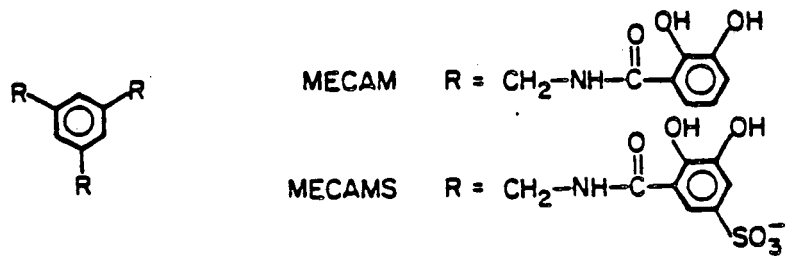
MECAM
R = CH2–NH–C
MECAMS
R = CH2–NH–C
SO3−

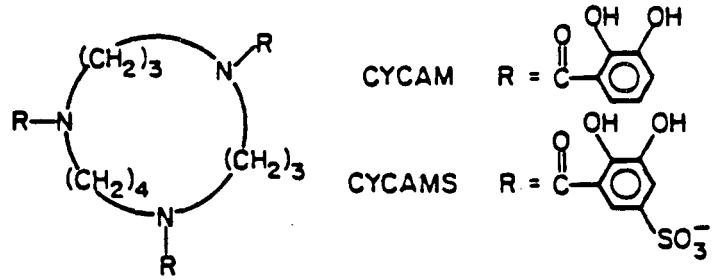
CYCAM
R =
CYCAMS
R =
SO3−

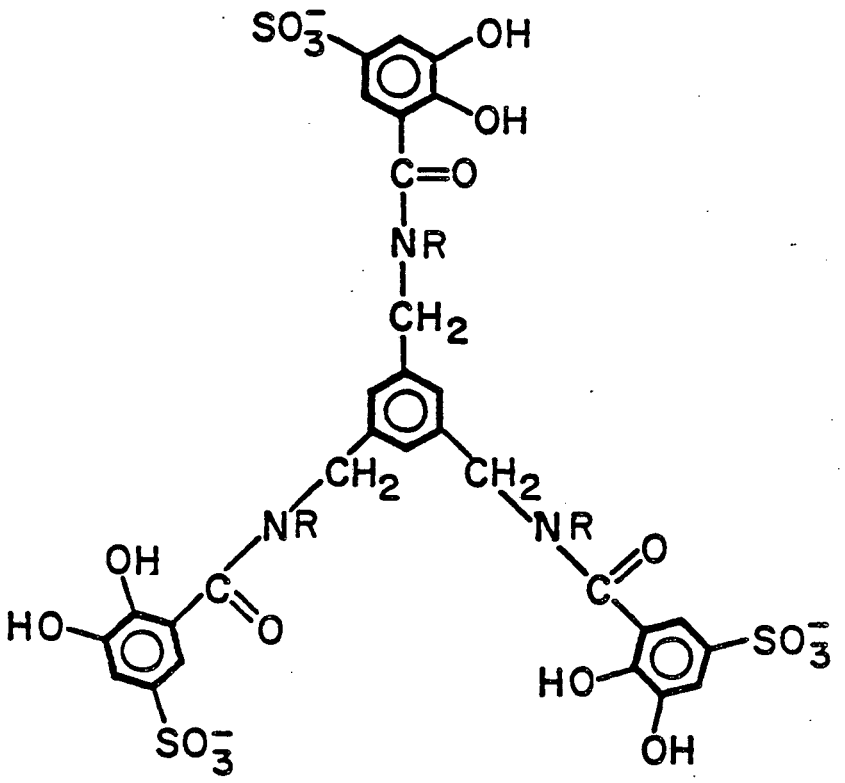

R = CH_3 R = $CH(CH_3)_2$

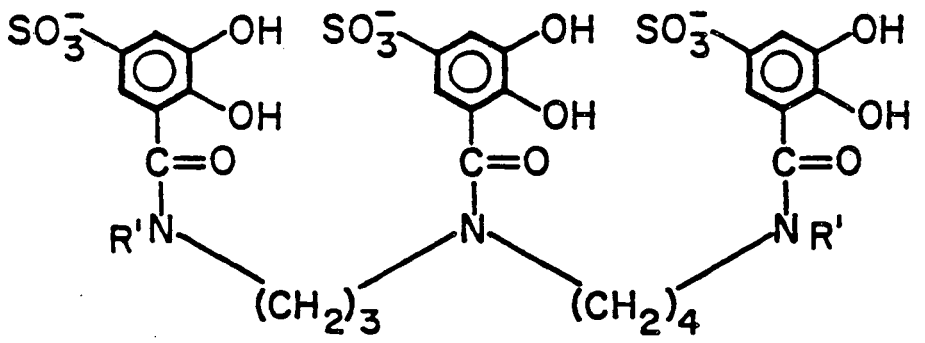

R' =  R' = $CH(CH_3)_2$

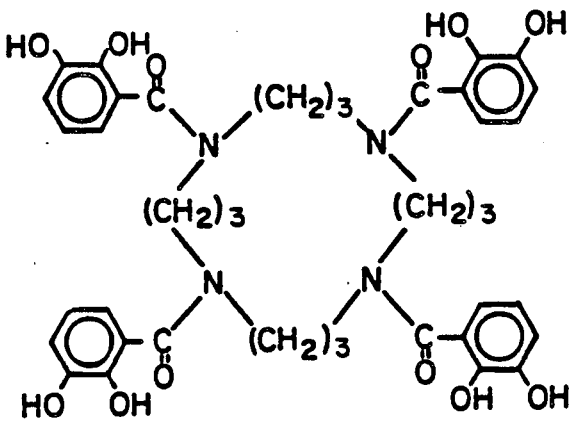

CYCAM

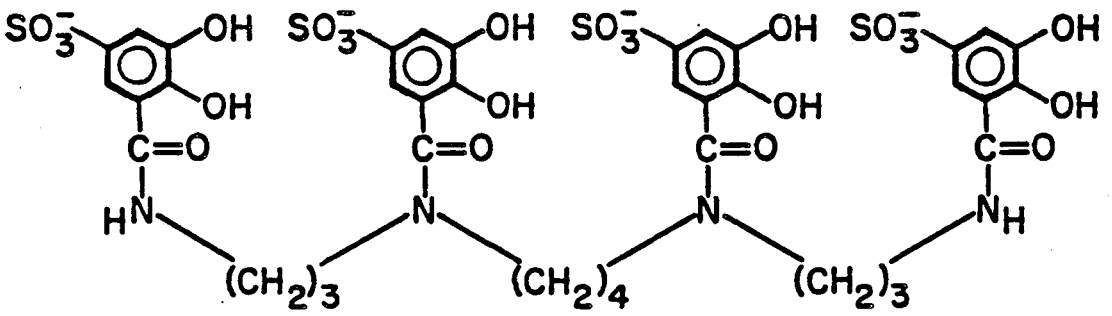

3,4,3-LICAMS

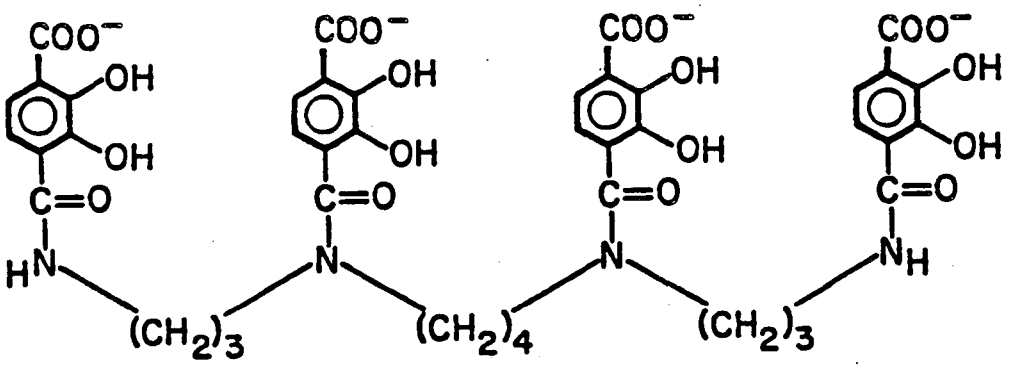

3,4,3-LICAMC

CHAPTER II

Selectivity of Sulfonated Polycatechoylamides for Ferric Ion

Chelation therapy as a means of treatment for removal of metals or metalloids from the body has been used since British anti-Lewisite (2,3-dimercapto-propanol) was discovered to be an effective sequestering agent for arsenic in the early 1940's.[1] Subsequent development of poly(carboxylate)amines such as ethylenediaminetetra-acetic acid (EDTA) and diethylenetriaminepentaacetic acid (DTPA), are effective in vivo sequestering agents for a variety of metal ions,[2] has spurred the search for the development of other effective chelating agents.

Although the synthetic chelating agents EDTA and DTPA effectively remove toxic metals from the body, they also bind divalent calcium and zinc[3] , as well as most other divalent metals, and must be administered as the calcium or zinc salts to avoid depletion of these elements from the body. Even then, toxicity results when these ligands are administered to test animals over prolonged periods.[4] Laboratory animals die, apparently at least in part as a result of Zn(II) depletion, when a high level of DTPA is maintained in the blood by

multiple injections.[5] Thus, there is a need for development of chelating agents which are capable of selectively chelating the toxic metal without removing biologically significant divalent metal ions.

The in vivo sequestering of ferric ion is of particular interest because of its toxicity if in excess in the body as mentioned in Chapter I. The synthetic catechoylamide ligands have been designed to bind ferric ion and other metals with high charge to ionic radius ratios such as Ga(III), In(III), and Pu(IV). Chapter I describes the details of the development and rational design concepts for the synthetic catechoylamide ligands. In addition, several comprehensive reviews have been published on this subject.[6-8]

For catechoylamide ligands to be considered as possible alternatives to chelating agents presently in use, the evaluation of their selectivity for ferric ion or Pu(IV) is important. This chapter reports the stabilities determined by potentiometric titrations of Ca(II), Mg(II), Cu(II), Zn(II), Ni(II), and Co(II) with several sulfonated catechoylamide ligands; a dicatechoylamide, N,N'-bis(2,3-dihydroxy-5-sulfobenzoyl)-1,6-diazahexane [4-LICAMS]; a tricatechoylamide, 1,3,5-N,N',N"-tris(2,3-dihydroxy-5-sulfobenzoyl)triaminomethylbenzene [MECAMS]; and a tetracatechoylamide, N,N',N",N'"-tetra(2,3-dihydroxy-5-sulfobenzoyl)-1,5,10,14- tetraazadecane [3,4,3-LICAMS]. Structural formulas for these ligands are shown in Figure 2.1.

Experimental

Reagents. Stock solutions of $Zn(NO_3)_2$ and $Mg(NO_3)_2$ were standardized by direct titration with disodium ethylenediaminetetraacetic acid (EDTA) using Eriochrome Black T as an indicator. Stock solutions of $Ca(NO_3)_2$, $Co(NO_3)_2$, and $Ni(NO_3)_2$ were standardized by back titration of a measured excess of disodium EDTA with a standardized solution of $Zn(NO_3)_2$ using Eriochrome Black T as the indicator. The $Cu(NO_3)_2$ solution was standardized with Pyrocatechol Violet by direct titration with disodium EDTA. Details of the standardization procedures are presented elsewhere.[9] Carbonate-free 0.1 M KOH was prepared by dilution of Baker Dilut-It KOH ampoules with twice-distilled degassed water. It was stored under a positive pressure of argon and standardized with potassium acid phthallate. Gran plots were performed to confirm the absence of carbonate.[10]

The synthesis and characterization of the ligands studied are reported elsewhere.[11,12] Equivalent weights of the ligands were determined by potentiometric titration.

Potentiometric Measurements. The apparatus used for the potentiometric titrations consisted of a Sargent Welch 10 mL automatic buret connected to a reservoir of 0.1 M KOH, a Corning 130 pH meter equipped with a standard saturated calomel electrode and a Ag/AgCl glass membrane electrode, a specially designed water-jacketed titration cell with constant temperature bath, and a Commodore PET 8K microcomputer with memory expansion interfaced to the buret, a stirrer, and the pH meter. All titrations were performed

automatically with the computer. Aliquots of 0.05 mL or 0.1 mL of base were added automatically only after the pH meter had stabilized. Usually the criteria used provided that a point on the titration curve was recorded and another aliquot of base was added only after the pH drifted less than 0.0005 pH unit per minute. Solutions were prepared for titration by weighing out the appropriate amount of ligand, adding 4.0 mL of 1.0 M KNO_3 and 36.0 mL of twice-distilled water for a constant ionic strength of 0.1 M. Stoichiometric amounts of stock metal solution were then added. The solution was degassed with argon for at least 30 minutes and equilibrated to 25.0 $\pm$ 0.05°C at which temperature the titration was run. The pH meter was calibrated with a standard solution of HNO_3 and a buffered acetic acid solution. Standardization of the meter was then completed by titrations of acetic acid to read $-\log[H^+]$ where $[H^+]$ is the hydrogen ion concentration, not activity. Equilibrium constants were calculated by a weighted non-linear least-squares refinement in which the $\log \beta$'s[13] were varied to minimize the sum of the squared differences between the observed and calculated pH at each point in the titration curve.[14] See the Appendix for further details on the refinement program.

Results and Discussion

4-LICAMS Titrations. The potentiometric titration curve of the free dicatechol ligand, 4-LICAMS, is shown in Figure 2.2. [The abscissa of the graph in this titration is moles base per mole ligand.] The curve shows a break at two equivalents. This is

indicative of the deprotonation of the two phenolic oxygens which are ortho to the carbonyl. The increased acidity of the ortho phenolic hydrogens over the meta phenolic hydrogens is due to the combined resonance and inductive effects of the carbonyl and sulfonate groups.[15] The average ligand protonation constants for the two monoprotonated catechoylamide arms have been estimated[16] to be $K \simeq 10^{11.5}$. These estimated protonation constants are based on literature values reported for similar, but simple, sulfonated benzamide ligands.[17] Work is currently in progress to measure the high protonation constants of the sulfonated catecholate ligands by monitoring the change in the uv spectrum with pH, since the $\pi \rightarrow \pi^*$ transition of the catechol rings and the $\pi \rightarrow \pi^*$ transition of the amide carbonyl appear to be perturbed by changes in pH. Preliminary results seem to indicate that the previous estimates for these protonation constants are accurate.[18] The ligand protonation constants for the ortho phenol moieties of 4-LICAMS are listed in Table I.

The titration curves of one to one 4-LICAMS to divalent metal are shown in Figure 2.2. The Cu(II), Zn(II), Co(II), and Ni(II) curves show breaks at four equivalents due to formation of a biscatecholate metal complex. From simple stoichiometric considerations, it is impossible to determine whether the complexes formed are monomeric or dimeric. Analysis of the buffer regions using the model-dependent computer program (See Appendix) yielded refinements for monomeric and dimeric complexes. However, the stability constants obtained assuming dimeric complexes present had errors ten to twenty times greater than

the stability constants obtained assuming formation of monomeric complexes. In addition, titrations were performed varying the metal concentration while keeping the ligand concentration constant. No shift of the buffer region to lower pH was observed at higher metal concentrations-as is expected if dimeric complexes were formed. Bis(catecholate) complexes of Cu(II), Co(II), Ni(II), and Zn(II) for simple monocatechol ligands are known.[19] Even at higher ratios of 4-LICAMS to metal there was no evidence of the formation of tris(catecholate) complexes.

By the depression of the titration curves, the relative stabilities of the 4-LICAMS divalent metal complexes are Cu(II) > Zn(II) > Co(II), Ni(II) > Mg(II) > Ca(II). These relative stabilities are reflected in the refined log β values listed in Table II. It is noteworthy that both Ca(II) and Mg(II) show very little affinity for the ligand and that their titration curves illustrate only slight depressions of the free ligand titration curve.

The ferric ion titration with 4-LICAMS (Figure 2.2) is performed with a three to two ligand to metal ratio due to the hydrolytic tendencies of Fe(III). Ratios less than this lead to hydrolysis of the metal and subsequent "drifts" in the pH readings. This problem is not encountered with the divalent metals due to their smaller hydrolysis constants.[3] The break at $\underline{a}$ = 6 indicates that six phenolic oxygens bind each ferric ion. Such a structure is probably dimeric in character, and may be analogous to the coordination of ferric ion by rhodotorulic acid, a dihydroxamate ligand in which metal complexation also occurs in a three to two ligand to metal ratio.[20] In addition,

x-ray structures performed on a synthetic dihydroxamate Fe(III)[21] complex as well as a di(N-hydroxypyridone)Fe(III)[22] complex show that the complexes are dinuclear. The refined value of $\log \beta_{230}$ for the dimeric Fe(III) complex is 76(1).[13]

MECAMS Titrations. The titration of the free tri-catechol MECAMS ligand is shown in Figure 2.3. The ligand protonation constants have been reported previously[16] and are listed in Table I. The break at a = 3 (moles base per mole ligand) denotes deprotonation of the three more acidic phenol groups ortho to the carbonyl on each of the catechol moieties.

One to one titrations of MECAMS with divalent zinc, cobalt, nickel, and magnesium (Figure 2.3) show no other features than a break at a = 5. This indicates the formation of a biscatecholate complex followed by deprotonation of the remaining phenol ortho to the carbonyl. A distinct inflection at a = 4 following the formation of the biscatecholate complex is present only in the titration of Cu(II) with MECAMS, in which case metal complex formation is strong enough not to overlap with the equilibrium of ligand deprotonation. By monitoring the C-O stretch of the carbonyl adjacent to the catechol as a function of increasing pH in the Cu(II)-MECAMS complexes, one can assign the peak that develops at ν = 1611 cm^{-1} to that of a free catechol arm - similar to the stretch observed at ν = 1613 cm^{-1} for deprotonated MECAMS.[23]

The refined $\log \beta$ values[13] are listed in Table II. The relative

stabilities of these complexes are the same as those noted with 4-LICAMS. The Ca(II) complexation is very weak, that metal again showing little affinity for the catecholate moieties.

The ferric MECAMS titration curve (Figure 2.3) indicates formation of a triscatecholate complex with concomitant release of six protons (a = 6). Spectrophotometric titration results as well as competitions performed with EDTA are reported elsewhere.[16] The strong one-to-one MECAMS to ferric ion complex which is formed with no free catecholate arms can be compared to the one to one MECAMS to divalent metal complexes which have one free catecholate arm and weaker complexation. It is clear that ferric ion forms a stronger complex and better utilizes the coordinating capability of the ligand.

3,4,3-LICAMS Titrations. The titration curve of the free tetracatechol ligand 3,4,3-LICAMS (a is moles base per mole ligand) is shown in Figure 2.4. This curve shows an inflection at a = 4. Analogous to the 4-LICAMS and MECAMS deprotonation curves, this represents the dissociation of the four phenolic hydrogens ortho to the carbonyl. The ligand protonation constants are given in Table I.

The one to one ligand to metal titration curves for 3,4,3-LICAMS with Mg(II), Ni(II), Co(II), and Zn(II) (Figure 2.4) only show a break at a = 6; while the Cu(II) curve also shows an inflection at a = 4 as well as a = 6. The buffer region from a = 0 to a = 4 of the Cu(II) curve is attributed to the formation of a biscatecholate complex. This is followed by the deprotonation of the phenols ortho to the carbonyl on the remaining catechoylamide arms (a = 4 to a = 6). The

stronger complexation of Cu(II) by the catecholate moieties allows the break at $\underline{a}$ = 4 to be seen and is the basis for proposing biscatecholate formation. Once again, no break at $\underline{a}$ = 4 occurs for the other divalent metals studied due to the overlapping equilibria of metal complexation and ligand deprotonation. Thus, as in the case of MECAMS, all the divalent metals studied except Ca(II) show formation of biscatecholate complexes. It is interesting to note that the titration curves of all the divalent metals except Mg(II) and Ca(II) with 3,4,3-LICAMS intersect at $\underline{a}$ = 5.5. At the intersection point the pH is equal to the pKa of the ortho phenol that is remaining on one of the free catecholate arms, analogous to the Bjerrum half integral $\bar{n}$ plots.[24] However at pH values more basic than the intersection point, the curves differ significantly, indicating different species are in solution. The logβ values ($\beta_{114}\beta_{113}\beta_{112}$) refined from these titrations are given in Table II. The relative stabilities of the metals with 3,4,3-LICAMS are the same as those noted with 4-LICAMS and MECAMS.

The ferric titration with 3,4,3-LICAMS breaks at $\underline{a}$ = 7. This is in keeping with the formation of a triscatecholate complex followed by deprotonation of the one remaining phenol which is <u>ortho</u> to the carbonyl. The fact that only one catecholate arm is free in the fully formed ferric ion 3,4,3-LICAMS complex demonstrates that ferric ion more effectively employs the ligand denticity of 3,4,3-LICAMS than do the divalent metals. Ferric ion also forms a stronger complex with 3,4,3-LICAMS.

Because of the expanded (octadentate) coordinating capabilities

of 3,4,3-LICAMS, titrations were also performed at two to one divalent metal to ligand ratios. These titration curves are shown in Figure 2.5. (For the free ligand curve, which is retained for the sake of comparsion, the abscissa should read moles base per 1/2 mole ligand.) Note that divalent zinc, copper, cobalt, and nickel show definite breaks at $\underline{a} = 4$, forming a dinuclear complex. The Ca(II) and Mg(II) curves indicate very weak complexation even at these higher metal concentrations. The relative stabilities are the same as in the previous complexes studied; this is reflected in the logβ values given in Table II (β_{210}).

Attempts were made to titrate Mn(II) with MECAMS and 3,4,3-LICAMS. All the titrations were characterized by large "drifts" in the pH readings. This can probably be attributed to the oxidation of Mn(II) to Mn(III) or Mn(IV) by any residual oxygen in the titration vessel (whose design does not allow for the truly rigorous exclusion of O_2) combined with the ability of the catechol ligand to stabilize the higher oxidation state.[25] Qualitatively, the Mn(II) complexes were slightly less stable than those formed with Co(II).

Although one can directly compare β values of a series of divalent metals with the same ligand (e.g., β_{110} of Cu[4-LICAMS] vs. β_{110} of Co[4-LICAMS]), problems arise when one attempts to compare β values of divalent metals with different ligands (e.g., β_{110} of Cu[4-LICAMS] vs. β_{110} of Cu[MECAMS]). This is because the ligands differ in acidity and proton dependence. In addition, one cannot compare values of divalent metal complexes to ferric complexes of the same or different ligands (e.g., β_{110} of Fe[MECAMS] vs. β_{111} of

Cu[HMECAMS]). In this case, the coordination around the metal differs; bis(catecholate) vs. tris(catecholate) coordination. As a standard by which to measure and compare the effectiveness of a potential chelating agent for a metal at physiological pH, one can calculate the concentration of the uncomplexed, aquated ion in a solution which is 10 μM in ligand, 1 μM metal, at pH 7.4. These calculations are performed using refined β values, or when β values are not directly obtainable, by using proton-dependent formation constants as in the case of ferric MECAMS and ferric 3,4,3-LICAMS. The concentrations which are calculated are expressed as pM, where pM = $-\log [M(H_2O)_x]$. Using pM values direct comparisons can be made: the larger the pM value, the greater the affinity of the chelate for the metal under the defined conditions. Under the conditions specified, the minimum pM value that is possible is 6.0. Keep in mind that the pM definition includes the stability of the soluble hydroxo complexes of the metal ion. The stability of complexes with hydroxide are insignificant in comparison to the stabilities demonstrated by the ligands for the metal ions studied. The pM values for the divalent metals and ferric ion with 4-LICAMS, MECAMS, 3,4,3-LICAMS, EDTA, DTPA, and desferrioxamine B (DFO), the current chelating agent used for treatment of iron overload, are tabulated in Table III.

Analysis of Table III reveals several important points regarding these chelating agents. None of the polycatechoylamides bind the important biological ions Ca(II) or Mg(II) to any significant extent; whereas the polycarboxylateamines, EDTA and DTPA, have an enhanced affinity for Ca(II) and Mg(II). Generally, EDTA and DTPA do not bind

ferric ion as tenaciously as do the polycatechoylamides, nor do they demonstrate specificity in binding.

The specificity of desferrioxamine B for ferric ion is impressive. However, it does not show as great an affinity for ferric ion as does MECAMS and 3,4,3-LICAMS: also, the differences in the Cu(II) pM value and the ferric ion pM value (ΔpM = 14.8) is less than that demonstrated by 3,4,3-LICAMS (ΔpM = 16.4). Desferrioxamine B also does not bind Ca(II) or Mg(II) to any great extent.

Just as MECAMS was designed to bind ferric ion, the ligand 3,4,3-LICAMS has been designed to complex tetravalent actinides, in particular Pu(IV). The ligand is octadentate, which satisfies the eight-coordinate nature of Pu(IV), via four catecholate moieties. The length and substitution pattern of the linear backbone has been determined from the structure of simple tetrakis catecholato actinide(IV) complexes[26] to allow for the best fit of the large Pu(IV) ion. In view of the similarities between Fe(III) and Pu(IV) (vide supra), 3,4,3-LICAMS is expected to bind Pu(IV) effectively. [See Chapter IV of this thesis.] In vivo tests of 3,4,3-LICAMS shows it is very effective in removing plutonium from mice.[27]

It is apparent from this study that 3,4,3-LICAMS demonstrates greater selectivity and greater affinity for metals of high charge to radius ratio than does DTPA, the current chelating agent used for plutonium decorporation. The difference in specificity between DTPA and 3,4,3-LICAMS confirms that catechoylamides may provide a promising alternative to DTPA for chelation therapy of plutonium contamination.

An interesting correlation is observed if one compares the pM of

each metal to its charge to ionic radius ratio. Figure 2.6 is a graph of charge to ionic radius ratio versus pM for MECAMS. A similar correlation exists for 4-LICAMS and 3,4,3-LICAMS. The ionic radii used for Zn(II) and Cu(II) were those listed by Shannon[28] for four coordinate species. The other ions were assumed to be six coordinate. Copper(II) is the smallest of the divalent metals studied and it demonstrates the greatest affinity for the catechoylamide. Ferric ion, with its high charge and small size, demonstrates the greatest stability. Plutonium(IV) also exhibits a high charge to ionic radius ratio, and this explains the qualitative observation of its high affinity for polycatechoylamide ligands. [See Chapter IV of this thesis.]

Summary

The synthetic polycatechoylamide ligands generally form very stable complexes with ferric ion and other ions of high charge to ionic radius ratios including Pu(IV) and Th(IV). The common divalent metals which are present in the body, e.g. Mg(II) and Ca(II), are large enough and of sufficiently low charge not to be chelated effectively by the polycatechoylamides. The effectiveness of the ligands as a whole can be attributed not only to the intrinsic affinity of the phenolic oxygens for ligation of highly charged ions, but also can be attributed to the structural design of the entire ligand for encapsulation of the desired ion. It is the combination of these two factors which contribute to the excellent selectivity of the polycatechoylamides to sequester Fe(III) or Pu(IV).

REFERENCES

1. Peters, R.A.; Stocken, L.A.; Thompson, R.H.S., Nature (1945), 156, 616- 619.

2. Seven, M.J.; Johnson, L.A., Eds. "Metal Binding in Medicine," Lippincott: Philadelphia, 1959.

3. Martell, A.E.; Smith, R.M., "Critical Stability Constants," Plenum Press: New York, 1977.

4. Foreman, H., "Metal Binding in Medicine," Seven, M.J.; Johnson, L.A., Eds., Lippincott: Philadelphia, 1959; p. 82-94.

5. Taylor, G.N.; Williams, J.L.; Roberts, L.; Atherton, D.R.; Shabestari, L., Health Phys. (1974), 27, 285-288.

6. Raymond, K.N.; Harris, W.R.; Carrano, C.J.; and Weitl, F.L., ACS Symp. Ser. (1980), No. 140, 313-332.

7. Raymond, K.N.; Smith, W.L., Struct. Bond. (Berlin) (1981), 43, 159-186.

8. Raymond, K.N.; Smith, W.L.; Weitl, F.L.; Durbin, P.W.; Jones, E.S.; Abu-Dari, K.; Sofen, S.R.; Cooper, S.R., ACS Symp. Ser. (1980), No. 131, 143-172.

9. Welcher, T.J., "The Analytical Uses of Ethylenediaminetetraacetic Acid," Van Nostrand: Princeton, N.J., 1958.

10. Rossotti, F.; Rossotti, H., J. Chem. Ed. (1965), 42, 375-378.

11. Weitl, F.L.; Harris, W.R.; Raymond, K.N., J. Med. Chem. (1979), 22, 1281-1283.

12. Weitl, F.L.; Raymond, K.N., J. Am. Chem. Soc. (1980), 102, 2289-2293.

13. The formation constant, β_{mlh}, is written in terms of free metal, free ligand, and free hydrogen concentrations, where the subscript mlh denotes the number of metal, ligand, and hydrogen ions incorporated in the complex. Protons associated with the sulfonate groups are ignored, since their pKa's are about 3.0 and under the conditions of these experiments they remain deprotonated. For example, the stability constant of the complex formation given by the reaction

$$Cu^{2+} + MECAMS^{9-} + 2H^{+} = Cu(H_2MECAMS)^{5-}$$

is β_{112} ,where

$$\beta_{112} = [Cu(H_2MECAMS)^{5-}]/([Cu^{2+}][MECAMS^{9-}][H^+]^2)$$

In contrast, the formation constant, K, is a stepwise formation constant. For example, for the $CuH_2MECAMS^{5-}$ complex written above

$$K_{MHL} = [Cu(HMECAMS)^{6-}]/([CuMECAMS^{7-}][H^+])$$

$$K_{MH_2L} = [Cu(H_2MECAMS)^{5-}]/([Cu(HMECAMS)^{6-}][H^+])$$

such that $\beta_{112} = \beta_{110} \cdot K_{MHL} \cdot K_{MH_2L}$

14. The weighted residual for each data point is

$$r_i = (1/\sigma_i)(pH_{obsd} - pH_{calc})_i.$$

The derivatives $D_{ij}=(\partial r_i / \partial \log \beta_j)$ were computed numerically and the shifts in β values, computed to minimize the sum of the squares of the residuals, were applied from the vector-matrix equation:

$$\Delta \log \beta = (D^T D)^{-1} D^T r.$$

The weighting factor, $1/\sigma_i$, was based on the estimated uncertainty in the pH reading at each point in the titration curve. This uncertainty has two components: the precision of the pH meter itself and the precision of titrant delivery (volume V_T). Thus the weight was calculated as

$$\sigma_i^2 = \sigma_{meter}^2 + (\partial pH/\partial V_T)_i^2 \sigma_{V_T}^2$$

where σmeter=0.003 pH unit, σV_T=0.002 mL and $\partial pH/\partial V_T$ is the slope of the titration curve at each point in the titration. This weighting scheme emphasizes the more accurate data from buffer regions and minimizes the relatively inaccurate pH readings from the steep inflections.

15. Bordwell, F.G.; Cooper, G.D., J. Am. Chem. Soc. (1952), 74, 1058-1070.

16. Harris, W.R.; Raymond, K.N.; Weitl, F.L., J. Am. Chem. Soc. (1981), 103, 2667-2675.

17. Avdeef, A.; Sofen, S.R.; Bregante, T.L.; Raymond, K.N., J. Am. Chem. Soc. (1978), 100, 5362-5370.

18. Pecoraro, V.; Scarrow, R.; Kappel, M.; Raymond, K., manuscript in preparation.

19. Rohrscheid, F.; Balch, A.L.; Holm, R.H., Inorg. Chem. (1966), 9, 1542-1551.

20. Carrano, C.J.; Cooper, S.R.; Raymond, K.N., J. Am. Chem. Soc. (1979), 101, 599.

21. Barclay, S.J.; Riley, P.R.; Raymond. K.N., J. Am. Chem. Soc. (1982), 104, 6802.

22. White, D.: Scarrow, R.; Raymond, K., unpublished results.

23. Pecoraro, V.L.; Harris, W.R.; Wong, G.; Raymond, K.N., submitted to J. Am. Chem. Soc.

24. Rossotti, F.; Rossoti, H., "The Determination of Stability Constants, and other Equilibrium Constants in Solution" McGraw-Hill: New York, 1961.

25. Magers, K.D.; Smith, C.G.; Sawyer, D.T., Inorg. Chem. (1978), 17, 515-523.

26. Sofen, S.R.; Cooper, S.R.; Raymond, K.N., Inorg. Chem. (1979), 18, 1611-1616.

27. Durbin, P.W.; Jones, E.S.; Raymond, K.N.; Weitl, F.L., Radiat. Res. (1980), 81, 170-187.

28. Shannon, R.D., Acta Crystallogr., Sect. A (1976), A32 (5), 751-767.

Table I

Protonation constants[a] of sulfonated catecholate ligands[b]

Ligand	$\log K_3^H$	$\log K_4^H$	$\log K_5^H$	$\log K_6^H$	$\log K_7^H$	$\log K_8^H$	$\log K_{ave}^H$
4-LICAMS	6.61(1)	5.96(1)	-	-	-	-	6.3
MECAMS[c]	-	7.26(2)	6.44(2)	5.88(2)	-	-	6.5
3,4,3-LICAMS	-	-	8.26(2)	7.62(3)	6.69(2)	6.13(1)	7.3

[a] $K_N^H = \frac{[H_nL]}{[H_{n-1}L][H]}$

[b] Measurements were made at 25°C and 0.10 M (KNO_3) ionic strength.

[c] See Ref. 16.

Table II

Equilibrium constants[a] of divalent metals with sulfonated catecholate ligands[b]

	Cu(II)	Zn(II)	Ni(II)	Co(II)	Mg(II)	Ca(II)	Fe(III)
MECAMS							
$\log \beta_{111}$	35.88(5)	30.2(1)	26.5(2)	26.3(2)	22.3(2)	-	-
$\log \beta_{112}$	42.21(5)	37.01(6)	34.17(8)	33.9(1)	27.9(1)	-	-
$\log \beta_{110}$	-	-	-	-	-	-	41[c]
3,4,3-LICAMS							
$\log \beta_{114}$	60.8(2)	54.75(7)	53.42(8)	53.24(6)	50.5(3)	48.89(8)	-
$\log \beta_{113}$	54.1(2)	47.8(5)	45.9(3)	45.7(3)	42.5(4)	39.86(6)	-
$\log \beta_{112}$	46.0(2)	39.9(2)	37.9(2)	37.7(2)	34.3(3)	30.12(4)	-
$\log \beta_{210}$	43.8(2)	31.8(1)	28.2(2)	27.9(2)	19.9(2)	16.2(2)	-
$\log \beta_{111}$	-	-	-	-	-	-	43[d]
4-LICAMS							
$\log \beta_{110}$	21.2(2)	15.63(5)	14.0(2)	13.6(1)	-	-	27.4(1)
$\log \beta_{121}$	-	-	-	-	-	-	51.1(5)
$\log \beta_{122}$	-	-	-	-	-	-	58.3(5)
$\log \beta_{230}$	-	-	-	-	-	-	76(1)

[a] $\beta_{m\ell h} = \frac{[M_m L_\ell H_h]}{[M]^m [L]^\ell [H]^h}$; [b] Measurements were made at 25°C and 0.10 M (KNO_3) ionic strength; [c] See Ref. 16; [d] See Ref. 6.

Table III

Equilibrium free metal ion concentrations expressed as pM[a]

	4-LICAMS	MECAMS	3,4,3-LICAMS	EDTA[b]	DTPA[b]	DFO[c]
Cu(II)	13.6	16.9	14.7	16.9	18.2	11.8
Zn(II)	8.3	11.3	8.7	14.6	15.1	7.2
Ni(II)	6.8	8.0	7.2	16.7	17.0	7.0
Co(II)	6.5	7.7	7.0	14.5	16.0	6.5
Mg(II)	6.0	6.0	6.0	7.0	6.4	6.0
Ca(II)	6.0	6.0	6.0	8.8	7.6	6.0
Fe(III)	23.3	29.3	31.1	22.2	24.7	26.6

[a] $pM = -\log [M(H_2O)_x^{N+}]$; calculated for 10 μM ligand, 1 μM metal, pH 7.4 at 25°C and 0.1 M KNO_3.

[b] Ref. 3.

[c] Anderegg, G.; L'Eplattenier, F.; Schwarzenbach, G. Helv. Chim. Acta 1963, 46, 1400.

Figure Captions for Chapter II

Figure 2.1. Structural formulas of sulfonated catechoylamide ligands.

Figure 2.2. Potentiometric equilibrium curves of 4-LICAMS free ligand, 1:1 4-LICAMS to divalent metal, and 3:2 4-LICAMS to ferric ion, [M]≃ 1.1 x 10^{-3}M; [Fe] = 6.6 x 10^{-4}M; μ = 0.10 M (KNO_3); T = 25°C.

Figure 2.3. Potentiometric equilibrium curves of MECAMS free ligand and 1:1 MECAMS to metal. [M]≃1.1 x 10^{-3}M; [Fe]≃1.3 x 10^{-3}M; μ = 0.10 M (KNO_3); T = 25°C.

Figure 2.4. Potentiometric equilibrium curves of 3,4,3-LICAMS free ligand, and 1:1 3,4,3-LICAMS to metal. [M] = [Fe]≃1.1 x 10^{-3}M; μ = 0.10 M (KNO_3); T = 25°C.

Figure 2.5. Potentiometric equilibrium curves of 3,4,3-LICAMS free ligand and 1:2 3,4,3-LICAMS to divalent metal. [M]≃1.80 x 10^{-3}M; μ = 0.10 M (KNO_3); T= 25°C.

Figure 2.6. Graph of charge to ionic radius ratio versus pM for MECAMS.

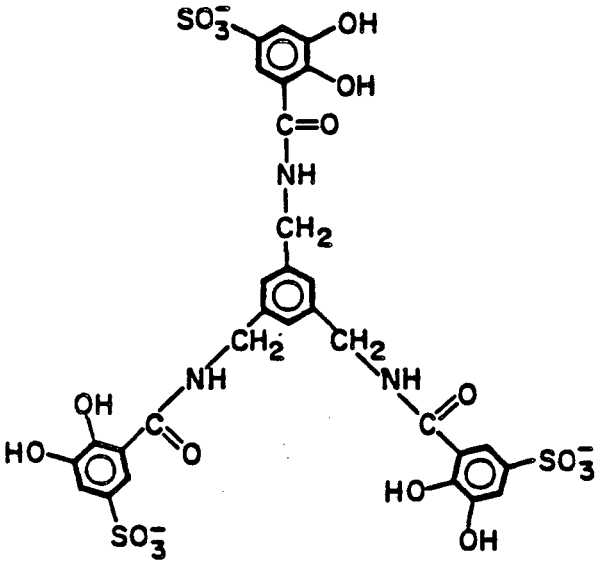

MECAMS

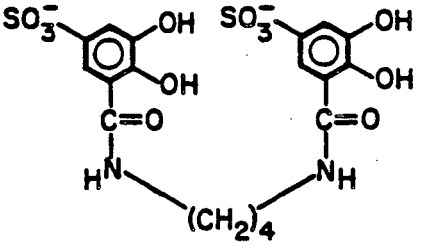

4-LICAMS

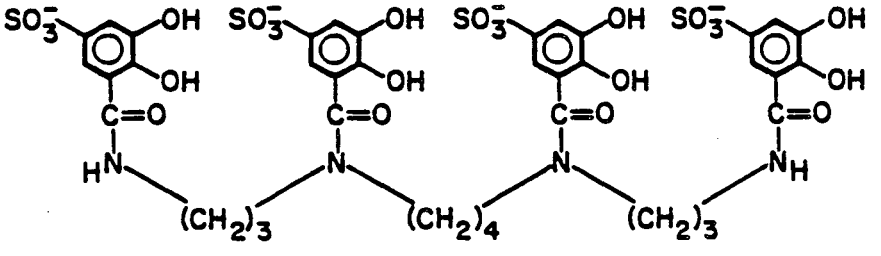

3,4,3-LICAMS

Titration Curves of 4-LICAMS

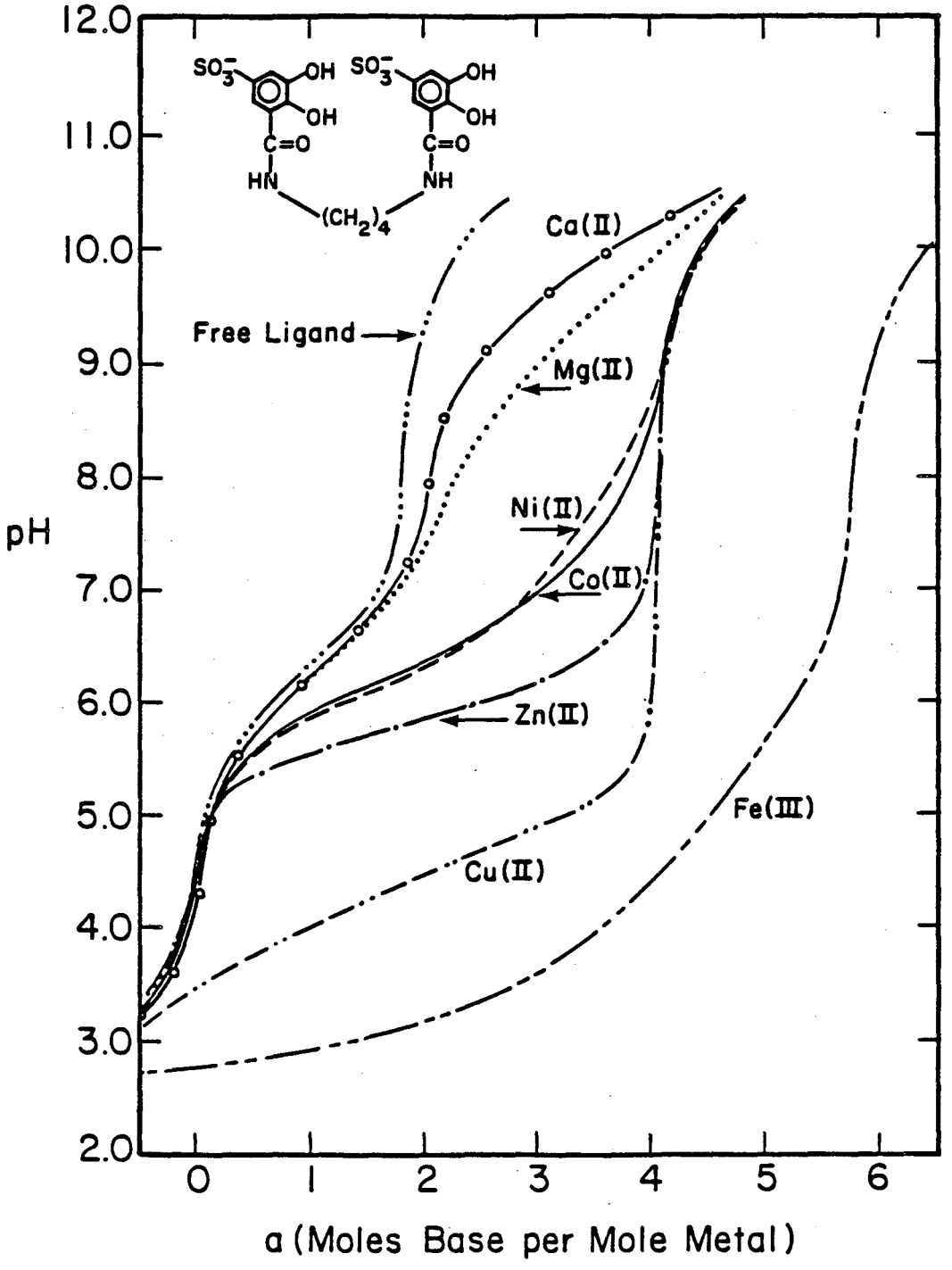

XBL 8010-12615

Titration Curves of MECAMS

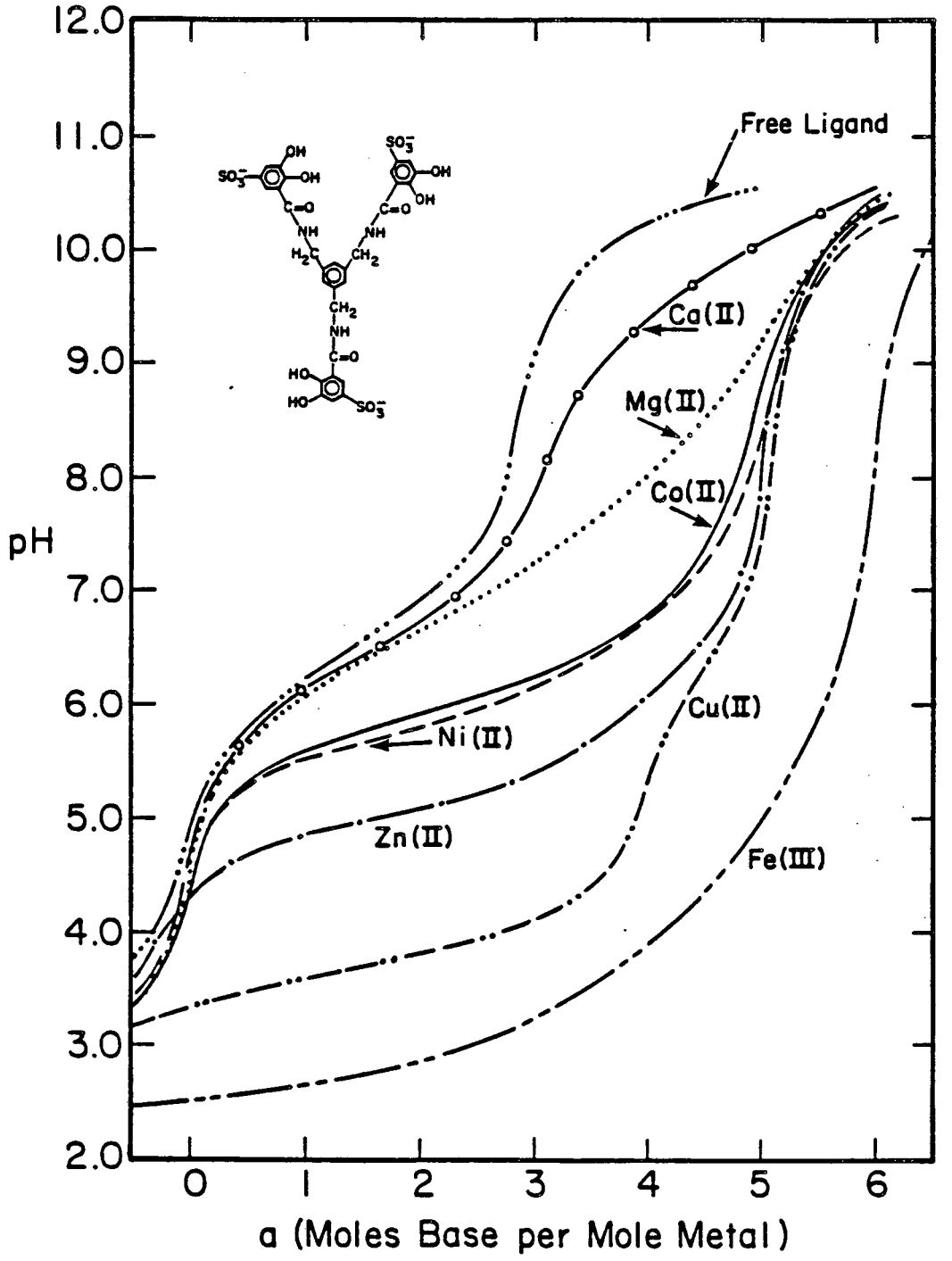

Titration Curves of 1:1 Metal to 3,4,3-LICAMS

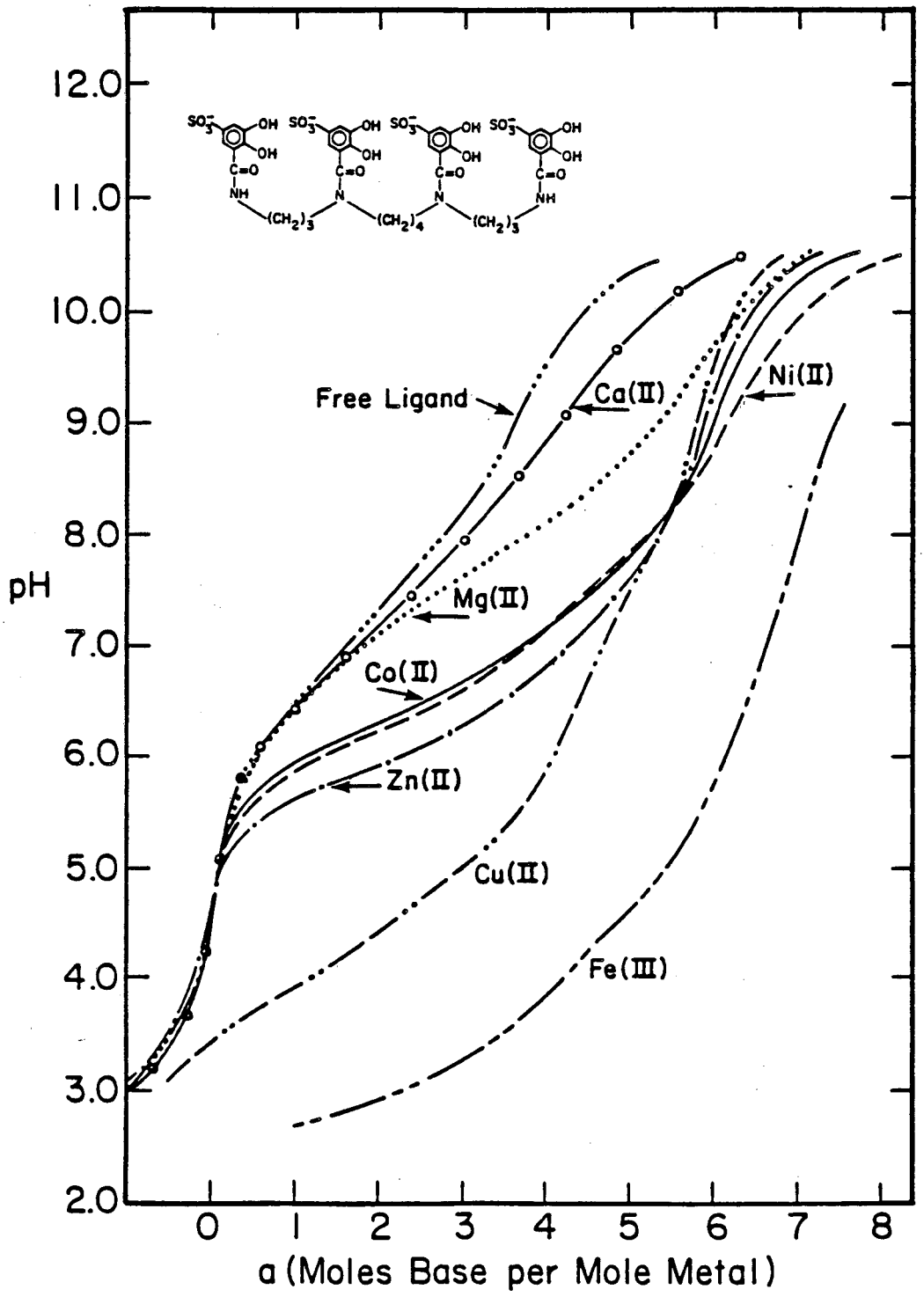

Titration Curves of 2:1 Metal to 3,4,3-LICAMS

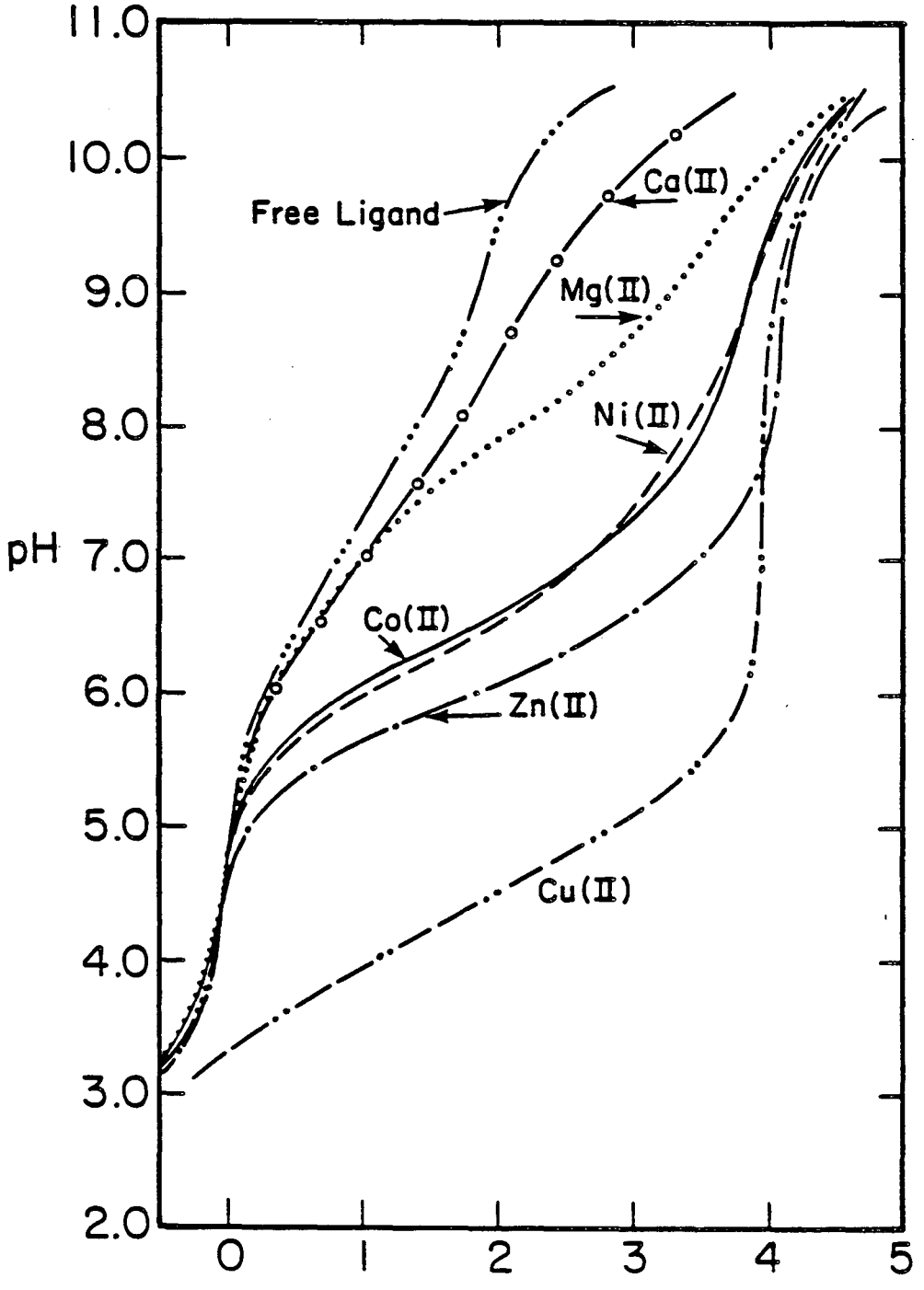

Metal Hardness vs. pM for MECAMS Complexes

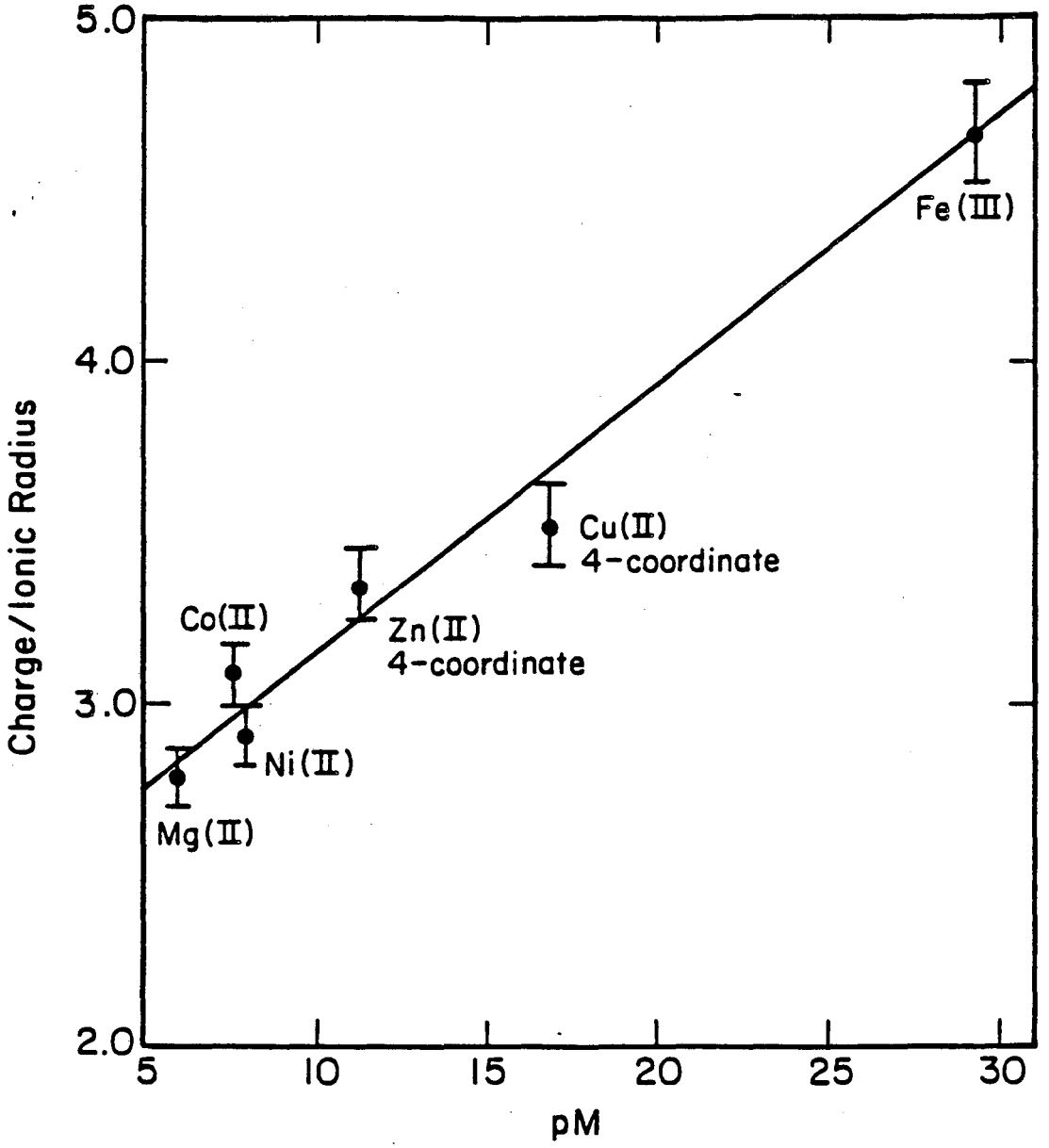

CHAPTER III

Complexation of Ga(III) and Fe(III) by Terminally N-Substituted Catechoylamide Ligands

In Chapter I we discussed the rationale and design concepts for the preparation of a series of tricatecholate chelating agents for Fe(III),[1,2] Ga(III), and In(III).[3,4] Functionalization of the amide nitrogen of catechoylamide ligands with various alkyl and aromatic substituents affects the *in vivo* distribution of the ligand.[3,5] Indeed, the derivative having an n-octyl chain attached to the amide nitrogen crosses the blood-brain barrier,[6] an uncommon property for most chemical substances.[7] Increasing the lipophilicity of a ligand by such modifications can also affect the stabilities of metal complexes formed as well as the kinetic ability of the ligand to remove the target metal from the transport protein transferrin. Correlation of structural modifications of ligands with complex stabilities and kinetic lability is helpful in determining future paths to be followed in ligand design and synthesis.

The use of radiopharmaceuticals incorporating ^{67}Ga and ^{111}In relies on the chemical similarities of these trivalent ions with Fe(III) and the radiological properties of the particular isotopes.

Although In(III) is somewhat larger, Ga(III) and Fe(III) are nearly identical in size,[8] and it is significant to note that both Ga(III) and In(III) are transported by the iron transport protein transferrin.[9,10] Radiopharmaceuticals incorporating ^{67}Ga and ^{111}In are used for imaging abscesses and tumors, a process which relies on the unusually rapid uptake of iron by such tissues and a correspondingly greater concentration of radionuclide.[9] Administration of chelating agents shortly after administration of the radionuclide as a citrate complex is done to renove excess radionuclide from the body, thereby enhancing the image by lowering the background and decreasing the radiation exposure to the patient.[3]

In one respect the requirements of chelate pharmaceuticals for ferric ion are very different from those for gallium or indium: while Fe(III) is present in gram amounts, the radiopharmaceuticals contain nanogram amounts of gallium and indium.[9] Thus for radiopharmaceuticals, only small amounts of chelating agent are necessary if it forms a very stable complex and if competition from other metal ions is not significant.

This chapter summarizes the thermodynamic and kinetic evaluation of Ga(III) and Fe(III) complexes of four terminally N-substituted catechoylamide ligands: N,N"-diisopropyl-N,N',N"-tris(5-sulfo-2,3-dihydroxybenzoyl)-1,5,10-triazadecane [DiP-3,4-LICAMS]; N,N"-sulfobenzyl-N,N',N"-tris(5-sulfo-2,3-dihydroxybenzoyl)-1,5,10-triazadecane [Dibenzyl-3,4-LICAMS]; N,N"-dicyclohexyl-N,N',N"-tris(5-sulfo-2,3-dihydroxybenzoyl)-

1,5,10-triazadecane [Dicyclohexyl-3,4-LICAMS]; 1,3,5-N,N',N"-triisopropyl-N,N',N"-tris(5-sulfo-2,3-dihydroxybenzoyl) triaminomethylbenzene [TiP-MECAMS]. Structural formulas are shown in Figure 3.1.

Experimental

Potentiometric Measurements. A detailed account of the apparatus used and the procedure followed for potentiometric titrations has been given in Chapter II. In short, measurements were made with a Corning 130 digital pH meter equipped with a Corning glass and a saturated calomel electrode The meter was calibrated with standard acetate and nitric acid solutions to read hydrogen ion concentration, not activity. Solutions (40 mL of about 0.1 mM ligand) were kept under argon and were maintained at 25.0 $\pm$ 0.05°C by a circulating water bath. The ionic strength was maintained at 0.1 M with KNO_3 for Fe(III) titrations or KCl for Ga(III) titrations. Carbonate-free 0.1 M KOH was prepared from Baker Dilut-It ampoules with freshly boiled, doubly distilled water. Back titrations with HNO_3 were also performed with each ligand and the resulting titration curves were compared with those obtained by titrating with base to assure that there was no hysteresis of the curves. Potentiometric data were refined using a weighted nonlinear least-squares analysis in which log β's were varied to minimize the sum of the squared differences between the observed and calculated pH at each point in the titration curve. (See Appendix for further details.)

Spectrophotometric Measurements. Spectrophotometric titrations

were recorded on a Hewlett-Packard 8450A vis/uv spectrophotometer. The visible spectra of ≈0.2 mM ferric-ligand complexes (0.1 M KNO_3) were monitored as a function of pH. After each small addition of ≈3 M HNO_3, the pH was measured, an aliquot was removed, the spectrum was recorded, and the sample was returned to the solution. Absorbance measurements for the spectrophotometric competitions with Na_2H_2EDTA were taken on a Cary 118 vis/uv spectrophotometer. For the Fe(III)-catechoylamide competitions, twelve replicates were made for each of the ligands with varying amounts of ferric ion, ligand , and Na_2H_2EDTA. The pH range studied was from 5.5 to 7.0. Equilibrium was approached from both directions; i.e., ferric EDTA plus free catechoylamide and ferric catechoylamide plus Na_2H_2EDTA. The absorbance was checked after 72 hours and after 144 hours to ensure that equilibrium had been attained. The Ga(III) catechoylamide competitions were carried out as previously described,[11] using the Fe(III)-catechoylamide complex as the spectral probe. These competitions were allowed to equilibrate for as long as four weeks to ensure that equilibrium had been reached.

Fourier Transform Infrared Spectra. Fourier transform infrared spectra of D_2O solutions were obtained on a single-beam Nicolet 7199 FT IR spectrometer at 1.0 cm^{-1} resolution (300 scans). A Perkin-Elmer AgCl ∿0.2 mm cell was used for all spectra. First the cell was filled with D_2O and a background spectrum was taken. Typical ligand concentrations used were about 0.1 M, and spectra of ferric complexes were done with 5 to 10% excess metal ion added as solid $FeCl_3 \cdot 6H_2O$ to assure complexation of all ligand. After these spectra were taken the

contribution due to D_2O was subtracted to yield a spectrum of the ligand or metal complex alone. The pH measurements were made using a Beckman Instruments pH-102 Metrohm pH meter equipped with a Sigma combination electrode. The pH meter was standardized using Mallinckrodt pH 4.01 and 7.00 buffers. The pH values reported here for D_2O solutions were obtained by taking pH meter readings in the usual manner and correcting the readings for D_2O using the method of Perrin.[12] The pH was decreased incrementally by addition of approximately 3 M DCl to each solution with adjustments in pH by use of NaOD.

Metal Stock Solutions. The ∿0.1 M $Fe(NO_3)_3$ solution was prepared by dissolving $Fe(NO_3)_3 \cdot 9H_2O$ (Mallinckrodt) in ∿0.1 M HNO_3. The solution was standardized with Na_2H_2EDTA and Eriochrome Black T indicator by back titration with standardized Mn(II) as described elsewhere.[13]

The ∿0.1 M $GaCl_3$ solution was prepared by dissolving gallium metal in ∿0.2 M HCl. The solution was then standardized by direct titration with Na_2H_2EDTA using Pyrocatechol Violet as the indicator.[13]

The hydrogen ion concentration of both solutions was determined by potentiometric titration of the EDTA complex.

Preparation of Diferric Transferrin. Apotransferrin (Tf) obtained from Sigma (98%) was loaded with ferric ion using a procedure similar to that outlined by Bates and Schlabach.[14] The modified procedure is given here. Apotransferrin (250 mg-MW 76600) was dissolved in 0.1 M $NaClO_4$/0.05 M TRIS buffer at pH 7.4 and diluted to 5.0 mL. To this solution approximately two equivalents of sodium

bicarbonate were added, since bicarbonate/carbonate is a necessary synergistic anion for ferric ion binding to Tf. A solution of ~20 mM of $Fe(NTA)_2$ freshly prepared at pH 7.4 was added (0.692 mL) and the solution was allowed to stir for 30 minutes. The remaining operations were performed in the cold room at 5°C. The diferric transferrin (Fe_2Tf) was run down a G-25 Sephadex column equilibrated and eluted with 0.1 M $NaClO_4$ and 0.05 M TRIS at pH 7.4 to remove excess NTA. The Fe_2Tf gives a salmon-colored band the collection of which took about 1-1/2 hours. The protein solution was concentrated using an Amicon membrane filter which had first been washed with 0.1 M TRIS (pH 7.4). To the concentrated protein solution (<1 mL) was added 6-7 mL of 0.1 M TRIS (pH 7.4) and the resultant solution filtered through the membrane to dilute the $NaClO_4$. This filtration was done five times. The visible spectrum of the resulting Fe_2Tf indicated Abs_{280}/Abs_{466}= 18, the ratio required for >95% saturation of Tf by Fe(III).[15] In addition, Abs_{428}/Abs_{466}= 0.88, an indication of protein robustness (should be 0.85). The protein solution was also passed through a 0.45 μ millipore filter to remove particulates before any kinetic measurements were performed. The stock Fe_2Tf was stored at 5°C.

Kinetic Measurements. The kinetics of iron removal from Fe_2Tf at 25°C by the N-substituted ligands were done in the following manner. To 2.0 mL of 0.1 M TRIS buffer (pH 7.4) in the sample cuvette (reference is TRIS buffer) was added 80 μL of the Fe_2Tf stock solution ($[Fe_2Tf]$ = 0.02 mM). To maintain psuedo first order conditions and to compare rate constants to other values previously obtained,[15,16] buffered (pH 7.4) solutions of the ligands were added

so that the initial ligand concentration was 0.2 mM. The kinetics were followed by monitoring the increase in absorbance at 484 nm with a Cary 118 and a HP8450A vis/uv spectrophotometer over a period of two to three half-lives.

Syntheses. All syntheses were performed by Dr. Fred Weitl, formerly of Lawrence Berkeley Laboratory. The syntheses of the unsulfonated derivatives are reported in detail elsewhere,[17,18] as is the sulfonation procedure for the catechoylamide ligands.[2] Briefly, the unsulfonated derivative is added to 30% fuming H_2SO_4 in ice and stirred overnight. The solution is brought to neutral pH by addition of NaOH. Excess Na_2SO_4 is removed by extractions with $MeOH/H_2O$ mixtures. This yields the hygroscopic white trisodium salt of the ligand. Elemental analyses were performed by Analytical Services, Chemistry Department, University of California, Berkeley. Titration of the free ligand samples gave molecular weights which agreed to within 1% to those obtained by elemental analysis. The ^1H NMR spectra in d_6-DMSO were recorded on a 90 MHz JEOL FX90Q Fourier Transform NMR at Lawrence Berkeley Laboratory or on a 250 MHz Fourier Transform NMR in the Chemistry Department at the University of California, Berkeley.

DiP-3,4-LICAMS

Anal. Calcd for $C_{34}H_{40}N_3O_{18}S_3Na_3 \cdot 4H_2O$: C, 40.20; H, 4.73,; N, 4.14. Found: C, 40.13; H, 4.62; N, 4.04.

^{1}H NMR at 74°C: δ =1.1 ppm (doublet, 12H, -CH($\underline{CH_3}$)$_2$); δ =1.3 -1.9 ppm (b, 6H, -NCH$_2$$\underline{CH_2}$-); δ =3.5-2.9 ppm (b, 10H, -NC$\underline{H}$(CH$_3$)$_2$ and -NC$\underline{H_2}$-); δ =6.82 ppm (quartet, 3H, 4-$\underline{H}$ on sulfonated catechol); δ =7.10 ppm (triplet, 3H, 6-$\underline{H}$ on sulfonated catechol).

dicyclohexyl-3,4-LICAMS

Anal. Calcd. for $C_{40}H_{48}N_3O_{18}S_3Na_3 \cdot 6H_2O$: C, 42.44; H, 5.30; N, 3.71. Found: C, 42.37; H, 4.94; N, 3.69.

^{1}H NMR at 22°C: δ =2.0-0.75 ppm (b, -NCH$_2$$\underline{CH_2}$-); δ =4.5-2.6 ppm (b, -NC$\underline{H_2}$-); δ =6.75 and 7.10 (doublet of doublets, Ar$\underline{H}$).

dibenzyl-3,4-LICAMS

Anal. Calcd. for $C_{42}H_{38}N_3O_{24}S_5Na_5 \cdot Na_2SO_4 \cdot 2CH_3OH \cdot 3H_2O$: C, 35.18; H, 3.46; N, 2.80. Found: C, 35.17; H, 3.46; N, 2.86.

^{1}H NMR at 22°C: δ =1.9-1.2 ppm 9b, -NCH$_2$$\underline{CH_2}$-); δ =3.4 (b, $\underline{CH_3}$OH); δ =3.5-2.8 ppm (b, -NC$\underline{H_2}$-); δ =4.7 ppm (b, SO_3^--C$_6$H$_4$-$\underline{CH_2}$-N-); δ =6.8 ppm (b, 4H, -$\underline{H}$ on sulfobenzyl); δ =7.5-7.1 ppm (t, 6H, 4,6-$\underline{H}$ on 5-sulfocatechol); δ =7.55 ppm (b, 4H, -$\underline{H}$ on sulfobenzyl).

TiP-MECAMS

Anal. Calcd. for $C_{39}H_{42}N_3O_{18}S_3Na_3 \cdot Na_2SO_4 \cdot 2CH_3OH \cdot 3H_2O$: C, 38.89; H, 4.43; N, 3.32. Found: C, 38.74; H, 4.18; N, 3.32.

^{1}H NMR at 22°C: δ =1.1 ppm (b, -CH($\underline{CH_3}$)$_2$); δ =3.4 ppm (b, $\underline{CH_3}$OH); δ =4.7 ppm (b, Ar-$\underline{CH_2}$-); δ =6.90 ppm (s, 3H, Ar$\underline{H}$); δ =7.4-7.15 (t, 6H, 4,6-$\underline{H}$ on sulfocatechol).

Results and Discussion

Ligand Protonation Constants. The ligand protonation constants obtained by potentiometric titration for the N-substituted ligands are shown in Table I. Those constants represented as log K^{H}_{4-6} [19] are the protonation constants of the phenolic oxygen anion ortho to the carbonyl group. The protons of the phenolic oxygen anion meta to the carbonyl dissociate at higher pH in a range inaccessible by potentiometric methods.

Comparison of the protonation constants of the N-substituted-3,4-LICAMS derivatives to the protonation constants of 3,4-LICAMS[20] indicates that the N-substituted derivatives are considerably less acidic, due to the inductive effect of the alkyl group, through the carbonyl, to the aromatic ring. A similar phenomenon can be observed by comparing the pKa's of salicylaldehyde (pKa = 8.22) to 2-acetylphenol (pKa = 9.94),[21] in which case the alkyl group is directly attached to the carbonyl and the effect is greater. Comparison of the protonation constants of MECAMS,[20] trimethyl- MECAMS [(Me)$_3$MECAMS] [16](which has methyl groups on the amide nitrogen), and TiP-MECAMS (Table I) shows a gradual decrease in acidity as the alkyl chain gets larger. This could be due to a change in local dielectric

in the presence of larger alkyl chains.

The protonation constants of the phenolic oxygens meta to the phenol have been estimated to be log K^{H}_{1-3} =11.7 for the 3,4-LICAMS N-substituted derivatives and log K^{H}_{1-3}=11.8 for TiP-MECAMS.[16] These estimates are based on the estimated high protonation constants for 3,4-LICAMS and MECAMS, (log K^{H}_{1-3}=11.5),[20,22] which have been shown to be good estimates from preliminary data obtained by monitoring changes in the uv spectrum of the ligands at high pH, [23]and with the knowledge that the N-substituted derivatives are less acidic than their unsubstituted counterparts.[16]

Fe(III) Thermodynamics. The ferric complexes of the N-substituted catechoylamides have been investigated by both spectrophotometric and potentiometric methods.

The potentiometric titration curves of the Fe(III) complexes are shown in Figure 3.2. All ligands form triscatechol complexes with concomitant release of six protons (a is moles base added per mole metal ion). In addition, the titration curves of the ferric complexes of dicyclohexyl-3,4-LICAMS and DiP-3,4-LICAMS show distinct inflections at a = 4. The metal complex protonation constants, K_{MH_nL},[19] refined by a nonlinear least-squares program are found in Table IIA.

The spectra of the tris(catecholato) Fe(III) complexes show λ_{max} at 485 nm, characteristic of the ligand to metal charge transfer band of other Fe(III) tris(catecholates),[20,24] with extinction coefficients (in units of $M^{-1}cm^{-1}$) of 4900 for DiP-3,4-LICAMS and dicyclohexyl-3,4-LICAMS and 4350 for

dibenzyl-3,4-LICAMS and TiP-MECAMS. These extinction coefficients are considerably less than those observed for 3,4-LICAMS and MECAMS ($\varepsilon \sim 6200$)[20] and just slightly less than that observed for $(Me)_3$MECAMS ($\varepsilon \sim 5200$).[16]

By monitoring the absorbance of the Fe(III) complexes as a function of pH the tris(catecholato) to bis(catecholato) equilibrium can be studied. Previous studies have shown that the ferric complexes of 3,4-LICAMS and MECAMS protonate via two sequential one-proton steps rather than by a single two-proton step with concomitant dissociation of a catecholate arm.[20] We have proposed that the one-proton stoichiometry of the complex corresponds to protonation at the phenolic oxygen meta to the carbonyl (the least acidic phenol) followed by a shift in coordination of the Fe(III) ion to the carbonyl oxygen adjacent to the catecholate ring. The experiment performed to confirm this hypothesis was to follow the vibrational stretching frequency of the amide carbonyl as a function of pH to determine whether or not the carbonyl oxygen is bound to the metal ion.[25] The results of these experiments for Fe(III)MECAMS and Fe(III)(3,4-LICAMS) support the proposed "salicylate-type" binding mode. The absorbance shift monitored as a function of pH for ferric complexes of dibenzyl-3,4-LICAMS, dicyclohexyl-3,4-LICAMS, and TiP-MECAMS all demonstrate sequential one-proton stoichiometry. The spectra taken at varying pH values of these complexes contain an isosbestic point at 532, 540, and 542 nm, respectively. The spectra of ferric TiP-MECAMS and dicyclohexyl- 3,4-LICAMS retained this isosbestic point over a range in pH which can be correlated to the potentiometric titration

curves-indicating that one equivalent of acid has been added and that only two species are in solution. A graphical method developed by Schwarzenbach[26] may be used to determine the proton stoichiometry. For A_o, the initial absorbance of the tris(catecholato) complex at high pH; n, the proton stoichiometry of the reaction; and A_{obs}, the observed absorbance at any particular wavelength and pH, a graph of A_{obs} versus $(A_o - A_{obs})/[H^+]^n$ will be linear if n corresponds to the reaction stoichiometry. The slope of this line is $1/K_{MH_nL}$, where K_{MH_nL} is defined as $[MH_nL]/([ML][H^+]^n)$. Thus, the full equation is

$$A_{obs} = \varepsilon_{MH_nL} C_T + \frac{A_o - A_{obs}}{[H^+]} \cdot \frac{1}{K_{MH_nL}} \qquad (1)$$

where C_T is the total concentration of absorbing species in solution and ε_{MH_nL} is the extinction coefficient of the protonated species. These plots were linear for n = 1 for both ferric TiP-MECAMS and ferric dicyclohexyl- 3,4-LICAMS, indicating bis(catecholato) mono(salicylate) coordination about the Fe(III). The resultant values of the protonation constants, K_{MHL} and K_{MH_2L}, agree well with those obtained from potentiometric measurements as shown in Table IIA.

Although the titration spectra of the ferric complexes of dibenzyl-3,4-LICAMS displayed an isosbestic point at 532 nm, this point was not retained through a one equivalent addition of protons. In the region from a = 6 to 4 two equilibria overlap:

$$Fe(\text{dibenzyl-3,4-LICAMS})^{6-} + H^+ \underset{K_{MHL}}{=} Fe(H\text{dibenzyl-3,4-LICAMS})^{5-} \qquad (2)$$

$$Fe(H\text{dibenzyl-3,4-LICAMS})^{5-} + H^+ \underset{K_{MH_2L}}{=} Fe(H_2\text{dibenzyl-3,4-LICAMS})^{4-} \qquad (3)$$

A nonlinear least-squares refinement was used to calculate the extinction coefficients and protonation constants in these equilibria.[20] At each pH the absorbances were recorded at 490, 520, 560, and 592 nm. The sum of the squared differences between observed absorbance and the calculated absorbance was minimized in the refinement. At any wavelength the absorbance is given by Eq. 4.

$$Abs^{\lambda} = [ML]\left(\varepsilon^{\lambda}_{ML} + K_{MHL}[H^+]\,\varepsilon^{\lambda}_{MHL} + K_{MHL}K_{MH_2L}[H^+]^2\,\varepsilon^{\lambda}_{MH_2L}\right) \quad (4)$$

The values of [ML] can be calculated from mass balance by using an initial set of equilibrium constants

$$[Fe]_{total} = [ML](1 + K_{MHL}[H^+] + K_{MHL}K_{MH_2L}[H^+]^2) \quad (5)$$

The value of $\varepsilon^{\lambda_{1-4}}_{ML}$ is obtained directly from the spectrum at high pH. Thus there is a total of 10 parameters: $\varepsilon^{\lambda_{1-4}}_{MHL}$, $\varepsilon^{\lambda_{1-4}}_{MH_2L}$, K_{MHL}, K_{MH_2L}. These were refined simultaneously using 52 data points at 13 pH values between pH 8.5 and 4.7. Although highly correlated, the refinement proceeded to give the values for K_{MHL} and K_{MH_2L} as shown in Table IIA.

The protonation equilibria of the ferric complex of DiP-3,4-LICAMS differs from the other N-substituted ligands. Figure 3.3 shows the visible spectra from a = 6.0 to 4.1. The isosbestic point at 551 nm indicates that probably only two species are in solution over this pH range. This would imply that the protonation behavior of Fe(III)(DiP-3,4-LICAMS)$^{6-}$ differs from all other synthetic

catechoylamides that have carbonyl groups adjacent to the catechol ring and that it dissociates via one two-proton step. Indeed, the Schwarzenbach plot over this pH range is linear for n =2 (Figure 3.4). It is not clear why the ferric complex of DiP-3,4-LICAMS should protonate in this manner. The CPK space-filling model indicates that the the organic moieties on the amide nitrogen are directed away from the coordination sphere of Fe(III). However, the organic moiety could hinder the rotation about the amide bond, a rotation that is necessary if a Fe(III) mono(salicylate) bis(catecholate) complex is to form. Why this hindrance of rotation should be greater with DiP-3,4-LICAMS than with dicyclohexyl-3,4-LICAMS (both having tertiary carbons attached to the amide nitrogen) is not understood.

The Fourier Transform IR spectra of DiP-3,4-LICAMS in D_2O is quite different than the spectra of enterobactin, MECAMS, and 3,4-LICAMS.[25] Most notably, the amide I band, ν(C=O), that appears in the free ligand spectra of the latter ligands at low pH (1640 - 1630 cm^{-1}) is present for only secondary amides,[27,28] DiP-3,4-LICAMS is a tertiary amide with a broad band present at 1591 cm^{-1}. This broad band is present in both D_2O and KBr pellet and probably is actually two bands which are not resolvable, the ν(C=O) and ν(C=C) in the aromatic ring. It was the amide I band and its shift upon metal complexation at various pH values that allowed previous workers to evaluate the metal binding, i.e., catecholate binding, salicylate binding, or the presence of a free catecholate arm upon protonation of the complex.[25] In the case of ferric DiP-3,4-LICAMS, the amide band at 1591 cm^{-1} of the free ligand at pH 1 does shift to 1570 cm^{-1} with a

shoulder at 1548 cm^{-1} upon complexation by Fe(III) at pH 9.6. Protonation of the complex shifts the band to higher frequencies, but no new features appear, so this may not be a good diagnostic to follow for tertiary amides. However, the region from 1300 to 1000 wavenumbers contains the CO stretching and OH deformation modes.[28] Although there is much debate in the literature about the assignment of some of these bands, they appear to be affected by metal complexation in this case. Figure 3.4 shows the FT IR spectra of ferric complexes of DiP-3,4-LICAMS at various pH values as well as the spectrum of free DiP-3,4-LICAMS at pH 1. The free ligand spectrum (bottom) has sharp bands at 1290 and 1107 cm^{-1}. The ferric DiP-3,4-LICAMS complex at pH 9.6 (top) has no band at 1290 cm^{-1} and a band at 1095 cm^{-1}. As the pH is lowered, a band at 1104 appears at pH 2.9 and the band at 1095 disappears. At pH 1, the spectrum of the ferric complex now has a band at 1290 and 1106 cm^{-1} which is very similar to the free ligand. As mentioned before, the Fe(III) tris(catecholato) complex of DiP-3,4-LICAMS protonates via one two-proton step in which case two possibilities are most likely: either a simultaneous protonation of two phenolic oxygens meta to the carbonyl and a resultant bis(salicylate) mono(catecholato) complex is formed, or a protonation of one catecholate arm occurs and a Fe(III) bis(catecholato) complex is formed. The latter complex has an uncoordinated, protonated catechol arm present which should result in part of the spectrum resembling the free ligand spectrum.[25] In fact, this similarity to the free ligand spectrum is not seen until pH 2.9, or after the addition of four protons. This is by no means conclusive

evidence that from a = 4 to 6 the complex which predominates is a Fe(III) bis(salicylate) mono(catecholato) complex, but in light of further evidence it seems to be the best choice.

The overall formation constants of the Fe(III) complexes of tricatecholate ligands cannot be determined directly because the iron binding is so strong that the complexes are not appreciably dissociated into free ligand and free iron above pH 2. Therefore, proton-dependent stability constants have been determined spectrophotometrically by competition with EDTA.[20] Because the three largest ligand protonation constants are unknown, it is not possible to calculate standard formation constants, i.e., those written in terms of the fully deprotonated form of the ligand. Instead, the equilibria are expressed in terms of the H_3L species.

$$Fe^{3+} + H_3L \overset{K^*}{=} FeL + 3H^+ \qquad (6)$$

$$K^* = \frac{[FeL][H^+]^3}{[Fe^{3+}][H_3L]} \qquad (7)$$

Values of K* can be obtained from a competition constant, K_{comp}, using the stability constant for FeEDTA (log β_{110}^{FeEDTA}=25.0)[21]

$$K_{comp} = \frac{[FeL][H^+][EDTA]}{[FeEDTA][H_3L]} = \frac{K^*}{\beta_{110}^{FeEDTA}} \qquad (8)$$

The concentrations of all the species in Eq. 8 can be calculated using the ligand protonation constants of EDTA and the tricatecholate, the metal chelate protonation constants of FeEDTA and Fe tris(catecholato), the pH, the absorbance at 484 nm (where FeEDTA does not absorb significantly), and mass balance equations. Over the pH range studied the pertinent equations are

$$Abs^{484} = [FeL](\varepsilon_{FeL} + K_{FeHL}[H^+] \varepsilon_{FeHL} + K_{FeHL}K_{FeH_2L}[H^+]^2 \varepsilon_{FeH_2L}) \quad (9)$$

$$[Fe]_{total} = [FeL] + [FeHL] + [FeH_2L] + [FeEDTA] + [FeOHEDTA] \quad (10)$$

$$[L]_{total} = [H_3L](1 + K_4^H[H^+] + K_4^HK_5^H[H^+]^2 + K_4^HK_5^HK_6^H[H^+]^3) + [FeL] + [FeHL] + [FeH_2L] \quad (11)$$

$$[EDTA]_{total} = [EDTA](1 + K_1^H[H^+] + K_1^HK_2^H[H^+]^2) + [FeEDTA] + [FeOHEDTA] \quad (12)$$

The log K* values and the log β_{110} estimates for the ferric complexes of the N-substituted ligands are shown in Table III. The $\log \beta_{110}$ constants are approximate values based on the estimations of the high protonation constants of the free ligand (vide supra).

The formation constants of the ferric complexes of the N-substituted tricatechoylamides appear to be of comparable stability to the unsubstituted derivatives.[20] However, at physiological pH hydrogen ion is in sufficiently high concentration that it competes with Fe(III) for the oxygen anion of the tricatecholate, such that the complexing form of the ligand represented in β_{110}^{FeL}, the fully deprotonated form, is virtually nonexistent at pH 7. To facilitate comparison under biologically reasonable conditions, a pM scale has been introduced (see Chapter II). The pM values for a number of synthetic tricatechoylamide ligands as well as for several other

ligands are listed in Table IV. From the pM values it is apparent that the less acidic N-substituted ligands are not as effective in sequestering Fe(III) as are MECAMS or 3,4-LICAMS.[20] In particular, dibenzyl-3,4-LICAMS which has the highest value for log K* actually has a pM comparable to 3,4-LICAMS because of its less acidic protons. However, all the lipophilic derivatives do have pM values that are higher than the pM value for the iron-transport protein transferrin.[29] This is important since the most likely mechanism for successful iron removal is to administer chelating agents which will remove the iron from transferrin and facilitate iron excretion from the body, then allowing the apotransferrin to mobilize the less accessible iron stores.

Ga(III) Thermodynamics. Potentiometric titrations and spectrophotometric competitions with Na_2EDTA were performed to assess the stabilities of the complexes of Ga(III) with the N-substituted catechoylamides.

Figure 3.6 shows the potentiometric titration curves of the Ga(III) complexes. All the ligands form a tris(catecholato) complex with Ga(III) with concomitant release of six protons. Refinement of the buffer regions using a weighted nonlinear least-squares analysis (see Appendix) yielded the complex protonation constants found in Table IIB. The complex protonation constants for Ga(III) with DiP-3,4-LICAMS and dicyclohexyl-3,4-LICAMS only refined using a model assuming one two-proton step equilibrium, i.e., no Ga(III) mono (salicylate) bis(catecholato) complex is formed. This was observed previously in the analysis of the Ga(III) 3,4-LICAMS

equilibrium.[11] Refinement of the data assuming a model with two sequential one-proton steps yielded two identical constants (e.g., for Ga-DiP-3,4-LICAMS log K_{MH_2L} =12.1 for one two-proton step; log K_{MHL} = log K_{MH_2L} =6.05 for two one-proton steps, implying two simultaneous protonations). The refinements indicate that the complexes with dibenzyl-3,4-LICAMS and TiP-MECAMS do protonate via one-proton steps. As suggested previously, this protonation behavior may be due to the presence of a tertiary carbon which is attached to the amide nitrogen in dicyclohexyl-3,4-LICAMS and DiP-3,4-LICAMS, hindering the rotation about the amide bond and thus not allowing the formation of a mono(salicylate) complex. However, this is contrary to what is observed with Fe(III). The presence of the alkyl group may also contribute to the double bond character of the amide bond, thus hindering rotation due to electronic effects.

It is noteworthy that a study of the pH dependence of the carbonyl stretching frequency of the GaMECAMS complex indicated no dissociation of a catechol arm until pH 3.5.[11] The refinement of the potentiometric titration of this complex was inconclusive as to the stoichiometry of the first protonations since it could be refined as both a one two-proton step or as two one-proton steps. Thus the stoichiometry of protonation of these complexes as well as the coordination of the metal ion in these complexes is not well understood, and perhaps study of the ^{13}C NMR of the Ga complexes would do much to elucidate the extent of involvement of the carbonyl oxygen.

The spectrophotometric competitions with EDTA were performed using the absorbance of the Fe(catechoylamide) at 484 nm as a spectral

probe. In these experiments exchange of GaEDTA with Fe(catechoylamide) [or FeEDTA with Ga(catechoylamide)] was monitored.

$$GaEDTA + FeL = GaL + FeEDTA \quad (13)$$

$$K_{comp} = \frac{[GaL][FeEDTA]}{[FeL][GaEDTA]} \quad (14)$$

Knowledge of the formation constants of GaEDTA, FeEDTA, and Fe(catechoylamide), along with mass balance, absorbance and pH measurements allows calculation of a formation constant for Ga(catechoylamide).

$$K_{comp} = \frac{\frac{[GaL]}{[Ga][L]} \cdot \frac{[FeEDTA]}{[Fe][EDTA]}}{\frac{[GaEDTA]}{[Ga][EDTA]} \cdot \frac{[FeL]}{[Fe][L]}} = \frac{(\beta_{110})_{GaL} (\beta_{110})_{FeEDTA}}{(\beta_{110})_{GaEDTA} (\beta_{110})_{FeL}} \quad (15)$$

$$(\beta_{110})_{GaL} = \frac{K_{comp} (\beta_{110})_{GaEDTA} (\beta_{110})_{FeL}}{(\beta_{110})_{FeEDTA}} \quad (16)$$

The details of this calculation have been described previously.[11] The formation constants of the Ga(III) complexes are shown in Table III. Earlier published constants of Ga(III) DiP-3,4-LICAMS and TiP-MECAMS are thought to be in error due to inaccurate estimation of

the protonation constants of the ligands and due to the neglect of the protonation of the Ga tris(catecholato) complex.[3] Unlike the Fe(III) complexes, the Ga(III) formation constants of the N-substituted ligands are all significantly lower than the formation constants of Ga(III) with MECAMS and 3,4-LICAMS.[11]

Table IV contains the pM values for the Ga(III) complexes calculated from the formation constants. These values indicate a significant decrease in affinity for Ga(III) at physiological pH for the lipophilic derivatives compared to 3,4-LICAMS and MECAMS. In fact, the relative pM values indicate that TiP-MECAMS and dicyclohexyl-3,4-LICAMS may not be capable of removing Ga(III) from transferrin.[10] Biological studies of TiP-MECAMS and DiP-3,4-LICAMS with Ga(III) and In(III) indicate that TiP-MECAMS was less effective in removing excess ^{67}Ga from the blood than was DiP-3,4-LICAMS.[3] This difference may well be due to the limited ability of TiP-MECAMS to remove Ga(III) from transferrin. In vivo testing of dibenzyl-3,4-LICAMS with ^{67}Ga is currently in progress.

Transferrin Kinetics. The N-alkylated catechoylamides must also rapidly remove Fe(III) or Ga(III) from the transport protein transferrin to be effective in vivo. Since the protein-catecholate solutions become visibly turbid after about four half-lives, standard methods to obtain A_∞ were aborted and the results were analyzed by the Guggenheim method [plot $\ln(A_{t+\Delta} - A_t)$ vs. time with slope as k_{obs}][30] or by the method of Kezdy, Jaz, and Bruylants [plot A_t vs. $A_{t+\Delta}$ with $k_{obs} = \ln(\text{slope})/\Delta$],[31] independently developed also by Swinbourne.[32] The Δ chosen for these calculations was generally about

one half-life. In all cases these two methods gave nearly identical results with good convergence coefficients as reported in Table V. The spectral changes observed during a typical kinetic run are demonstrated in Figure 3.7 with an increase in absorbance occuring at 480 - 490 nm due to the formation of the Fe(III) tris(catecholato) complex.

The results (Table V) indicate some interesting trends. It is evident that the N-alkylated derivatives are slower at removing Fe(III) from Fe_2Tf than their unsubstituted counterparts. In fact, increase in steric bulk in going from MECAM to $(Me)_3$MECAMS to TiP-MECAMS shows a corresponding decrease in k_{obs}. Tufano has reported[33] the rate constants of the removal of Fe(III) from ferrioxamine B using the same N-alkylated ligands with the observation that the N-alkylated derivatives demonstrate slower kinetics than the unsubstituted catechoylamides, however he notes that these rates are virtually invariant with alkyl substituent. The dibenzyl-3,4-LICAMS appears to be slightly faster than DiP-3,4-LICAMS or dicyclohexyl-3,4-LICAMS at removal of Fe(III) from ferrioxamine B. In contrast, the dibenzyl-3,4-LICAMS removes iron from Fe_2Tf at slower rates than the other alkylated ligands. The important difference between ferrioxamine B and Fe_2Tf is that the former is monocationic at pH 7.4 while the latter is anionic at this pH. Recalling that the dibenzyl derivative carries an additional minus two charge because of the sulfonation of the benzyl group, its slower kinetics at removing iron from Fe_2Tf in comparison to the other N-alkylated derivatives may not be surprising due to larger charge repulsion. It may also be

hampered in removing iron due to the steric bulk of the pendant benzyl group, inhibiting access to Fe(III) in Fe_2Tf. In contrast, it is slightly faster at removing iron from ferrioxamine B.

Perhaps the most remarkable observation is that despite the substituent size and varying charge, these ligands do not show any great variation in k_{obs}.

Summary. The lipophilic analogues of enterobactin form stable complexes with ferric ion, thermodynamically capable of removing Fe(III) from the iron transport protein transferrin, and kinetically efficient. One ligand, DiP-3,4-LICAMS, forms a tris complex with Fe(III) which protonates via one two-proton step. Of all ligands studied to date, this is the only synthetic tricatechoylamide with a carbonyl adjacent to the ring which demonstrates this protonation behavior.

The Ga(III) complexes of the N-substituted ligands are not as stable as those formed with unsubstituted sulfonated tricatechoylamides. The TiP-MECAMS and dicyclohexyl-3,4-LICAMS may not be thermodynamically capable of efficiently removing Ga(III) from transferrin. However, DiP-3,4-LICAMS has been shown to be effective in in vivo sequestering of ^{67}Ga.

It appears that increasing lipophilicity of the ligand in this manner does lower the affinity of the ligand for the target metal. Some loss of stability can be sacrificed in the case of Fe(III) to test whether or not changing the tissue distribution of the ligand will make it a better chelating agent for iron overload. However, the

complexes with Ga(III) are of borderline stability if the ligands are to be capable of removing Ga(III) from transferrin.

REFERENCES

1. Weitl, F.L.; Raymond, K.N., J. Am. Chem. Soc. (1979), 101, 2728.

2. Weitl, F.L.; Harris, W.R.; Raymond, K.N., J. Med. Chem. (1979), 22, 1281.

3. Moerlein, S.M.; Welch, M.J.; Raymond, K.N.; Weitl, F.L., J. Nucl. Med. (1981), 22, 710.

4. Moerlein, S.M.; Welch, M.J., J. Nucl. Med. (1982), 23, 501.

5. Durbin, P.W.; Jeung, N.; Jones, E.S.; Weitl, F.L.; Raymond, K.N., manuscript in preparation.

6. Welch, M., personal communication.

7. Bloom, W.; Fawcett, D. "A Textbook of Histology" W.B. Saunders Co.: Philadelphia, Pa., (1975), 381.

8. Shannon, R.D., Acta Crystallogr., Sect A (1976), A32, 751.

9. Welch, M.J.; Moerlein, S.M., ACS Symp. Ser. (1980), No. 140, 121.

10. Harris, W.R.; Pecoraro, V.L., submitted to Biochemistry.

11. Pecoraro, V.L.; Wong, G.B.; Raymond, K.N., Inorg. Chem. (1982), 21, 2209.

12. Perrin, D.D.; Dempsey, B. "Buffers for pH and Metal Ion Control;" John Wiley and Sons, Inc.: New York, (1974), 81.

13. Welcher, T.J., "The Analytical Uses of Ethylenediaminetetraacetic Acid;" Van Nostrand: Princeton, N.J., (1958).

14. Bates, G.W.; Schlabach, M.R., J. Biol. Chem. (1973), 248, 3228.

15. Carrano, C.J.; Raymond, K.N., J. Am. Chem. Soc. (1979), 101, 5401.

16. Pecoraro, V.L.; Weitl, F.L.; Raymond, K.N., J. Am. Chem. Soc. (1981), 103, 5133.

17. Weitl, F.L.; Raymond, K.N., J. Org. Chem. (1981), 46, 5234.

18. Kappel, M.J.; Pecoraro, V.L.; Raymond, K.N., manuscript in preparation.

19. The stepwise formation constant K_2^H is written

$$K_2^H = [H_2L]/([H^+][HL])$$

In contrast, the overall formation constant, β_{mlh}, is written in terms of free ligand, free metal, and free hydrogen concentrations, such that for H_2L

$$\beta_{012} = \frac{[H_2L]}{[H^+]^2[L]}$$

consequently, $\beta_{012} = K_2^H \cdot K_1^H$.

20. Harris, W.R.; Raymond, K.N.; Weitl, F.L., J. Am. Chem. Soc. (1981), 103, 2667.

21. Martell, A.E.; Smith, R.M. "Critical Stability Constants;" Plenum Press: New York, (1977).

22. Avdeef, A.; Sofen, S.; Bregante, T.; Raymond, K., J. Am. Chem. Soc. (1978), 100, 5362.

23. Pecoraro, V.; Scarrow, R.; Kappel, M.; Raymond, K., manuscript in preparation.

24. Harris, W.R.; Carrano, C.J.; Raymond, K.N., J. Am. Chem. Soc. (1979), 101, 2213.

25. Pecoraro, V.L.; Harris, W.R.; Wong, G.B.; Carrano, C.J.; Raymond, K.N., J. Am. Chem. Soc., in press.

26. Schwarzenbach, G.; Schwarzenbach, K., Helv. Chim. Acta (1963), 46, 1390.

27. Nakanishi, K., "Infrared Absorption Spectroscopy;" Holden-Day Inc.: San Francisco, Ca, (1962).

28. Bellamy, L.J., "The Infrared Spectra of Complex Molecules;" Methued and Co.,Ltd.: London, (1966).

29. Aasa, R.; Malmstrom, B.G.; Saltman, P.; Vanngard, T., Biochim. Biophys. Acta (1963), 75, 203.

30. Guggenheim, E.A., Philos. Mag. (1926), 2, 538.

31. Kezdy, F.J.; Jaz, J.; Bruylants, A., Bull. Chem. Soc. Chim. Belg. (1958), 67, 687.

32. Swinbourne, E.S., Aust. J. Chem. (1958), 11, 314.

33. Tufano, T.; Ph.D. thesis, University of California, Berkeley, (1982).

Table I. Ligand Protonation Constants[a]

Ligand	log K_4^H	log K_5^H	log K_6^H	log K_{ave}^H
DiP-3,4-LICAMS	8.50(3)	7.78(1)	7.13(1)	7.8
Dibenzyl-3,4-LICAMS	8.51(1)	7.84(1)	7.03(3)	7.8
Dicyclohexyl-3,4-LICAMS	8.49(5)	7.77(1)	7.05(3)	7.8
TiP-MECAMS	8.61(2)	7.85(1)	6.60(2)	7.7
Me_3-MECAMS[b]	8.52(2)	7.57(2)	6.72(2)	7.6
MECAMS[c]	7.26	6.44	5.88	6.5
3,4-LICAMS[c]	8.28	7.07	6.11	7.2

[a] $K_n^H = \frac{[H_nL]}{[H^+][H_{n-1}L]}$.

[b] Ref. 16.

[c] Ref. 20.

Table IIA. Ferric Complex Protonation Constants[a]

Ligand	log K_{MHL}		log K_{MH_2L}		log K_{MH_3L}	
	Potentiometric	Spectral	Potentiometric	Spectral	Potentiometric	Spectral
DiP-3,4-LICAMS			12.66(4)[b]	12.9(1)[b]		
Dibenzyl-3,4-LICAMS	6.48(10)	6.27(11)[c]	4.65(8)	4.72(13)[c]	3.41(7)	-
Dicyclohexyl-3,4-LICAMS	6.68(4)	6.85(7)	6.02(2)	5.78(8)	3.62(3)	-
TiP-MECAMS	7.85(8)	7.83(7)	6.07(8)	6.06(8)	3.84(8)	3.81(7)
$(Me)_3$MECAMS[d]	-	6.80(3)	6.61(5)	-	5.80(5)	-
MECAMS[e]	5.74(2)	5.19(3)	4.10(4)	-	3.46(5)	-
3,4-LICAMS[e]	6.16(6)	5.85(2)	5.3(1)	5.32(7)	3.10(4)	3.05(4)

Table IIB. Gallium Complex Protonation Constants[a,f]

Ligand	log K_{MHL}	log K_{MH_2L}	log K_{MH_3L}
DiP-3,4-LICAMS	-	12.1(1)[b]	-
Dibenzyl-3,4-LICAMS	6.6(1)	4.8(1)	3.3(1)
Dicyclohexyl-3,4-LICAMS	-	12.0(1)[b]	-
TiP-MECAMS	7.20(2)	5.8(1)	3.1(1)
MECAMS[g]	5.7(1)	4.9(2)	-
3,4-LICAMS[g]	-	10.2(1)[b]	-

[a] $K_{MH_nL} = \dfrac{[MH_nL]}{[MH_{n-1}L][H^+]}$.

[b] One two-proton step occurs.

[c] By non-linear least-squares refinement (see text). Correlation coef ~ .9

[d] Ref. 16.

[e] Ref. 20.

[f] By refinement of potentiometric data.

[g] Ref 11.

Table III. pH Dependent Equilibrium Constants and Normal Formation Constants of a Series of Iron(III) and Gallium(III) Complexes

Ligand	log K^{*a}	log β_{110} for Fe(III)	log β_{110} for Ga(III)
DiP-3,4-LICAMS	5.36(13)	40	36
Dibenzyl-3,4-LICAMS	7.0(4)	42	36
Dicyclohexyl-3,4-LICAMS	4.85(15)	40	35
TiP-MECAMS	4.15(15)	40	35
$(Me)_3$MECAMS[c]	5.21(3)	41	-
MECAMS	6.57(10)	41[d]	38[e]
3,4-LICAMS	6.40(9)	41[d]	38[e]

[a] $K^* = \frac{[FeL][H^+]}{[H_3L][Fe]}$.

[b] Ref. 19.

[c] Ref. 16.

[d] Ref. 20.

[e] Ref. 11.

Table IV. pM[a] Values

Ligand	Fe(III) pM	Ga(III) pM
Enterobactin	35.5[b]	-
MECAMS	29.4[c]	26.3[d]
3,4-LICAMS	28.5[c]	26.0[d]
Dibenzyl-3,4-LICAMS	28.4	22.4
$(Me)_3$MECAMS	26.9[e]	-
DiP-3,4-LICAMS	26.8	22.3
Ferrioxamine B	26.6[f]	-
Dicyclohexyl-3,4-LICAMS	26.3	21.3
TiP-MECAMS	26.2	21.0
Transferrin	23.6[g]	21.3[h]
EDTA	22.2[f]	21.6[f]

---

[a]Conditions are $[L]_T = 10^{-5}$M; $[M]_T = 10^{-6}$M; pH 7.4.
[b]Ref. 24.
[c]Ref. 20.
[d]Ref. 11.
[e]Ref. 16.
[f]Calculated from stability constants in Ref. 21.
[g]Calculated from stability constants in Ref. 29.
[h]Ref. 10.

Table V. Rate Constants for Iron Removal from Diferric Transferrin to Catechoylamide Sequestering Agents

Ligand	k_{obs}[a] (X 10^3 min^{-1})	$t_{1/2}$ (hours)	Convergence coefficient[b]
Dibenzyl-3,4-LICAMS	0.86[0.80][c]	13.8	0.999[0.992]
Dicyclohexyl-3,4-LICAMS	1.6 [1.6]	7.1	0.998[0.995]
DiP-3,4-LICAMS	1.8 [1.8]	6.3	0.999[0.994]
TiP-MECAMS	1.2 [1.2]	9.6	0.999[0.995]
$(Me)_3$MECAMS[e]	1.9	6.0	-
MECAM[d]	3.4	3.4	-
3,4-LICAMS[d]	2.2	5.2	-
enterobactin[d]	2.2	5.2	-

[a] $[Fe_2Tf]$ = 0.02 mM; $[ligand]_T$ = 0.2 mM; pH 7.4 (0.1 M TRIS); 25°C.

[b] From linear least squares defined as $R = \frac{n\Sigma(x-\bar{x})(y-\bar{y})}{n^2\Sigma(x-\bar{x})^2\Sigma(y-\bar{y})^2}$.

[c] Non-bracketed numbers by method of Kezdy, Jaz, and Bruylants (Ref. 31); bracketed numbers by method of Guggenheim (Ref. 30).

[d] Ref. 15.

[e] Ref. 16.

Figure Captions for Chapter III

Figure 3.1. Structural formulas for N-substituted catechoylamides: TiP-MECAMS, dicyclohexyl-3,4-LICAMS, DiP-3,4-LICAMS, and dibenzyl-3,4-LICAMS.

Figure 3.2. Potentiometric titration curves of Fe(III) with (····) TiP-MECAMS; (—·—) dicyclohexyl-3,4-LICAMS; (— — —) DiP-3,4-LICAMS; (———) dibenzyl-3,4-LICAMS. Taken at 25.0°C in 0.1 M KNO_3. [Fe(III)] ≈1.3 mM.

Figure 3.3. Spectrophotometric titration of Fe(III) DiP-3,4-LICAMS from pH 8.85 to 5.17. [Fe(III)]≈ 0.4 mM.

Figure 3.4. Schwarzenbach plot of Fe(III) DiP-3,4-LICAMS indicating protonation via one two-proton step.

Figure 3.5. FT IR spectra of ferric complexes of DiP-3,4-LICAMS and DiP-3,4-LICAMS. In order from top to bottom, ferric complexes at pH 9.6, 4.9, 2.9, 1.0 and uncomplexed DiP-3,4-LICAMS at pH 1.

Figure 3.6. Potentiometric titration curves of Ga(III) with (· · · ·) TiP-MECAMS; (·—·—) dicyclohexyl-3,4-LICAMS; (— — —) DiP-3,4-LICAMS; (———) dibenzyl-3,4-LICAMS. Taken at 25.0°C in 0.1 M KCl. [Ga(III)] ≈1.3 mM.

Figure 3.7. Spectral changes observed for the removal of Fe(III) from

Fe_2Tf by dicyclohexyl-3,4-LICAMS over 15 hours. [ligand] ≈0.20 mM, $[Fe_2Tf]$ ≈0.02 mM.

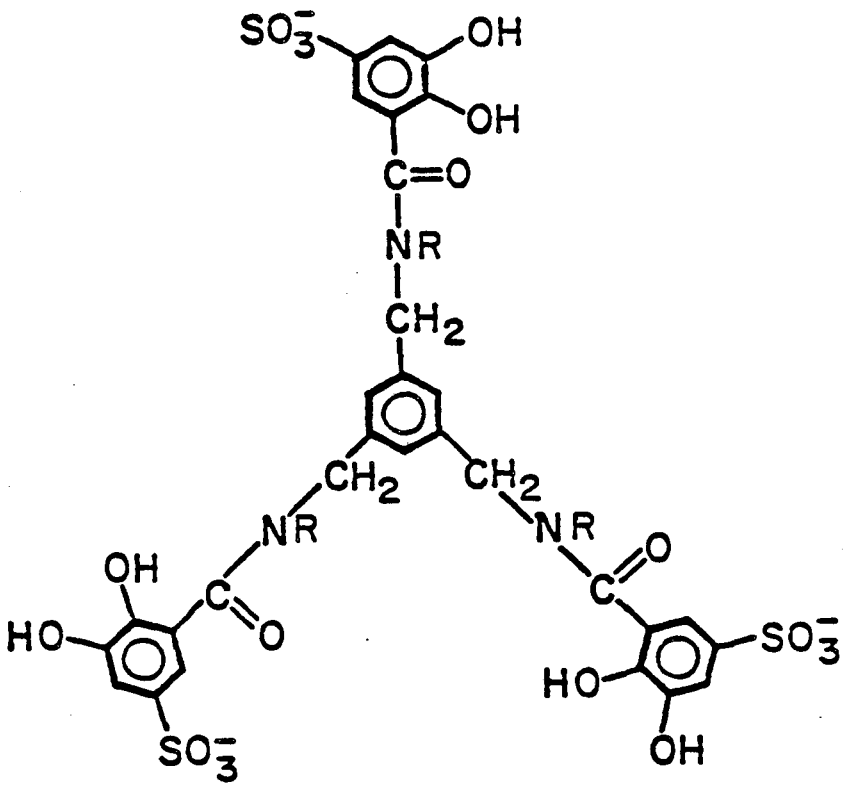

R = $CH(CH_3)_2$

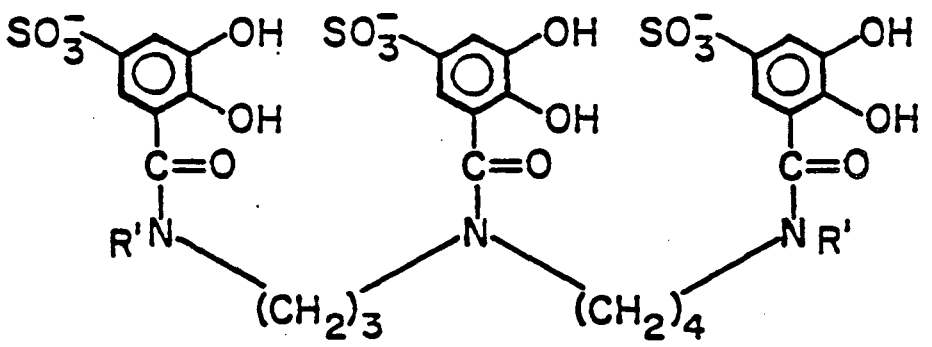

R' = 

R' = $CH(CH_3)_2$

R' = 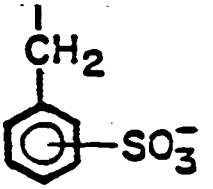

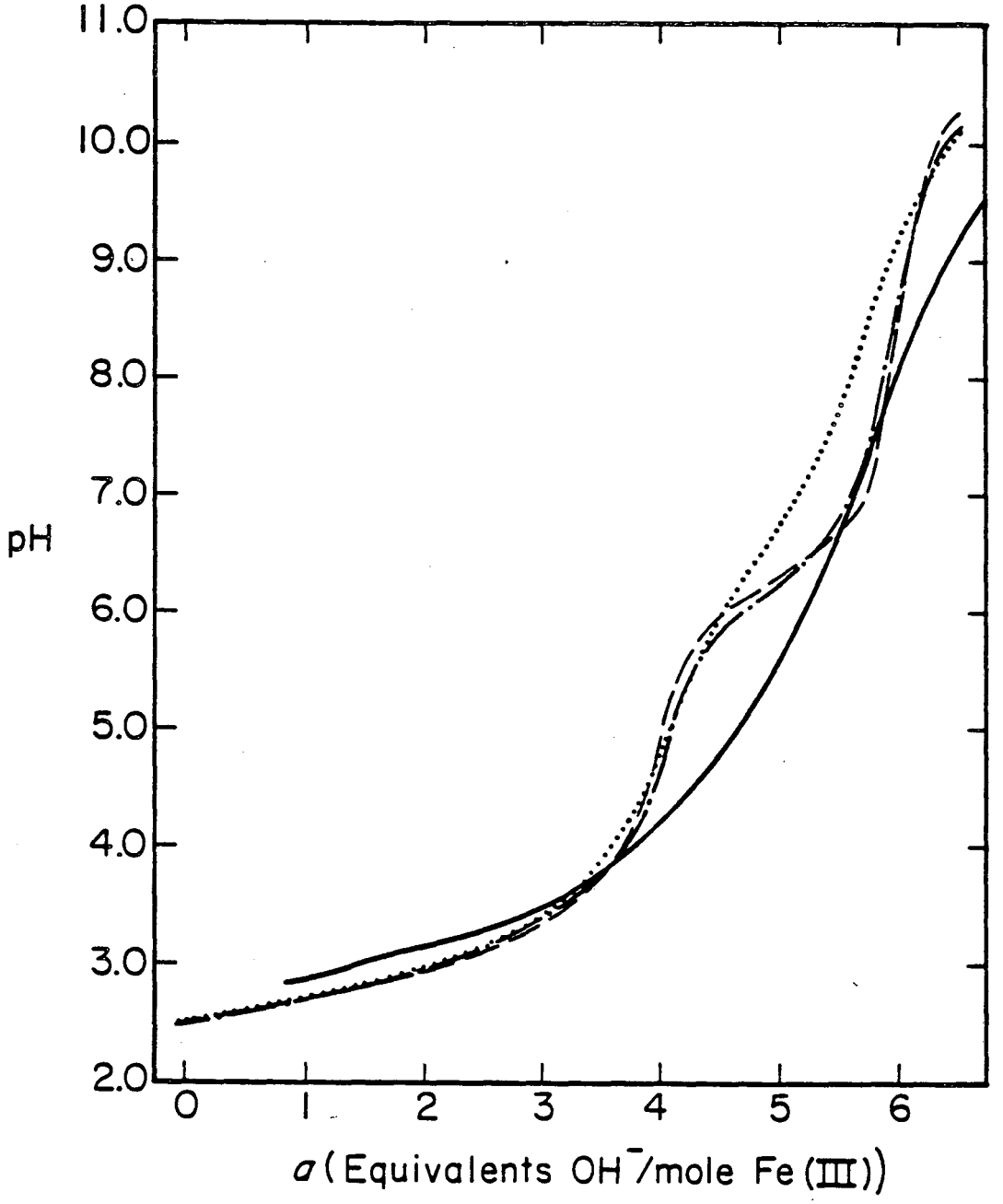
11.0
10.0
9.0
8.0
7.0
6.0
5.0
4.0
3.0
2.0
pH
0
1
2
3
4
5
6
σ (Equivalents OH⁻/mole Fe (III))

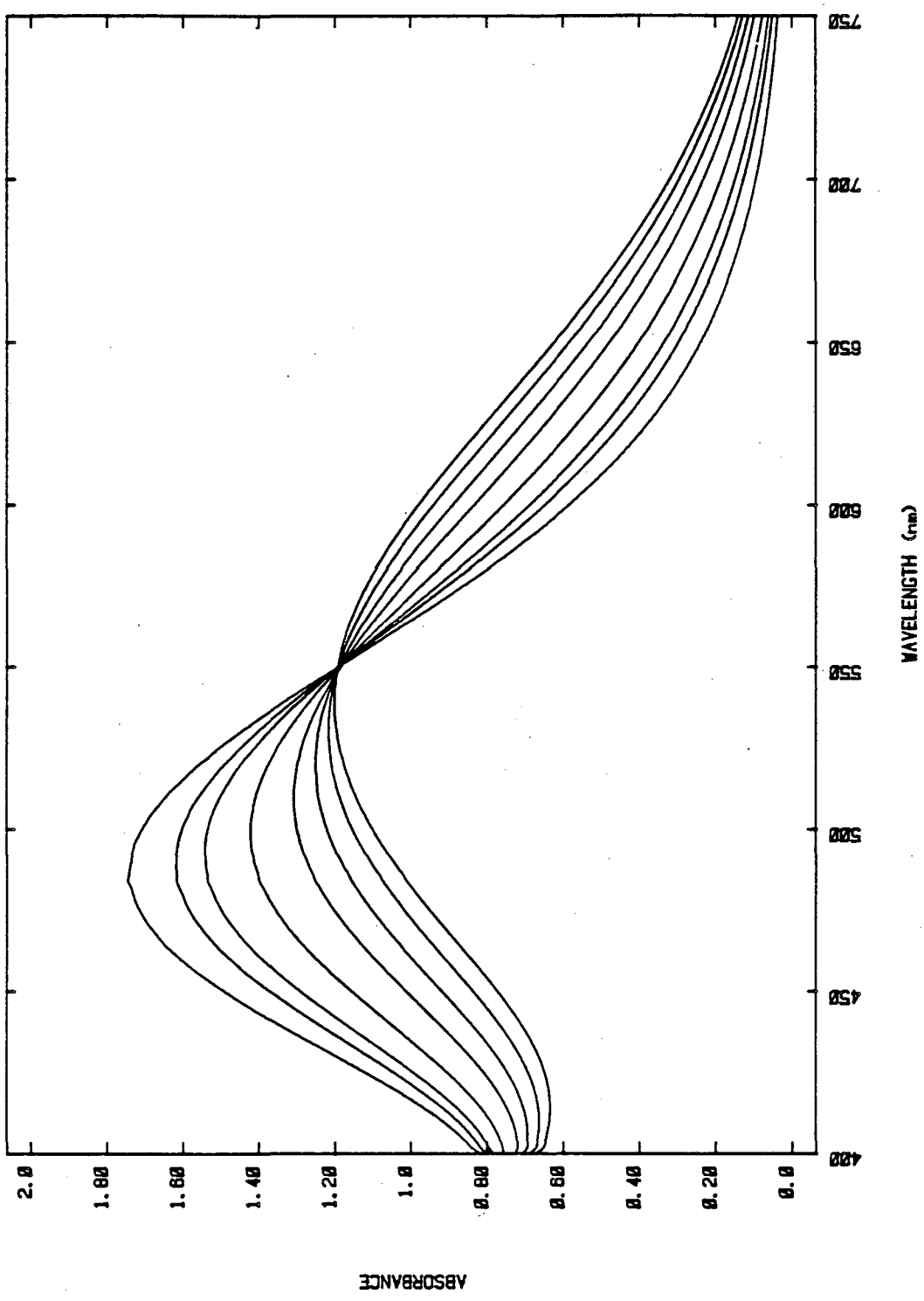
ABSORBANCE
2.0
1.80
1.60
1.40
1.20
1.0
0.80
0.60
0.40
0.20
0.0
400
450
500
550
600
650
700
750
WAVELENGTH (nm)

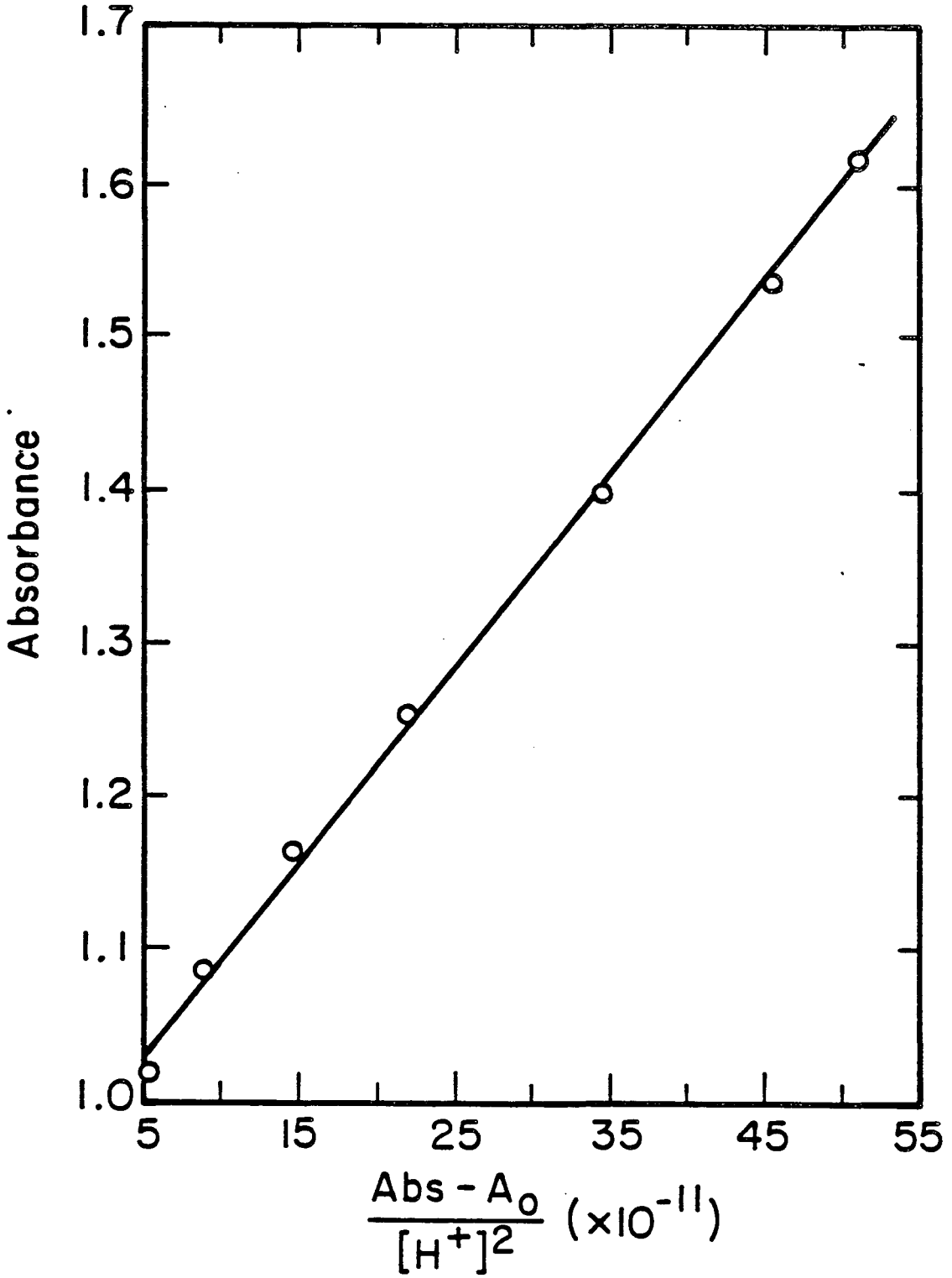
1.7
1.6
1.5
1.4
1.3
1.2
1.1
1.0
Absorbance
5
15
25
35
45
55
Abs - A0 / [H+]2 (×10-11)

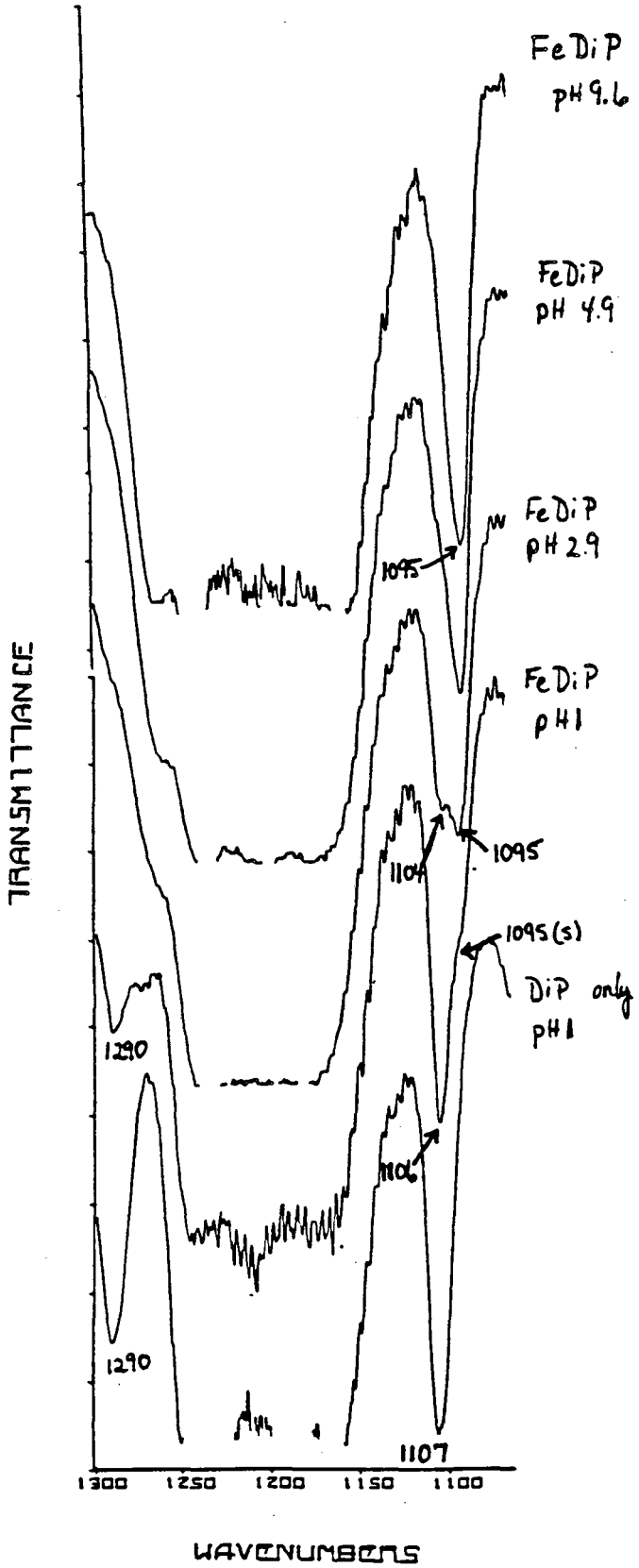
FeDiP
pH 9.6
FeDiP
pH 4.9
FeDiP
pH 2.9
FeDiP
pH 1
DiP only
pH 1
1095
1104
1095
1095(s)
1290
1104
1290
1107
1300
1250
1200
1150
1100
TRANSMITTANCE
WAVENUMBERS

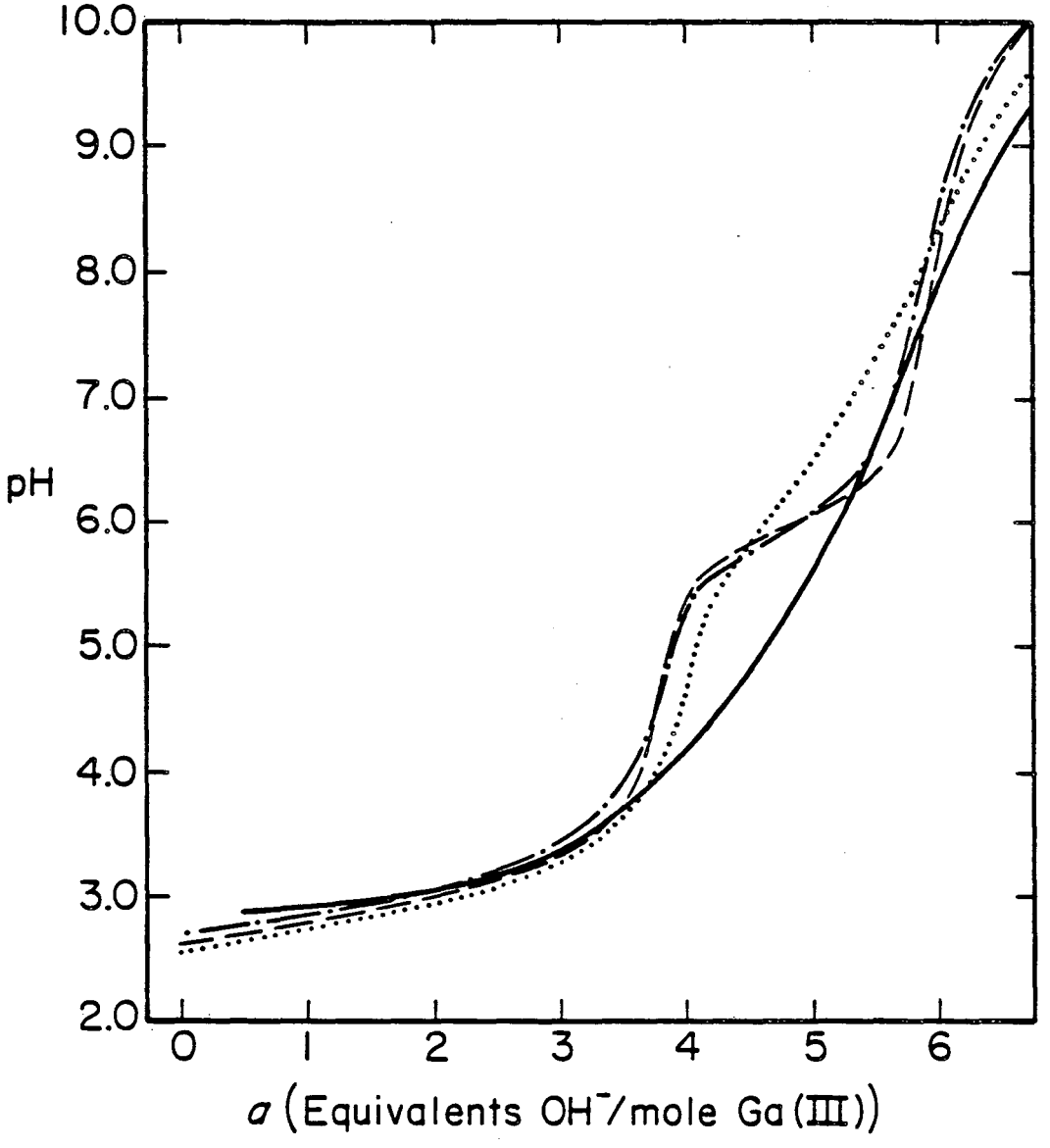
10.0
9.0
8.0
7.0
6.0
5.0
4.0
3.0
2.0
pH
0
1
2
3
4
5
6
a (Equivalents OH⁻/mole Ga(III))

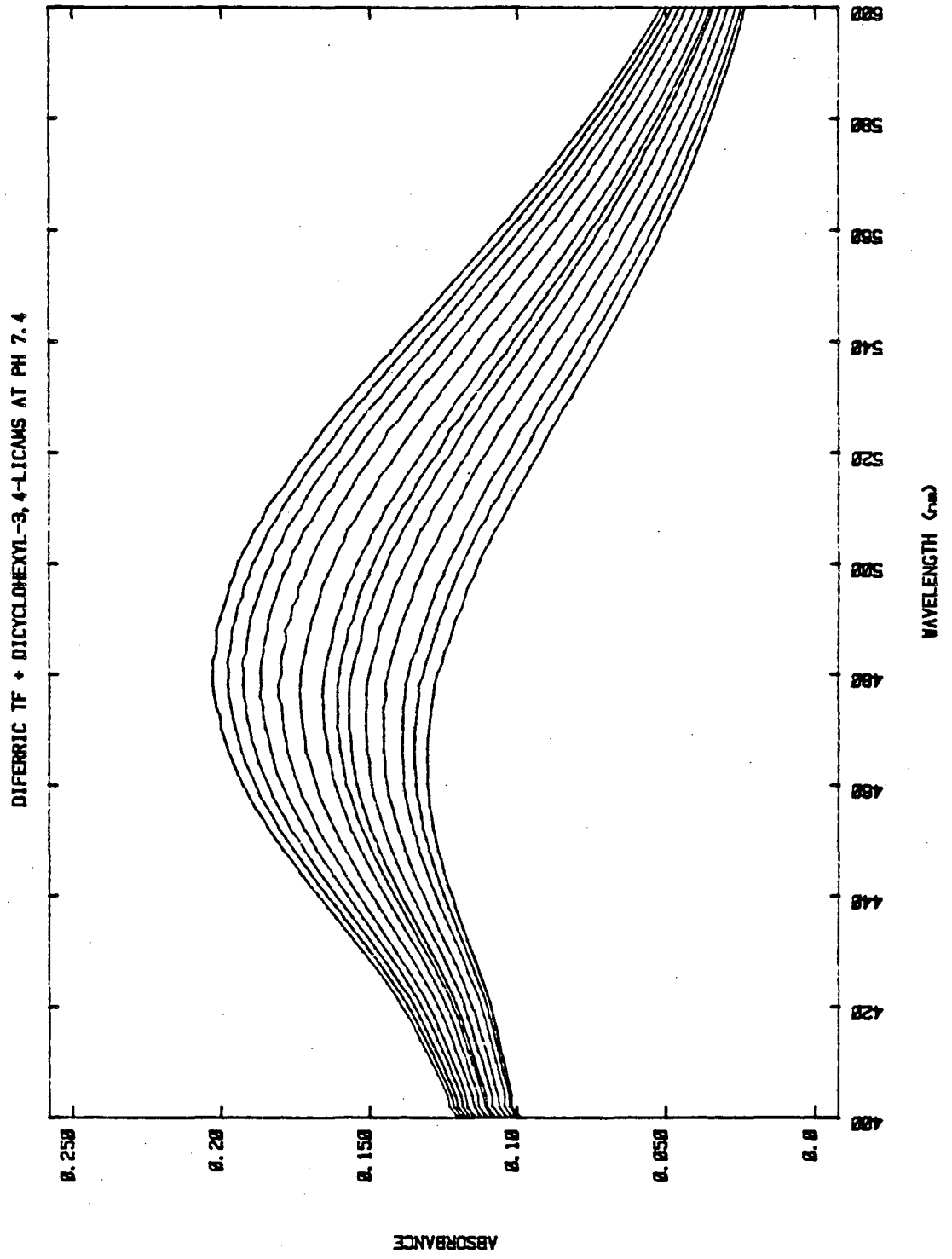
DIFERRIC TF + DICYCLOHEXYL-3,4-LICAMS AT PH 7.4
ABSORBANCE
0.250
0.20
0.150
0.10
0.050
0.0
400
420
440
460
480
500
520
540
560
580
600
WAVELENGTH (nm)

CHAPTER IV

Complexation of Plutonium(IV) and Cerium(IV) by Catecholate Ligands

Although a great deal of effort has been expended to synthesize catecholate ligands which are octadentate (tetracatecholates) and capable of encapsulating actinide(IV) ions,[1-3] there has been no direct evidence about the nature of complexes formed-aside from the fact that 3,4,3-LICAMS and 3,4,3-LICAMC (Figure 4.1) effectively complex Pu(IV) in vivo and promote excretion.[3,4]

There are a number of difficulties associated with studying Pu(IV) complexes. The Pu(IV) ion does not usually exist as a free, aquated ion except in $HClO_4$ or dilute HCl;[5] and its polymerization at low pH in aqueous solution is well documented.[6,7] In addition to its intrinsic insolubility as the hydroxide, its incorporation into bone upon introduction to the body and high specific activity necessitates that work be done in a glove box and that all items which enter the glove box be discarded or decontaminated.

Previous work demonstrated that catechols (Figure 4.1) are very good at stabilizing higher oxidation states of metal ions (Fe(III),[8] Ti(IV),[9] and Ce(IV)[10]). In fact, the reduction potentials

of the uncomplexed ions, normally obtained in noncoordinating acidic media, are known to shift negative in excess of 2.0 volts upon complexation of catechol in basic solution. Since the Pu(IV)/Pu(III) reduction potential is +0.98 volt versus NHE,[11,12] complexation by catechol should shift it to about -1.0 volt versus NHE, well within the operating range of a hanging mercury drop electrode in base.[13] By varying ligand concentrations and pH of Pu-catecholate solutions, electrochemistry can be used to elucidate not only the relative stability of Pu(IV) versus Pu(III) complexes, but also to study protonation behavior and stoichiometry of complexes.[14] These studies can be carried out in dilute solution (less than 0.2mM in Pu) utilizing differential pulse voltammetry,[15] allowing for experiments to be performed with relatively small amounts of ligand and radionuclide. The experimental section of this chapter contains a short description of differential pulse voltammetry as well as pertinent references.

The opportunity to do electrochemical experiments with transuranium actinides is rare, but more rare is the superb apparatus which is available to do these studies. The experiment is operated by a microcomputer and all the data obtained electrochemically are digitalized and stored on 8" floppy disks. As many as 100 different voltammograms will fit on one disk where they can be copied and manipulated. The design of the apparatus and accompanying software are discussed in the experimental section and is partly the subject of one UC Berkeley PhD thesis.[16] Professors Steve and Teri Brown of Washington State and the University of Idaho, respectively, are

largely responsible for the interfacing and software development of this system. In additon, a glove box was designed by Dr. Heino Nitsche of Lawrence Berkeley Laboratory to allow for easy preparation of solutions and it includes a cable from the potentiostat to conduct electrochemical experiments.

As well as the electrochemistry of Pu-catecholates, this chapter includes a study of Ce-catecholates. Tetravalent cerium has been used in the past as a model for Pu(IV)[5,17] and this prompted a parallel study of the Ce(IV)-catecholates using the same electrochemical methods. Similarities in the chemistry of Ce(IV), Ce(III), and Pu(IV), Pu(III) are to be expected considering their identical charges and nearly identical size.[18]

Briefly, chapter IV deals with the study of the Pu(IV)/(III) electrochemical couple with catechol; 3,4,3-LICAMS; 3,4,3-LICAMC; and 3,4-LICAMS as a function of ligand concentration and pH. Experiments were also performed with 4-nitrocatechol and tiron (disodium 3,5-disulfocatechol) with less interpretable results. The Ce(IV)/(III) couple was studied with catechol; 3,4,3-LICAMS; and 3,4,3-LICAMC. Again, experiments with 4-nitrocatechol and tiron were inconclusive. Protonation of the metal complexes and stoichiometry of the complexes will be discussed. Figure 4.1 shows the structural formulas of the ligands used.

Experimental

Reagents. $^{242}PuO_2$ was obtained from Oak Ridge National Laboratory, dissolved in HCl with a minimal amount of NaF, and cleaned

by an anion exchange process with HNO_3 as detailed elsewhere.[19] The resulting solution was checked for purity by spark emmision spectroscopy to ensure a minimum of contaminant metal ions.[20] The HCl stock solution (10 mM) of Pu(IV) was standardized with xylenol orange indicator by direct titration with disodium ethylenediaminetetraacetic acid (Na_2H_2EDTA).[21] For experiments with cerium, both Ce(III) and Ce(IV) were used. $CeCl_3$ obtained from Pfalz and Bauer was dissolved in water (0.1 M) and standardized by back titration of a measured excess of Na_2EDTA with standardized $Zn(NO_3)_2$ with Eriochrome Black T indicator.[22] $(NH_4)_2Ce(NO_3)_6$ was purified by recrystallization before use.[23] It was added as a solid.

Catechol (Crown Zellerbach) and 4-nitrocatechol (Aldrich, 97%) were recrystallized twice from benzene. Disodium 3,5-disulfocatechol (tiron) was obtained from Eastman and required no further purification. The synthesis and characterization of 3,4,3-LICAMS,[2] 3,4-LICAMS[24] and 3,4,3-LICAMC[3] are reported elsewhere. Equivalent weight determinations of 3,4-LICAMS and 3,4,3-LICAMS were done by potentiometric titration.

The 0.10 M KOH (carbonate-free) used was prepared from twice-distilled water and a Baker Chemical Co. Dilut-It ampoule. It was stored under argon to minimize CO_2 dissolution.

Electrochemical Apparatus. All experiments were carried out at room temperature and 1.0 M ionic strength. The electrochemical cell consisted of a saturated calomel electrode as reference electrode, a Pt wire as auxiliary electrode, and a Metrohm hanging mercury drop electrode as the working electrode. The cell itself (from Princeton

Applied Research (PAR)) required 10.0 mL of solution (0.9 M KCl and 0.1 M KOH) and provided for the close proximity of the reference and working electrode to minimize IR drop. The cell diagram is

$$Hg/Hg_2Cl_2/KCl(sat'd)//1.0\ M\ KCl//0.1\ M\ KOH,0.9\ M\ KCl/Hg.$$

High base concentrations were necessary to ensure full deprotonation of the catechol ligands and optimum complexation of metal. All measurements were done with at least 10-fold excess ligand. Metal concentrations were typically 0.2 to 0.5 mM. These conditions provide reversible electrode kinetics at the slow scan rates used with differential pulse. The high base concentrations required frequent silanisation of the capillary of the Hg electrode. Silanisation prevents the solution from creeping back into the tip after the Hg drop is dislodged. It also maintains constant surface area of the Hg drop. Most of the problems encountered during these experiments were rectified immediately after the capillary was resilanised. Details are provided with the Metrohm electrode[25] but the general procedure is included here. First, the capillary must be thoroughly cleaned. With the aid of a water aspirator suck through first HNO_3 to remove Hg residue, and then H_2O to rinse. Put the capillary in an ethanolic NaOH solution (1 M) overnight to remove old silanisation. Rinse the capillary with HCl and determine optically if it is clean, then rinse with H_2O and absolute EtOH. Dry for two hours at 140 -150°C in an oven. After cooling, silanise immediately. At room temperature dip the capillary tip into a small quantity of dimethyldichlorosilane

obtained from PAR. (CAUTION-- corrosive and poisonous, absorbed through the skin.) Only 1 to 2 cm of the capillary bore requires treatment. Repeat dipping 5-6 times. Suck through pure toluene and dry at 140 -150°C for two hours.

The potentiostat used was a PAR 173 for all Pu experiments. A new IBM EC225 potentiostat was used for some of the Ce experiments. One of the problems associated with the PAR 173 is the amount of high frequency noise associated with the signal when it is obtained digitally. Filtering routines using a Fourier filter were performed to eliminate this noise (vide infra). The IBM potentiostat was much less noisy and is capable of much greater sensitivity. The potentiostat is interfaced to a Digital Equipment Corp. (DEC) MINC 11-2/B microcomputer. The microcomputer has a DEC RX02 dual floppy disk drive and a Tektronix CRT. Toman's PhD thesis includes details.[16] A homemade staircase deck supplied pulses for the pulsed voltammetry and signaled initial and final voltages for the potentiostat. The programs used were DPASV for differential pulse and CVBOX for cyclic voltammetry. Initial and final potentials as well as scan rates, pulse height and width are all part of the program input. Parameters used for differential pulse and a short description of the method follows.

Differential Pulse Voltammetry. Pulsed voltammetry has been developed to increase the sensitivity of electrochemical methods by decreasing the contribution of the charging current to that of the total current observed in a faradaic process.[15] The electrode-solution interface acts as a capacitor and the current

generated by this process is called a charging current. This current decays with time as $i_c \propto e^{-kt}$.[13] The current generated by an electrochemical process is called a faradaic current and it decays $i_f \propto t^{-\frac{1}{2}}$.[26,27] It is precisely this difference in decay rates that differential pulse takes advantage of in limiting the contribution of the charging current. A schematic diagram (Figure 4.2) of potential versus time best demonstrates the pulse sequence, where

T = time between pulses (0.5-4.0 sec.)
Δt = duration of pulse (5-100 millisec.)
ΔE = pulse height (10-100 mV)
E'= potential step (0.5-5.0 mV)

The method is actually a slow scanning technique and the current is sampled at t_1, at the end of T, and at t_2, at the end of the pulse. The difference in current ($\Delta i = i_{t_1} - i_{t_2}$) is plotted versus potential for the typical voltammogram. This virtually subtracts out the charging current contribution to the total current under the proper choice of parameters, since the charging current decays at a different rate than the faradaic current.[28,29] The resulting peak in the voltammogram can be translated into $E_{\frac{1}{2}}$ by the relation[13]

$$E_{peak} = E_{\frac{1}{2}} - \frac{\Delta E}{2}$$

The parameters used for this experiment were those done on a time scale resulting in reversible electrode kinetics. No kinetic data were obtained from these studies since sensitivity to irreversible reactions is decreased with this method, i.e., peak shape analysis is

difficult.[26] The parameters for these experiments were T=0.5 second, Δt=34.0 msec., ΔE=75.0 mV, E'=3.0 mV. The conditions for reversibility are peak width at half height=94 mV, $i_{anodic}/i_{cathodic} = 1$; and a separation of the anodic and cathodic peaks of ΔE.

Data Analysis. A more powerful microcomputer was used for Fourier filtering and data analysis. The CPU is a DEC LSI-11 and it is about twice as fast as the 11/2. It is also equipped with a dual floppy disk drive (Data Systems DSD440) and a hard disk drive (DEC RL02). The method of filtering (program BAJSM) is described in detail elsewhere.[30] There are essentially three steps in the process:

(1) The voltammogram (current vs. potential) is fast Fourier transformed[31] into a frequency domain (amplitude vs. volts^{-1}).

(2) A smoothing function, usually a triangular cut (amplitude vs. volts^{-1}) is applied to the Fourier transform. This eliminates high frequency noise.

(3) The transform goes through an inverse Fourier transform to get a filtered voltammogram.

There is an additional manipulation done which rotates and translates the voltammogram before undergoing Fourier transform. This removes so-called "aliasing" effects and is best described elsewhere.[32]

After filtering, background voltammograms of the ligand solution before addition of the metal were subtracted out of the metal complex voltammograms (program BACK), usually with little consequence. One can then obtain the peak current and peak potential digitally ($\pm$1.0 mV) by using the program STAND. This program will also give the current and potential readings for any point in the voltammogram.

For cyclic voltammograms, the voltammogram must be split into an

anodic and cathodic scan (program SPLTCV) before they are filtered or background subtracted.

Files may be inspected by use of programs NSPCT2, NSPECT, or CVSPEC (for CV). Files may be edited by program UNARY to simply display certain potential ranges or to alter the current axis to display the correct units.

Results and Discussion

M(IV)/(III)Catechol Electrochemistry. As previously mentioned, the low acidity of catechol requires that the electrochemical experiments be conducted under very basic conditions. The measurements of electrochemical potential as a function of ligand concentration were always maintained at pH values >12.3. Above this pH the potential is independent of pH and demonstrates only a ligand dependence. The negative shift in potential for increasing total catechol concentrations is illustrated in Figure 4.3 for Pu-catechol. Note the abscissa units which demonstrate a tremendous negative shift in the potential as compared to Pu(IV)/Pu(III) (+0.98 V vs. NHE) in acidic medium.[11] This indicates a stabilization of the tetravalent ion relative to the trivalent ion by catechol. Similar stabilization of the Ce(IV)/Ce(III) couple with catechol is observed.[10](Table I) In addition, a similar negative shift in potential with increasing total ligand concentration is seen. Both systems are classified as quasi-reversible since there is a dependence of peak potential on scan rate, however at the slow scan rates employed here the electrode kinetics are reversible.

The x-ray structure of $Ce(IV)(cat)_4^{4-}$ has been determined previously under similar conditions of excess ligand and high base concentrations,[10] so the stoichiometry of the tetravalent cerium and presumably that of Pu(IV) are already known. The variation of potential of an electroactive metal complex with increasing ligand concentration gives information on the stoichiometry of the M(III) complexes which are formed.[14] For plutonium, using the two half reactions (L^{2-} = catechol^{2-})

$$Pu(IV) + e^- = Pu(III) \qquad E^\circ = +0.98 \text{ V vs. NHE}$$

$$Pu(IV)L_4^{4-} + e^- = Pu(III)L_q^{2q-3} + (4-q)L^{2-} \qquad E_f$$

and the two dissociation constants

$$K_{IV} = \frac{[Pu(IV)][L^{2-}]^4}{[Pu(IV)L_4^{4-}]} \qquad K_{III} = \frac{[Pu(III)][L^{2-}]^q}{[Pu(III)L_q^{2q-3}]}$$

a Nernstian expression can be written which includes a dependence on total ligand concentration (L_T) assuming reversible electrode kinetics at 25°C

$$E^\circ - E_f = 0.059 \left[\log\left(\frac{K_{IV}}{K_{III}}\right) - (4-q) \log L_T\right] \qquad (1)$$

Differentiation of this equation gives

$$d(E_f)/d(\log L_T) = -0.059\ (4-q)$$

Thus, a plot of potential versus the log of the total ligand concentration gives a line with a slope containing the value of 4-q, where q is the stoichiometric coefficient for M(III)catechol complexes. If the stoichiometry of the M(III)catechol complex is the same as that for the M(IV)catechol complex, there would be no variation of E_f with total ligand concentration and the total potential shift would be proportional to $\log(K_{IV}/K_{III})$. Such plots for cerium- and plutonium-catechol are illustrated by Figures 4.4 and 4.5. The slope of both of these lines indicate q=2.5. This implies a M(III)catechol complex of lower stoichiometry than the M(IV)catechol complex with two alternate interpretations, either under the conditions specified the M(III) complex may involve 2.5 catechols or at this pH there exists an equilibrium between the biscatecholate and triscatecholate complex. These results alter earlier interpretations regarding cerium catechol electrochemistry.[10] This previous study did not include an investigation of the ligand dependence of the potential, but measured a potential in 5 M NaOH and 1 M catechol assuming the Ce(III) complex was a tetracatechol complex. The value reported (-692 mV vs. SCE) is included as a point in Figure 4.4, indicating that the same ligand dependence on the potential exists at these extreme conditions. However, there appears to be no shift in potential above catechol concentrations of 2 M (5 M KOH) which means that under these forcing conditions a tetrakis(catecholato) complex of Ce(III) can be found in solution. The reduction potential for the Ce(IV)/Ce(III)-(catechol) couple is -732 mV versus SCE and implies a ratio of K(IV)/K(III) of 10^{41}. X-ray crystal structures of

$Gd(III)(cat)_3^{3-}$ and $Gd(III)(cat)_4^{5-}$ have been determined recently with the triscatecholato complex being isolated from solutions less concentrated in catechol (≃2 M) and more air stable.[33] A trivalent lanthanide(III) complex of lower stoichiometry, Eu(cat)OH, has also been isolated at neutral pH.[34]

Although the electrochemistry of these systems show quasi-reversible behavior, theory developed for reversible systems[14] appears to apply.

M(IV)/(III)3,4,3-LICAMS and M(IV)/(III)3,4-LICAMS Electrochemistry. Upon addition of Pu(IV) to a solution of 3,4,3-LICAMS at high pH (>12) a fairly intense amber color is observed due to a broad charge transfer band at 435 nm (ε=750 $M^{-1}cm^{-1}$). This same color is observed for Pu(IV)catechol at high pH. Lowering the pH of the Pu(IV)3,4,3-LICAMS (pH 10.9) shifts λ_{max} to 441 nm (ε=460 $M^{-1}cm^{-1}$), similar to the shifts and intensity loss seen for Fe(III)3,4-LICAMS upon protonation.[35] Complexes of $Ce(IV)(cat)_4^{4-}$ are purple,[10] as is the Ce(IV)3,4,3-LICAMS complex at high pH (λ_{max}=514 nm, ε=4400 $M^{-1}cm^{-1}$). Thus at high pH (>12) the 3,4,3-LICAMS complexes of Pu(IV) and Ce(IV) seem to be tetracatecholate complexes.

The negative shifts in potential for the Pu(IV)- and Ce(IV)3,4,3-LICAMS complexes as compared to free M(IV)/(III) are given in Table I. The shifts are larger than those observed with catechol.

Figure 4.6 illustrates the increase in current of the Pu(IV)/(III)3,4,3-LICAMS couple with time after addition of Pu(IV) stock solution to a solution of 3,4,3-LICAMS at pH 12.5 (0 to 3

hours). This indicates competition with hydroxide probably occurs over this period. The current reaches a maximum after this time.

The potential of the Pu(IV)/(III)- and Ce(IV)/(III)3,4,3-LICAMS couple does not appear to shift with increasing ligand concentration. This may mean that an M(IV) ion complexed by 3,4,3-LICAMS is bound by four catecholate arms of the same ligand. Upon reduction of the metal center to M(III) any concomitant reduction in the number of catecholate groups bound (as indicated by the Pu and Ce catechol studies) simply requires the removal of one or two catecholate arms of the ligand. This change in coordination environment upon reduction of M(IV) is then not reflected in a change of potential with varying total ligand concentration. Thus, a shift in potential dependent on total ligand concentration would not be expected for any encapsulating macrochelate. Of course, an alternate explanation is that the M(III) complex is a tetrakiscatecholato complex.

Assuming that the Pu(III)3,4,3-LICAMS complex is similar to the Pu(III)catechol complex, this would mean that at high pH there are one or possibly two pendant arms of the macrochelate which are unbound and deprotonated. Figure 4.7 shows the differential pulse voltammograms of Pu(IV)3,4,3-LICAMS as a function of pH. A positive shift in potential and a loss of current is seen between pH 10.8 and pH 6.5, whereas a small shift in potential and a small loss of current is observed between pH 12.1 and pH 11.0. Precipitation is evident at pH 9.4 and increases as the pH is lowered. Dependence of potential on pH can be interpreted in two ways.

CASE 1: Acidity of the oxidized complex causes the potential shift.

$$O + q\ H^+ = OH_q$$

$$OH_q + ne^- = RH_q$$

where

$$K = \frac{[OH_q]}{[O][H^+]^q}$$

oxidized species = $[OH_q] + [O]$
reduced species = $[RH_q]$

If the electrode kinetics are diffusion controlled (reversible), then $[RH_q] = [O] + [OH_q]$ at any pH value.

Then the expression for the Nernst equation is

$$E_{\frac{1}{2}} = E^\circ + \frac{0.059}{n} \log \left(\frac{[H^+]^q K}{[H^+]^q K + 1} \right) \qquad (2)$$

where E°=the formal potential of the electron-transfer process.

Therefore, if $[H^+]^q K >> 1$, then H_qO predominates and $E_{\frac{1}{2}}$ is independent of pH,

if $[H^+]\ K << 1$, then O predominates and in this region $E_{\frac{1}{2}}$ is dependent on pH and differentiation of (2) yields

$$dE_{\frac{1}{2}}/dpH = (-0.059/n)\ q \qquad (3)$$

CASE 2: Acidity of the reduced complex causes potential shift.

$$O + q\,H^+ + ne^- = RH_q$$

$$RH_q = q\,H^+ + R$$

where

$$K = \frac{[R][H^+]^q}{[RH_q]}$$

$$\text{oxidized species} = [OH_q] + [O]$$

$$\text{reduced species} = [RH_q] + [R]$$

If the electrode kinetics are reversible,

$[O] + [OH_q] = [RH_q] + [R]$ at any pH value.

Then the expression for the Nernst equation is

$$E_{\frac{1}{2}} = E^\circ - \frac{0.059}{n} \log \left(\frac{[H^+]^q}{[H^+]^q + K} \right) \qquad (4)$$

where E°=the formal potential of the electron-transfer process.

Therefore, under acidic conditions $[H^+]^q \gg K$, the reduced form will exist predominantly as RH_q and the variation in $E_{\frac{1}{2}}$ will be described by equation (3),

if $[H^+]^q \ll K$, then $E_{\frac{1}{2}}$ will be independent of pH.

A plot of $E_{\frac{1}{2}}$ versus pH for Pu(3,4,3-LICAMS) is shown in Figure 4.8. It shows a region at high pH with very little change in $E_{\frac{1}{2}}$ and a region between pH 10.8 and 6.5 with a slope of -0.053. Using equation (3), this corresponds to a one proton equilibrium described by Case 2, involving the acidity of the reduced species. The intersection of the two lines is at pH = pKa = 11.0. If the Pu(III)3,4,3-LICAMS has one or two pendant catechol arms free this pKa corresponds very well with the protonation of a phenolic oxygen meta to the carbonyl. In the free ligand, with no metal bound, this pKa is estimated to be about 11.5.[36] (see Chapter II)

An additional experiment performed to test this hypothesis of protonation of the free catechol arm of Pu(III)3,4,3-LICAMS involves monitoring the shift in $E_{\frac{1}{2}}$ with pH for Pu(3,4-LICAMS), this ligand being a tricatecholate (Fig. 4.1). Under conditions of ten-fold excess ligand one can envision that at pH>12, the plutonium(IV) may be surrounded by three catecholate arms of one ligand molecule and a fourth arm from another ligand molecule. However, upon reduction it is likely that the Pu(III) complex is bound by three catecholate arms of one 3,4-LICAMS molecule. Under these conditions a very small shift in $E_{\frac{1}{2}}$ with pH is observed; however a decrease in current is observed and precipitation is evident at pH 9.

The decrease in peak current with decreasing pH observed in Figures 4.7 and 4.9 can also be attributed to a protonation phenomenon, but the protonation here involves the Pu(IV)3,4,3-LICAMS complex. The bulk solution contains the Pu(IV) complex and the peak current is directly proportional to the concentration. For

differential pulse at a stationary electrode the peak current can be expressed as[26]

$$\Delta i_p = \frac{nFAD^{\frac{1}{2}}c}{\pi^{\frac{1}{2}} t^{\frac{1}{2}}} \cdot \frac{1-\beta}{1+\beta}$$

where

n = no. of electrons
F = Faraday constant
A = electrode area
D = diffusion coefficient of bulk electroactive species
C = concentration of bulk electroactive species
t = pulse width
β = $\exp[nF/RT\Delta E]$; ΔE = pulse height

Thus, one can consider that for two electroactive species in solution with differing diffusion coefficients the peak current is

$$\Delta i_p = kD_1^{\frac{1}{2}}c_1 + kD_2^{\frac{1}{2}}c_2$$

where k is a constant containing the aforementioned parameters. Consider that c_1 and c_2 be related by a protonation equilibrium

$$K_H = \frac{c_1[H^+]^n}{c_2}$$

and that $c_T = c_1 + c_2$.

For this relationship an expression can be developed

$$\Delta i_p = kD_2^{\frac{1}{2}}c_T + \frac{(\Delta i_p^{\circ} - \Delta i_p)K_H}{[H^+]^n} \qquad (5)$$

where Δi_p° = the peak current at high pH with only species c_1 present

Δi_p = the peak current at any pH other than Δi_p° where c_1 and c_2 are in equilibrium

This is analogous to an expression developed by Schwarzenbach for absorbtion, only in this case diffusion coefficients rather than extinction coefficients are used.[37]

A plot of Δi_p versus $(\Delta i_p^\circ - \Delta i_p)/[H^+]^n$ with proper choice of n gives a straight line with slope K_H. Figure 4.10 illustrates such a plot for Pu(IV)3,4,3-LICAMS (A) and Pu(IV)3,4-LICAMS (B). Two straight line segments are observed. The line segment with shallow slope corresponds to the protonation:

$$Pu(IV)3,4,3\text{-}LICAMS^{8-} + H^+ = Pu(IV)3,4,3\text{-}HLICAMS^{7-}$$

The shift in λ_{max} in the visible spectra obtained over this pH range also indicate that protonation is occuring. The plot shown in Figure 4.10 implies that the monoprotonated Pu(IV) complex has a diffusion coefficient 30-40% smaller than that of the deprotonated Pu(IV) complex. This seems unlikely, since to a first approximation, the diffusion coefficient is proportional to the volume of the complex. Therefore, large changes in the diffusion coefficient would not be expected upon a single protonation, but we believe that this correlation with current merits mention. Lowering the pH further, a white flakey precipitate is formed ($Pu(OH)_4$ is green and gelatinous) and a linear decrease in current is also observed and included in

Figure 4.10 for interest. This line segment can not be interpreted by the same method used for the line segment of shallow slope since two species are not in equilibrium in solution as is required to use this method. Instead, an alternate graphical method can be used. The formation constant for such a precipitate would be

$$K = \frac{1}{[Pu(IV)HLICAMS][H^+]^n} .$$

Therefore, a plot of ln Δi_p versus ln $[H^+]$ should give a line of slope -n. Such a plot for Pu(IV)3,4,3-HLICAMS is linear (correlation = -0.9999), but the slope is non-integral (slope = -0.20). This may indicate that the system was not in equilibrium when the measurements were obtained. It does appear that this precipitate is at least a diprotonated Pu(IV) complex. The presence of a precipitate, although not anticipated considering the high charge on the complex, can be understood by considering that upon protonation of the catecholate arms, space is available on the coordination sphere of Pu(IV). This ion is prone to hydrolysis and polymerization. In addition, the bridging capabilities of catechol is well illustrated in the $Gd(III)(cat)_3^{3-}$ structure, which contains two bridging catechol dianions.[33]

As mentioned previously, the coordination environment about Pu(IV) at high pH in the presence of excess 3,4-LICAMS may involve two ligands. Protonation of this complex may involve loss of a ligand.

One question which arises is why isn't a variation in $E_{\frac{1}{2}}$ with pH

seen for these Pu(IV) complexes, as theorized in Case 1? Only the equilibrium of the first protonation would be visible, since the second protonation does not produce a soluble product. The plot of Pu(IV)3,4,3-LICAMS protonation in Fig. 4.10A indicates that log K_{MHL} is 10.3. This is close to the protonation constant for Pu(III)3,4,3-LICAMS from Fig. 4.8 (log K_{MHL} = 10.9). A slight curvature in the pH region 10.0 to 10.7 in Fig 4.8 is noticeable which may be attributable to the two simultaneous protonations affecting the $E_{1/2}$. However, if Case 1 were the predominating factor a variation in $E_{1/2}$ at high pH (>11.0) would be expected. Another explanation would be that the kinetics for protonation of the free catechol arm of Pu(III)3,4,3-LICAMS may be faster than that of protonation of Pu(IV)3,4,3-LICAMS on the time scale of the experiment (6 mV/second scans). If polymerization of the protonated Pu(IV)3,4,3-LICAMS complex occurs (a relatively slow process), this might well be the reason the variation of $E_{1/2}$ with protonation of the oxidized specie is not seen.

In contrast to Pu(3,4,3-LICAMS), the Ce(3,4,3-LICAMS) differential pulse voltammogram shows no positive shift in potential with decreasing pH (Figure 4.11); however, it does show a decrease in peak current. It is not understood why $E_{1/2}$ does not shift with pH considering the similarities that exist between cerium and plutonium chemistry. Ce(IV)3,4,3-LICAMS demonstrated trends observed for plutonium, i.e., a decrease in current; however, there is greater scatter in the data. This may be a result of irreproducible Hg drop size in the study of cerium complexes, since a different model Hg

electrode was used outside the gloved box for cerium electrochemistry.

M(IV)/(III)3,4,3-LICAMC Electrochemistry. The electrochemistry of Pu(IV)/(III)3,4,3-LICAMC can be analyzed in the same manner as the complexes with 3,4,3-LICAMS. There is one notable difference, the phenolic oxygens of 3,4,3-LICAMC are considerably less acidic than those of the sulfonated ligand.[38] Thus, the protonation constants of the complexes are considerably higher.

Figure 4.12 illustrates the differential pulse voltammograms of Pu(3,4,3-LICAMC) as a function of pH. There is a positive shift in $E_{\frac{1}{2}}$ with a decrease in pH, similar to that observed for Pu(3,4,3-LICAMS). There is also a decrease in current with a decrease in pH. The features of the individual voltammograms do differ. Table I shows that the negative shift in potential for the complex as compared to the free ion is greater for LICAMC complexes than for LICAMS or catechol complexes. In addition, the Pu(3,4,3-LICAMC) voltammogram shows an additional peak at -1.07 V vs. SCE which has no pH dependence. This peak is not seen in the electrochemistry of the free ligand and is assumed to be a Pu complex. The carboxylate group para to the carbonyl does provide an additional binding mode for the Pu(IV) ion which does not exist in the sulfonated derivative and this may be the explanation for an additional peak. These scans also show a five-fold decrease in current as compared to the Pu(3,4,3-LICAMS) pulse voltammograms.

A plot of $E_{\frac{1}{2}}$ versus pH is shown in Figure 4.13 (slope =-0.068). The same reasoning used for the pH dependence in Pu(3,4,3-LICAMS) can

be used, i.e., the acidity of the reduced species is responsible for such a shift (Case 2); then the log of the protonation constant for Pu(III)3,4,3-LICAMC is above 13.0. The pKa of 2,3-dihydroxybenzoic acid, the monomer analog, is 13.1.[39]

Likewise, analysis of the decrease in current with decrease in pH (equation 5) gives two straight line segments for n = 1 (Fig. 4.10C). The line segment of shallow slope can be interpreted by Eq. 5. The protonation of Pu(IV)3,4,3-LICAMC occurs at pH values higher than that of Pu(IV)3,4,3-LICAMS with the appearance of a precipitate at pH 10.7 (log K_{MHL}=11.9).

The Ce(3,4,3-LICAMC) electrochemistry does show a positive shift in $E_{\frac{1}{2}}$ with decreasing pH, but potential shifts below pH 12 are out of the range of the hanging Hg drop electrode in basic medium. A decrease in current is also observed, but the data are few. Table I summarizes the shifts seen.

M(IV)/(III) Tiron and 4-nitrocatechol Electrochemistry. For some inexplicable reason the electrochemistry with 4-nitrocatechol and cerium or plutonium was not seen. The large peaks due to the reversible reduction of the nitro group to the radical anion and then to the amine were observed,[40] but no peaks due to metal complexation were seen. Any color changes due to metal complexation (purple for Ce(IV) or amber for Pu(IV)) are masked by the extremely intense red color of the dianion of 4-nitrocatechol.

The shifts observed for the cerium and plutonium complexes of tiron are in Table I. The voltammograms for metal complexes of this

ligand are irreversible. For plutonium, one sees a large cathodic wave and a small anodic wave. For cerium, the opposite is true. Part of the difficulty with irreversibility seen with this monocatechol may be its high charge when fully deprotonated (4-), causing charge repulsion in the metal complexes, particularly with the M(III) ion, and fewer catechols binding the metal ion. It is known, for instance, that only 1:1 complexes of tiron:Eu(III) and tiron:Lu(III) are formed at pH 9-10.[34] The Th(IV)-tiron complex is dinuclear (2 Th(IV); 3 tiron)[41] compared to Th(IV)(nitrocatechol)$_4^{4-}$ and Th(IV)(catechol)$_4^{4-}$.[42,43] Therefore, irreversibility may be due to major changes in coordination in reducing the M(IV) ion to the M(III) ion.

Summary

A summary of the protonation behavior of complexes of Pu(IV)- and Pu(III)- 3,4,3-LICAMS and 3,4,3-LICAMC as determined by electrochemical methods is diagrammed in Figure 4.14.

The implications of this study are that the complex of Pu(IV)3,4,3-LICAMS which exists at pH 7.4 (human plasma pH) is not a tetracatecholate complex, and may be a triscatecholate complex. In vivo work on Pu(IV) removal from mice using the same concentrations of 3,4,3-LICAMS and 3,4-LICAMS indicates that 3,4-LICAMS is more effective at removal of radionuclide per functional catechol group, thus Pu(IV) does not appear to utilize the full denticity of the tetracatechol, 3,4,3-LICAMS. Indeed, results obtained here indicate

that use of functional groups more acidic than catechol may be warranted. Development of macrochelates of the more acidic N-hydroxypyridinone ligand is currently underway.

Any concern over precipitation of Pu(IV) complexes of 3,4,3-LICAMS or 3,4,3-LICAMC in vivo is invalid since concentrations encountered in vivo are at least 1000-fold less than those encountered here. In addition, these studies were performed at 1 M ionic strength.

As to the validity of using Ce(IV), Ce(III) as a model for Pu(IV), Pu(III); one can definitely conclude from Table I that the relative potential shifts observed are the same. The electrochemistry with simple catechol also demonstrates a similarity in chemical nature. The differences observed in the protonation behavior of the macrochelate complexes is puzzling. It is fortuitous that the electrochemistry with plutonium yielded more information since this is the system we are most interested in, but this is little solace to the quizzical scientist who seeks a more definitive explanation.

REFERENCES

1. Weitl, F.L.; Raymond, K.N.; Smith, W.L.; Howard, T.R., J. Am. Chem. Soc. (1978), 100, 1170.

2. Weitl, F.L.; Raymond, K.N., J. Am. Chem. Soc. (1980), 102, 2289.

3. Weitl, F.L.; Raymond, K.N., J. Med. Chem. (1981), 24, 203.

4. Durbin, P.W.; Jones, E.S.; Raymond, K.N.; Weitl, F.L., Rad. Res. (1980), 81, 170.

5. Connick, R.E., "The Actinide Elements," Katz, J.J.; Seaborg, G.T., Eds. National Nuclear Energy Series. IV. 14-A, McGraw-Hill: New York (1954), p. 224.

6. Cleveland, J.M. "The Chemistry of Plutonium," Gordon and Breach Science Publishers: New York (1970), 83-89.

7. Brunstad, A. Ind. Eng. Chem. (1959), 51, 38.

8. Harris, W.R.; Carrano, C.J.; Cooper, S.R.; Sofen, S.R.; Avdeef, A.E.; McArdle, J.V.; Raymond, K.N., J. Am. Chem. Soc. (1979), 101, 6097.

9. Borgias, B.; Cooper, S.; Koh, Y.; Raymond, K., submitted to J. Am. Chem. Soc.

10. Sofen, S.R.; Cooper, S.R.; Raymond, K.N., Inorg. Chem. (1979), 18, 1611.

11. Connick, R.E.; McVey, W.H., J. Am. Chem. Soc. (1951), 73, 1798.

12. Rabideau, S.W.; Lemons, J.F., J. Am. Chem. Soc. (1951), 73, 2895.

13. Bard, A.J.; Faulkner, L.R., "Electrochemical Methods" J. Wiley and Sons: New York, 1980, back cover.

14. Meites, L., "Polarographic Techniques" Second Edition, J. Wiley and Sons: New York, 1965, 203-301.

15. Osteryoung, R.A.; Osteryoung, J., Phil. Trans. R. Lond. (1981), A302, 315-326.

16. Toman, J.J., PhD Thesis, University of California, Berkeley (1982).

17. Cotton, F.A.; Wilkinson, G., "Advanced Inorganic Chemistry" Third Edition, Wiley-Interscience: New York, 1972, 1072.

18. Shannon, R.D., Acta Crystallogr., Sect. A (1976), A32 (5),

751-767.

19. Coleman, G.H., Ed. "The Radiochemistry of Plutonium," National Academy of Sciences, available from Clearinghouse for Federal Scientific and Technical Information, National Bureau of Standards, Springfield, VA, (1965), p. 93.

20. Conway, J.G.; Moore, M.F., Anal. Chem. (1952), 24, 463.

21. Smirnov-Averin, A.P.; Kovalenko, G.S.; Ermoloev, N.P.; Krot, N.N., J. Anal. Chem.(USSR) (1966), 21, 62.

22. Welcher, T.J., "The Analytical Uses of Ethylenediaminetetraacetic Acid," Van Nostrand: Princeton, N.J., 1958.

23. Vogel, A.I., "Quantitative Inorganic Analysis," Third Edition, Longman: London, 1961, 315-316.

24. Weitl, F.L.; Harris, W.R.; Raymond, K.N., J. Med. Chem. (1979), 22, 1281-1283.

25. Instruction manual for the EA290/ Hanging Mercury Drop Electrode by Metrohm.

26. Keller, H.E.; Osteryoung, R.A., Anal. Chem. (1971), 43, 342-348.

27. Rifkin, S.C.; Evans, D.H., Anal. Chem. (1976), 48, 2174-2180.

28. Bennekom, W.P.; Schute, J.B., Anal. Chim. Acta (1977), 89, 71-82.

29. Klein, N.; Yarnitzky, C., Electroanal. Chem. Interfacial Electrochem. (1975), 61, 1-9.

30. Horlick, G., Anal. Chem. (1972), 44, 943-947.

31. Singleton, R.S., IEEE Trans. Audio Electroacoustics (1969), AU-17, 166.

32. Hayes, J.W.; Glover, D.E.; Smith, D.E.; Overton, M.W., Anal. Chem. (1973), 45, 277-284.

33. Freeman, G., work in progress.

34. Zhu, D.; Kappel, M.; Raymond, K., manuscript in preparation.

35. Harris, W.R.; Raymond, K.N.; Weitl, F.L. J. Am. Chem. Soc. (1981), 103, 2667-2675.

36. Pecoraro, V.; Scarrow, R.; Kappel, M.; Raymond, K., manuscript in preparation.

37. Schwarzenbach, G.; Schwarzenbach, K., Helv. Chim. Acta (1963), 46, 1390.

38. Kappel, M., unpublished results.

39. Avdeef, A.; Sofen, S.R.; Bregante, T.L.; Raymond, K.N., J. Am. Chem. Soc. (1978), 100, 5362.

40. Corvaja, C.; Farnia, G.; Vianello, E. Electrochim. Acta (1966), 11, 919-929.

41. Murakami, Y.; Martell, A., J. Am. Chem. Soc. (1960), 82, 5605-5607.

42. Zhu, D., work in rogress.

43. Sofen, S. R.; Abu-Dari, K.; Freyberg, D.P.; Raymond, K.N., J. Am. Chem. Soc. (1978), 100, 7882.

Table I. Potential Shifts of Catecholate-bound Pu and Ce

Ligand	Shift of Ce(IV)/Ce(III)[a] (Volts)	Shift of Pu(IV)/Pu(III)[b] (Volts)
Catechol	-2.00	-1.82
Tiron[c]	-1.97	-2.07
3,4-LICAMS	-	-1.87
3,4,3-LICAMS	-2.11	-1.91
3,4,3-LICAMC	-2.16	-2.03

[a]The potential of $Ce(IV) + e^- = Ce(III)$ has been determined in 1 M $HClO_4$ to be +1.7 V. vs. NHE. Hugus, Z., UCRL-1379, (1951).

[b]The potential of $Pu(IV) + e^- = Pu(III)$ has been determined in 1 M $HClO_4$ to be +0.98 V. vs. NHE. See Refs. 11 and 12.

[c]Irreversible.

Figure Captions for Chapter IV

Figure 4.1. Structural formulas for catecholate ligands: catechol, 4-nitrocatechol, tiron, 3,4,3-LICAMS, 3,4,3-LICAMC.

Figure 4.2. Schematic of differential pulse sequence with time.

Figure 4.3. Anodic differential pulse voltammogram of Pu-catechol (L_T= 9.0 to 32.0 mM).

Figure 4.4. Plot of the dependence of $E_{\frac{1}{2}}$ on total ligand concentration for Ce-catechol (L_T= 12.4 to 1000.0 mM).

Figure 4.5. Plot of the dependence of $E_{\frac{1}{2}}$ on total ligand concentration for Pu-catechol (L_T= 9.0 to 32.0 mM).

Figure 4.6. Differential pulse voltammogram of Pu(3,4,3-LICAMS) with time (0, 2, and 3 hours after addition of Pu(IV)).

Figure 4.7. Differential pulse voltammogram of Pu(3,4,3-LICAMS) as a function of pH (pH 10.59, 10.12, 9.90, 9.68, 9.36, 8.79, 7.39, 6.85).

Figure 4.8. Plot of the variation of $E_{\frac{1}{2}}$ with pH for Pu(3,4,3-LICAMS).

Figure 4.9. Differential pulse voltammograms of Pu(3,4-LICAMS) at pH 11.83 and pH 9.88.

Figure 4.10. Plots of the variation of peak current with pH.

(A) Pu3,4,3-LICAMS

(B) Pu3,4-LICAMS

(C) Pu3,4,3-LICAMC

Figure 4.11. Differential pulse voltammograms of Ce(3,4,3-LICAMS) at pH 11.90 and pH 7.20.

Figure 4.12. Differential pulse voltammogram of Pu(3,4,3-LICAMC) as a function of pH (pH 12.65, 12.30, 12.18, 11.82, 11.58, 11.07, 10.69).

Figure 4.13. Plot of the variation of $E_{\frac{1}{2}}$ with pH for Pu(3,4,3-LICAMC).

Figure 4.14. Summary of the Pu polycatecholate equilibria as determined by electrochemistry.

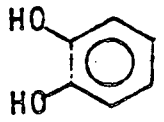

catechol

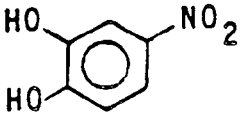

4-nitrocatechol

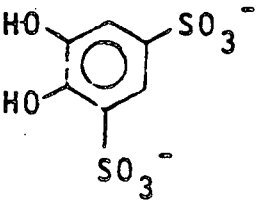

Tiron

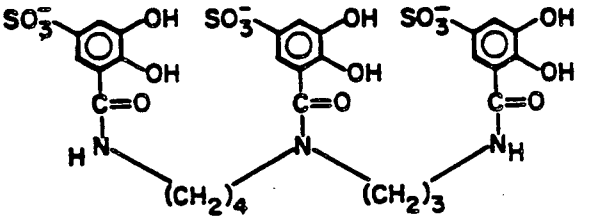

3,4 -LICAMS

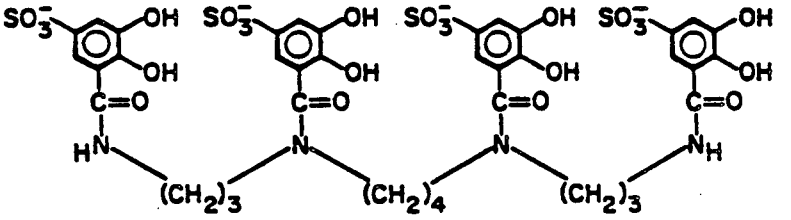

3,4,3-LICAMS

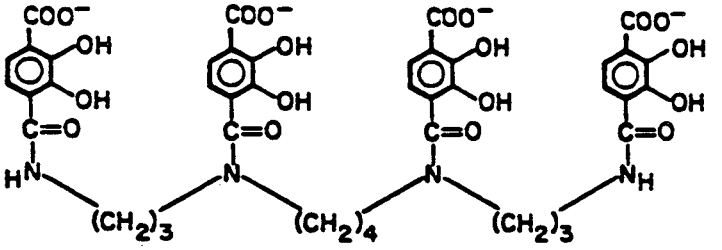

3,4,3-LICAMC

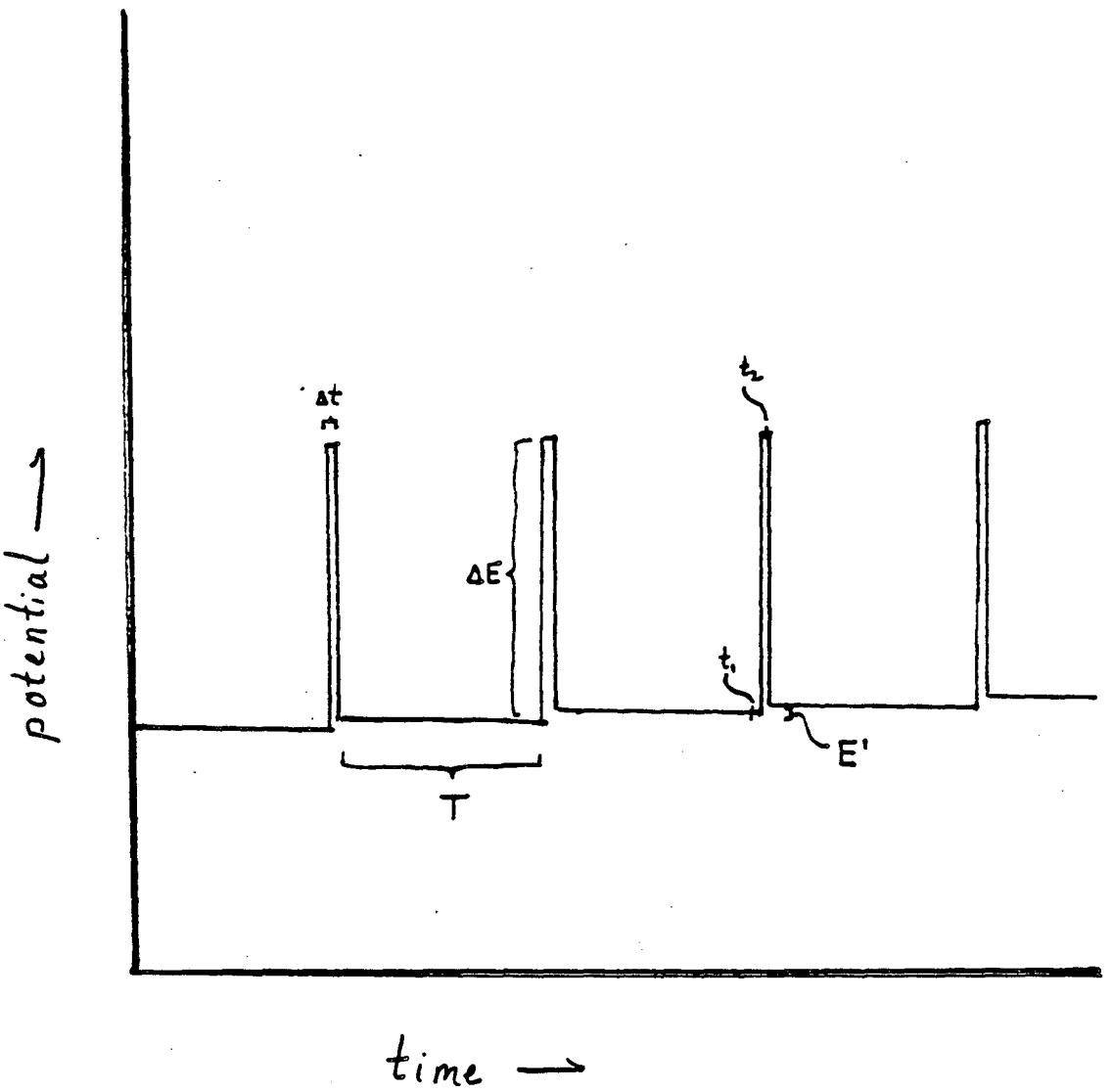
potential
time
Δt
ΔE
T
t_2
t_1
E'

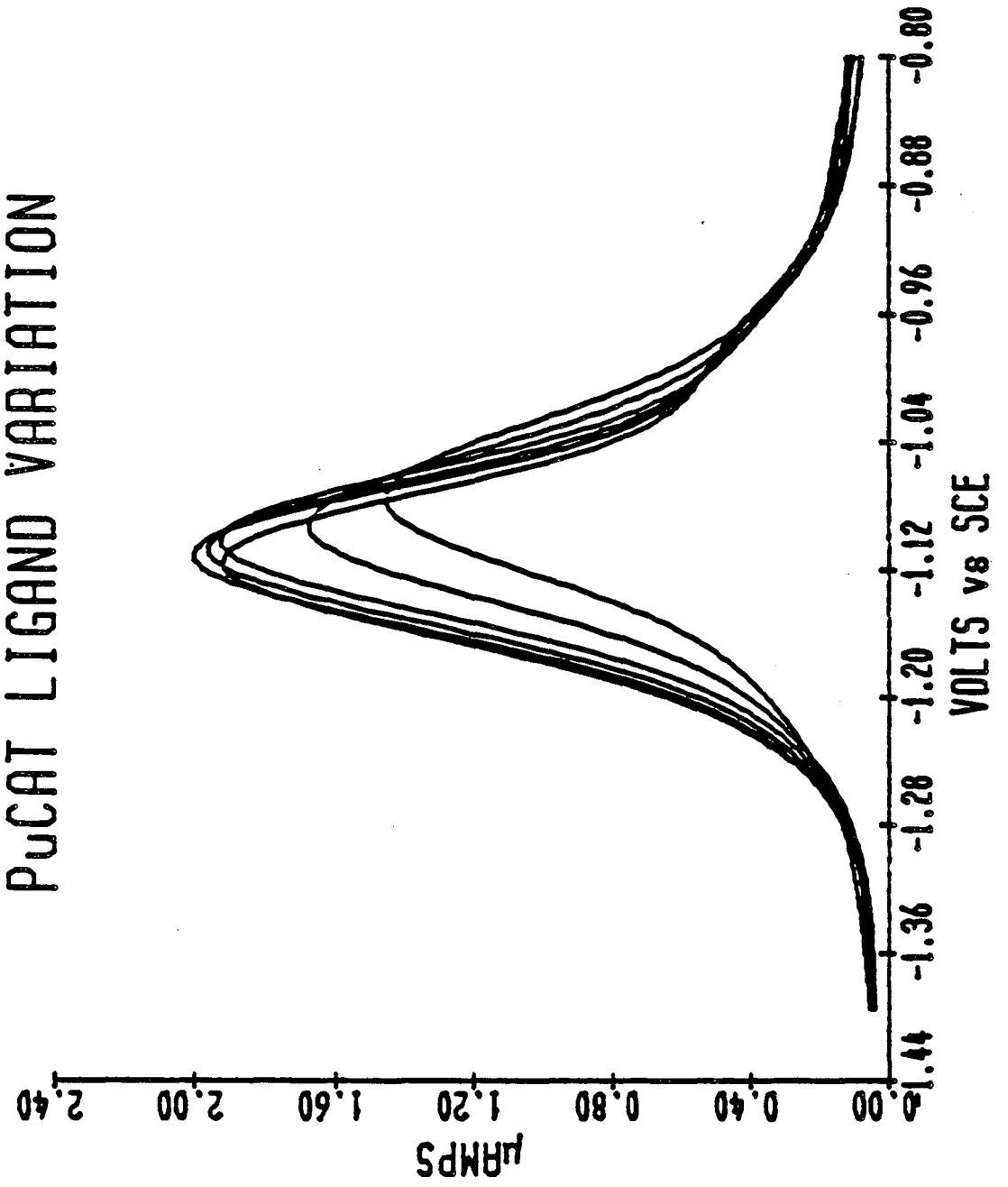
PuCAT LIGAND VARIATION
μAMPS
0.00
0.40
0.80
1.20
1.60
2.00
2.40
-1.44
-1.36
-1.28
-1.20
-1.12
-1.04
-0.96
-0.88
-0.80
VOLTS vs SCE

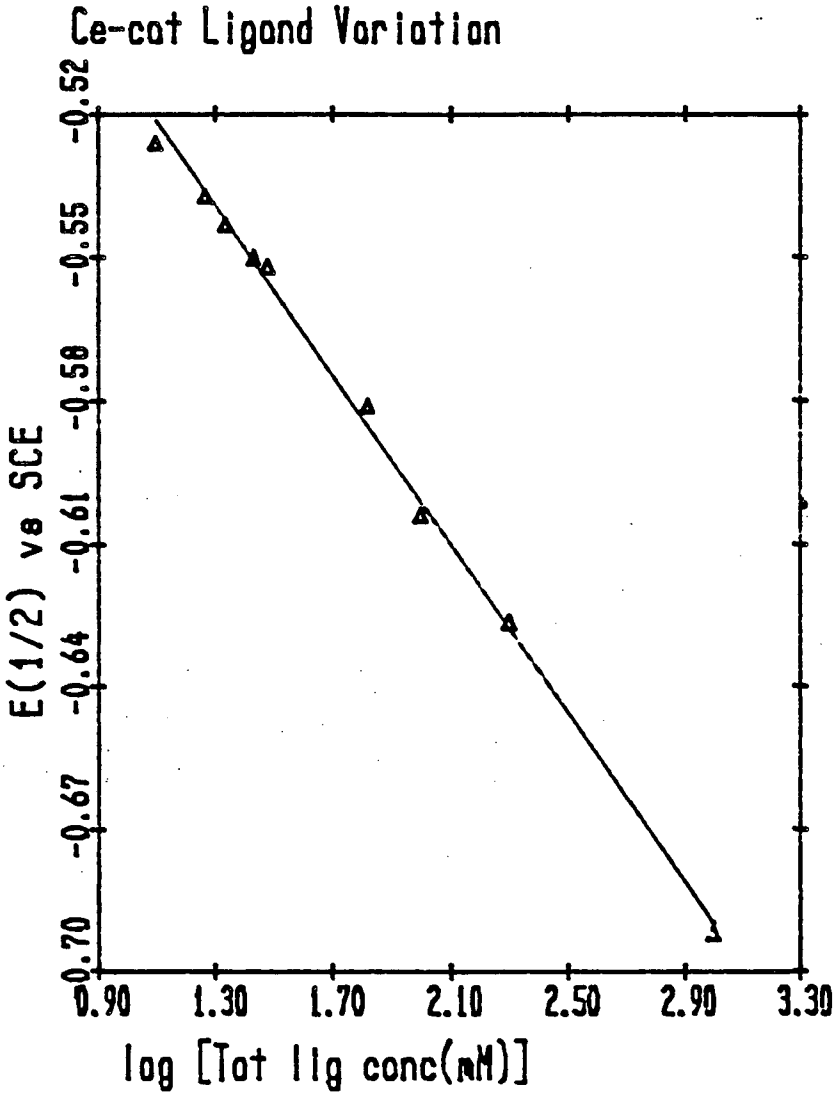
Ce-cat Ligand Variation
E(1/2) vs SCE
-0.52
-0.55
-0.58
-0.61
-0.64
-0.67
-0.70
0.90
1.30
1.70
2.10
2.50
2.90
3.30
log [Tot llg conc(mM)]

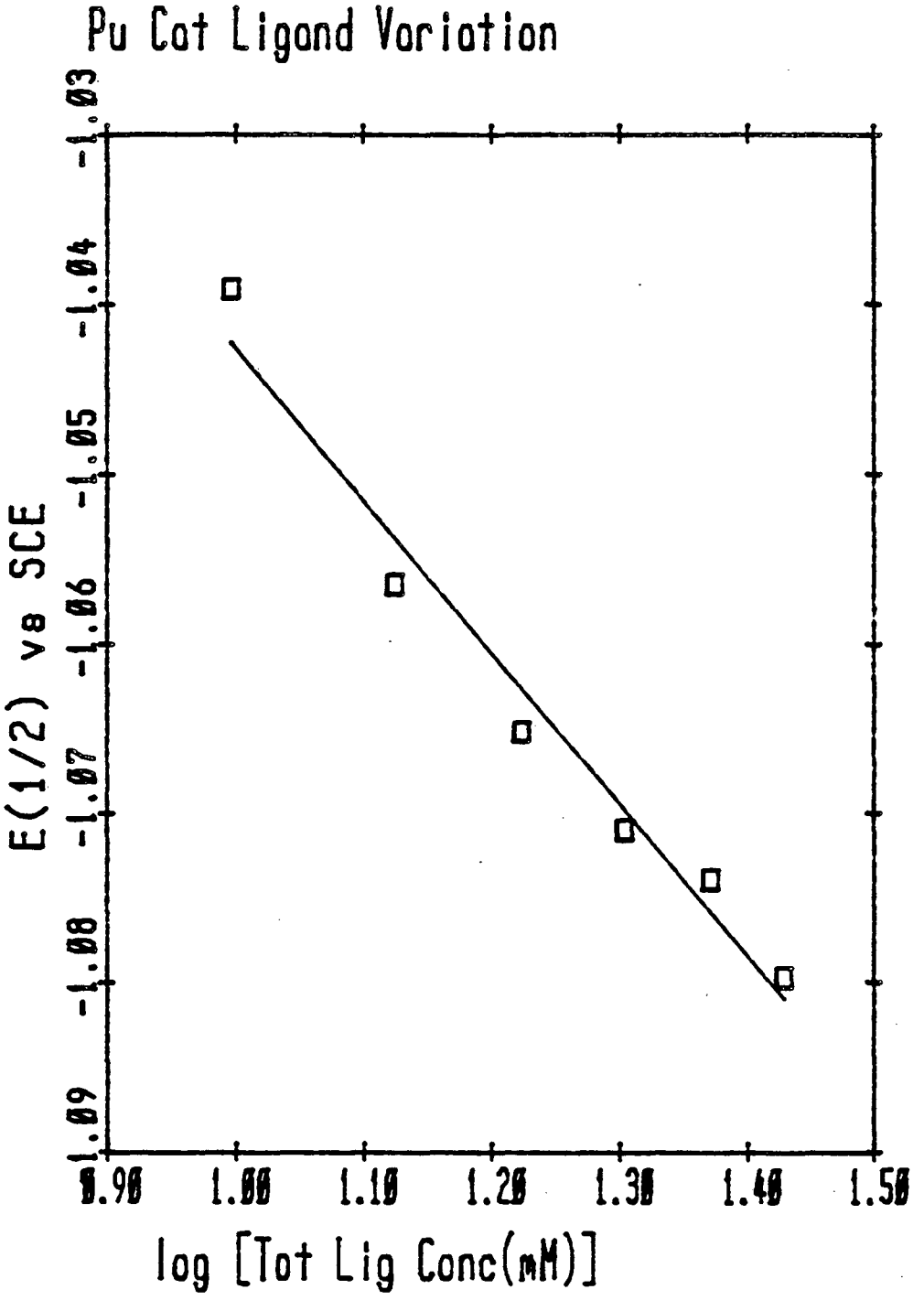
Pu Cat Ligand Variation
E(1/2) vs SCE
-1.03
-1.04
-1.05
-1.06
-1.07
-1.08
-1.09
0.90
1.00
1.10
1.20
1.30
1.40
1.50
log [Tot Lig Conc(mM)]

XBL 833-8709

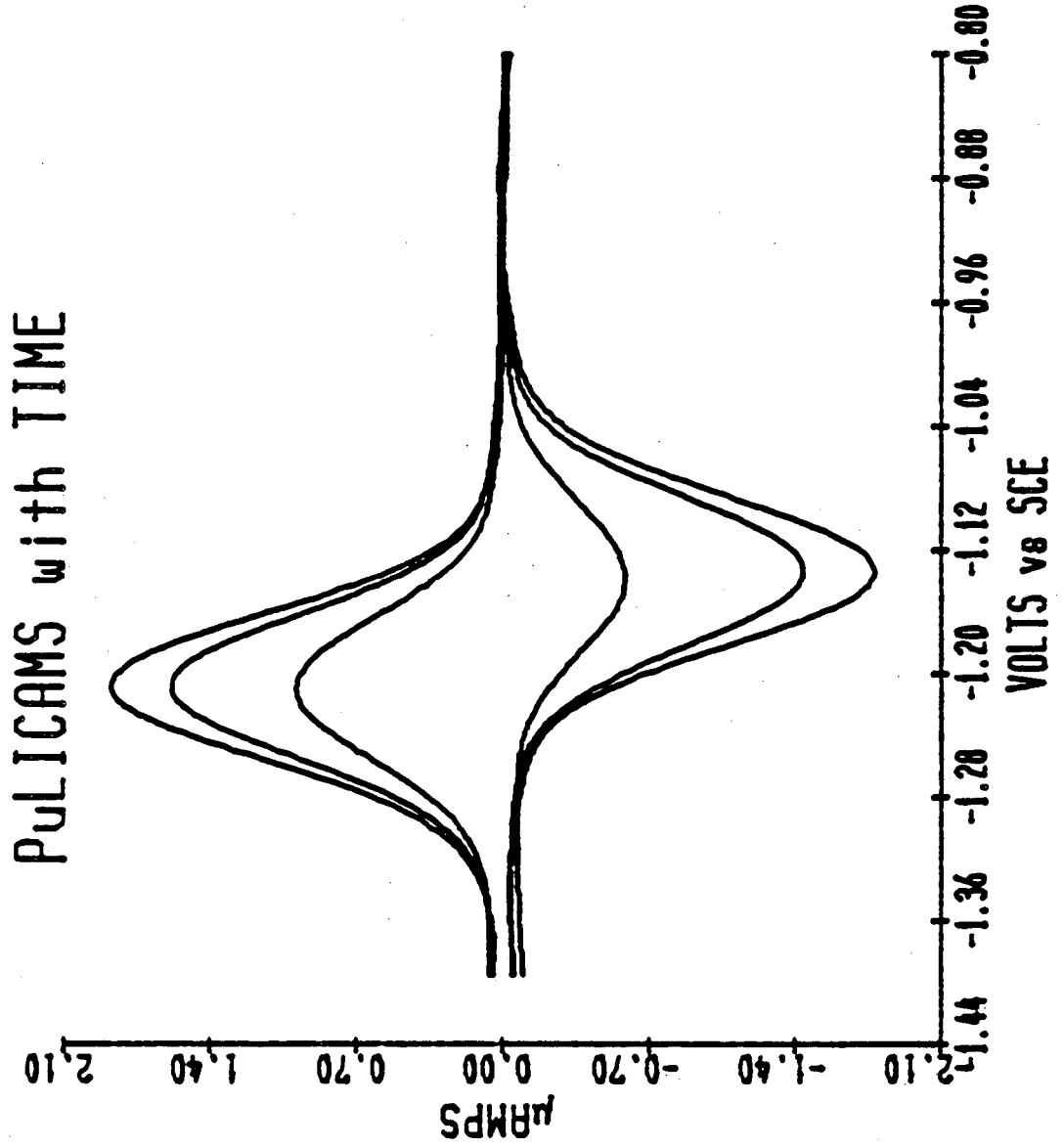
PuLICAMS with TIME
μAMPS
2.10
1.40
0.70
0.00
-0.70
-1.40
-2.10
VOLTS vs SCE
-0.80
-0.88
-0.96
-1.04
-1.12
-1.20
-1.28
-1.36
-1.44

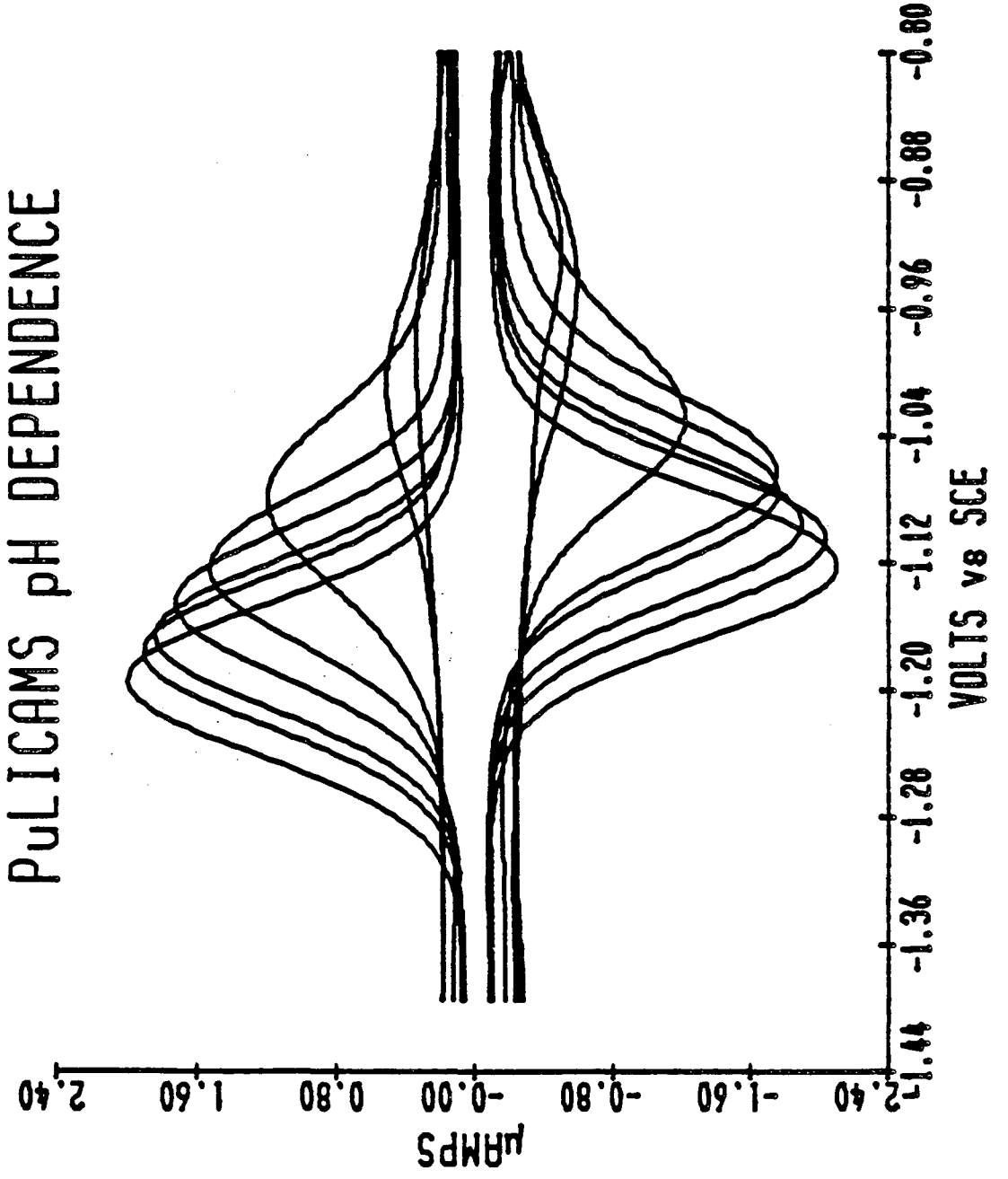
PuLICAMS pH DEPENDENCE
μAMPS
2.40
1.60
0.80
-0.00
-0.80
-1.60
-2.40
-1.44
-1.36
-1.28
-1.20
-1.12
-1.04
-0.96
-0.88
-0.80
VOLTS vs SCE

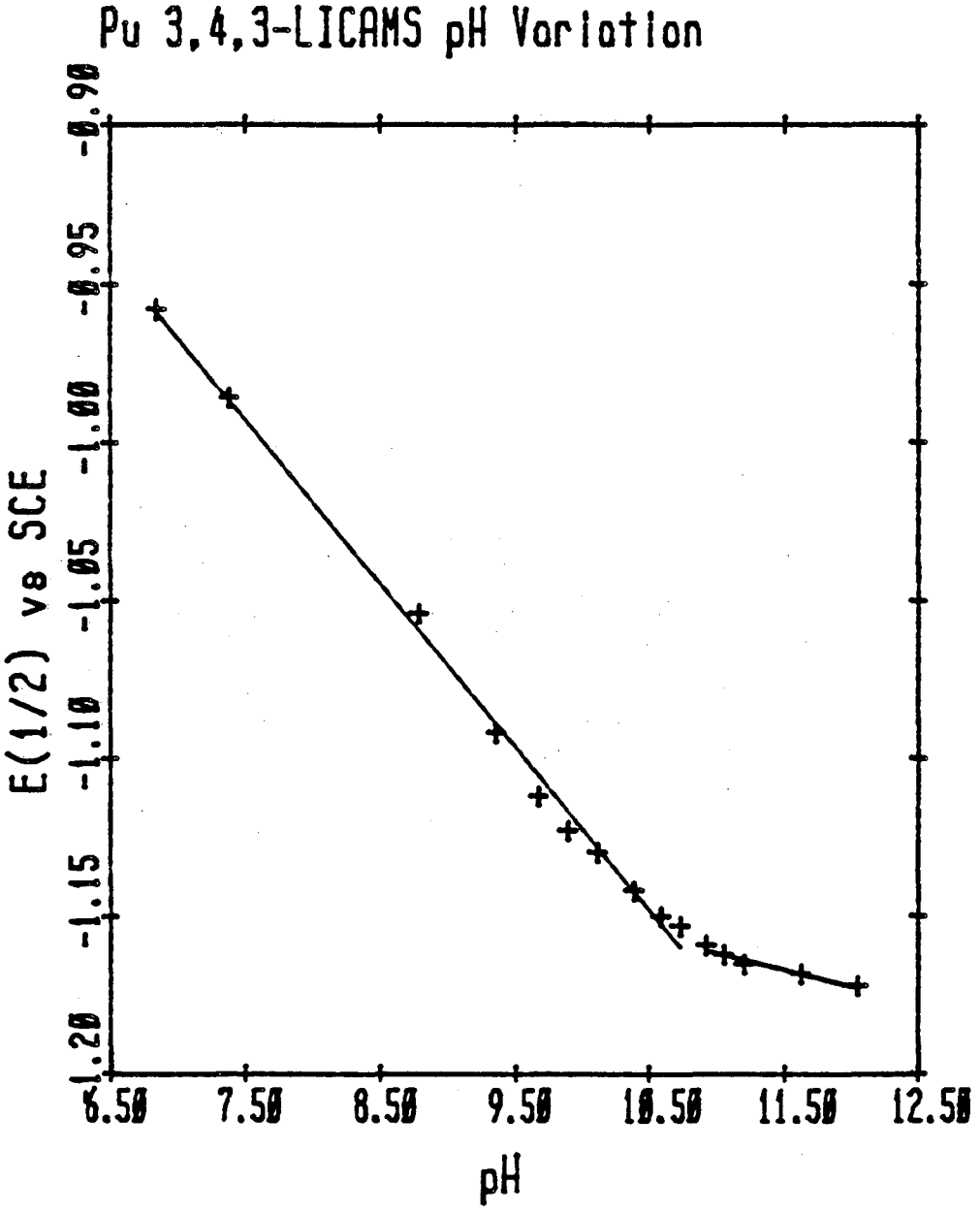
Pu 3,4,3-LICAMS pH Variation
E(1/2) vs SCE
-0.90
-0.95
-1.00
-1.05
-1.10
-1.15
-1.20
6.50
7.50
8.50
9.50
10.50
11.50
12.50
pH

XBL 833-8710

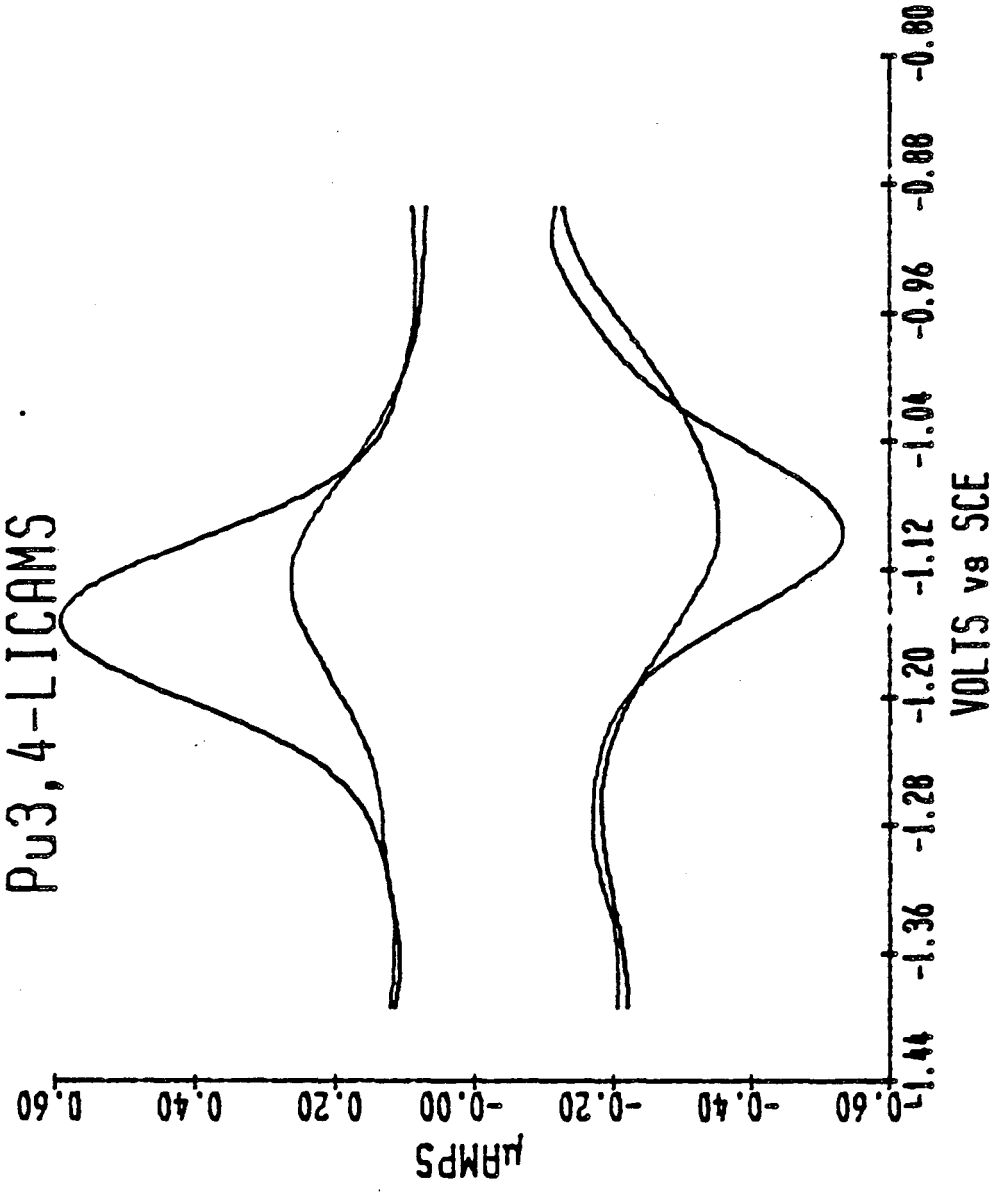
Pu3,4-LICAMS
μAMPS
0.60
0.40
0.20
0.00
-0.20
-0.40
-0.60
VOLTS vs SCE
-0.80
-0.88
-0.96
-1.04
-1.12
-1.20
-1.28
-1.36
-1.44

A

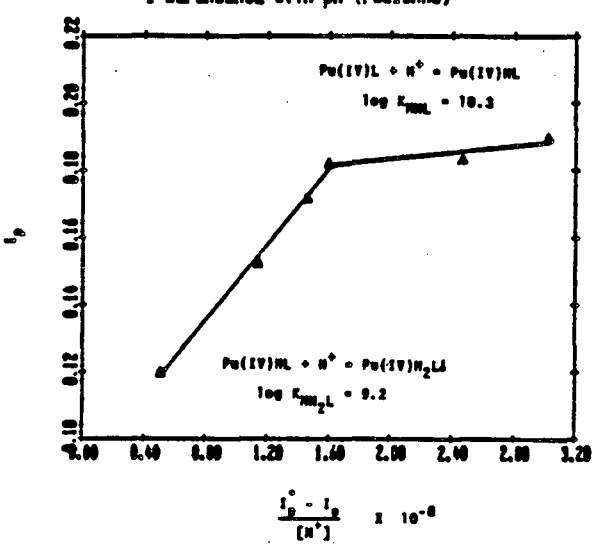
I DEPENDENCE with pH (PuLICAMS)
Pu(IV)L + H+ = Pu(IV)ML
log K = 10.3
Pu(IV)ML + H+ = Pu(IV)H2L
log K = 9.2
I0 - I / [H+] x 10-8

B

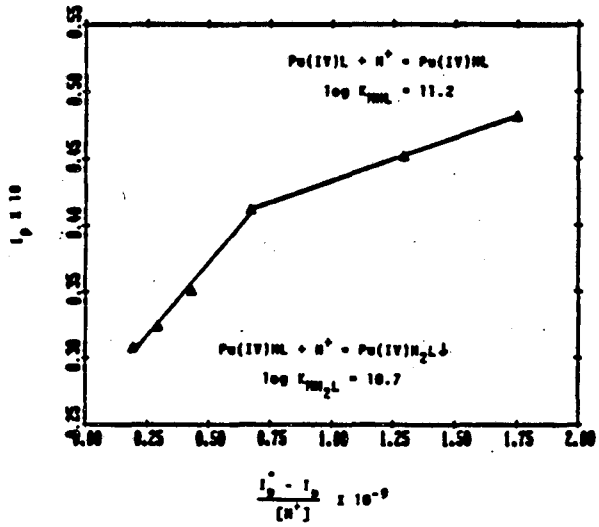
I DEPENDENCE with pH (Pu3.4LICAMS)
Pu(IV)L + H+ = Pu(IV)ML
log K = 11.2
Pu(IV)ML + H+ = Pu(IV)H2L
log K = 10.7
I0 - I / [H+] x 10-9

C

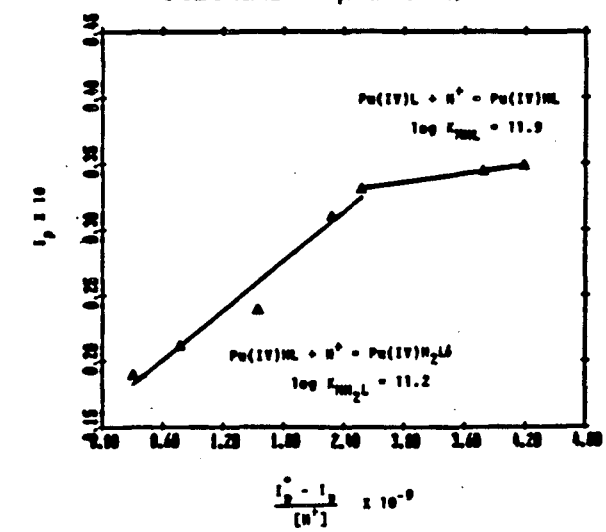
I DEPENDENCE with pH (PuLICAMC)
Pu(IV)L + H+ = Pu(IV)ML
log K = 11.9
Pu(IV)ML + H+ = Pu(IV)H2L
log K = 11.2
I0 - I / [H+] x 10-9

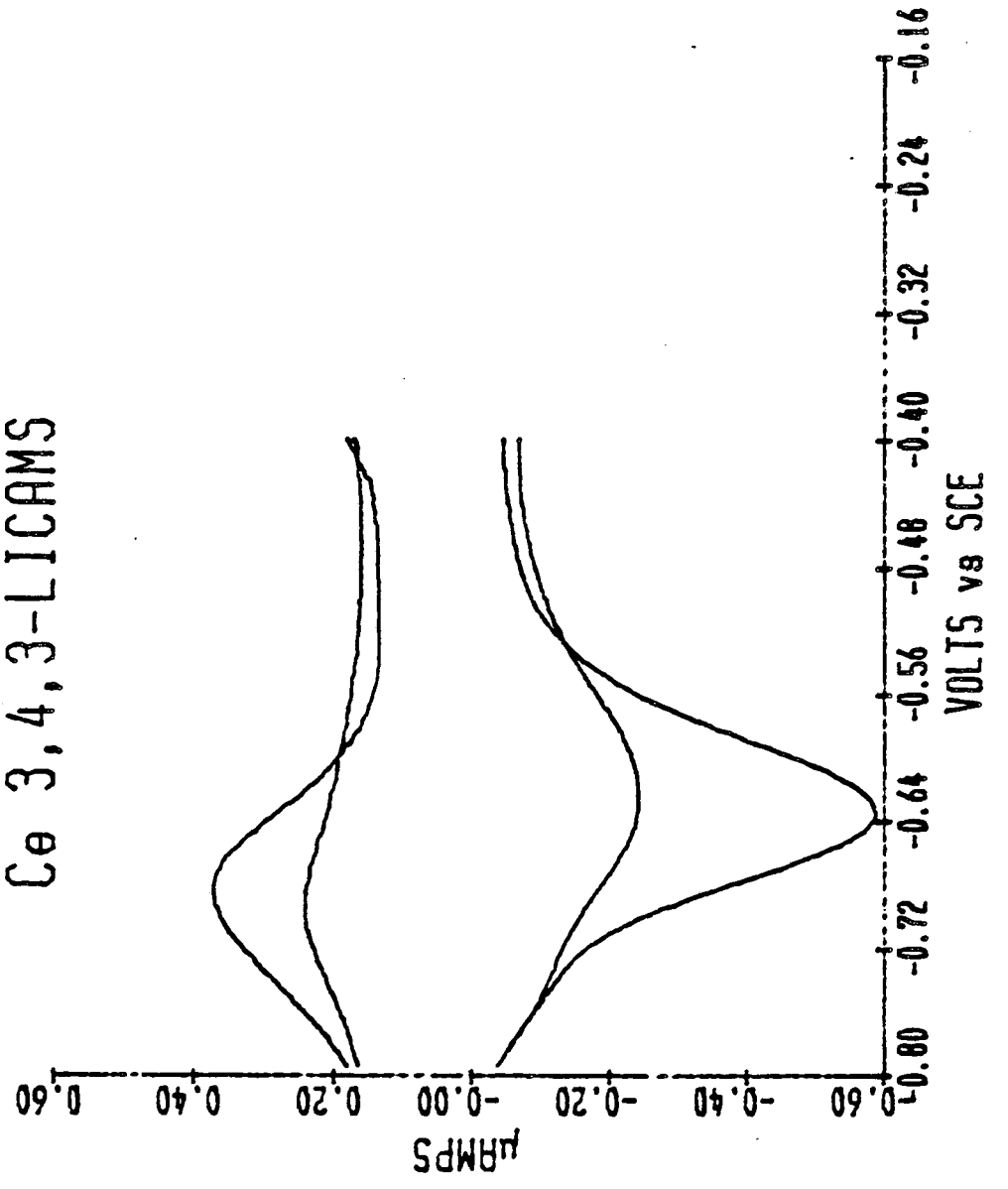
Ce 3,4,3-LICAMS
μAMPS
0.60
0.40
0.20
-0.00
-0.20
-0.40
-0.60
VOLTS vs SCE
-0.16
-0.24
-0.32
-0.40
-0.48
-0.56
-0.64
-0.72
-0.80

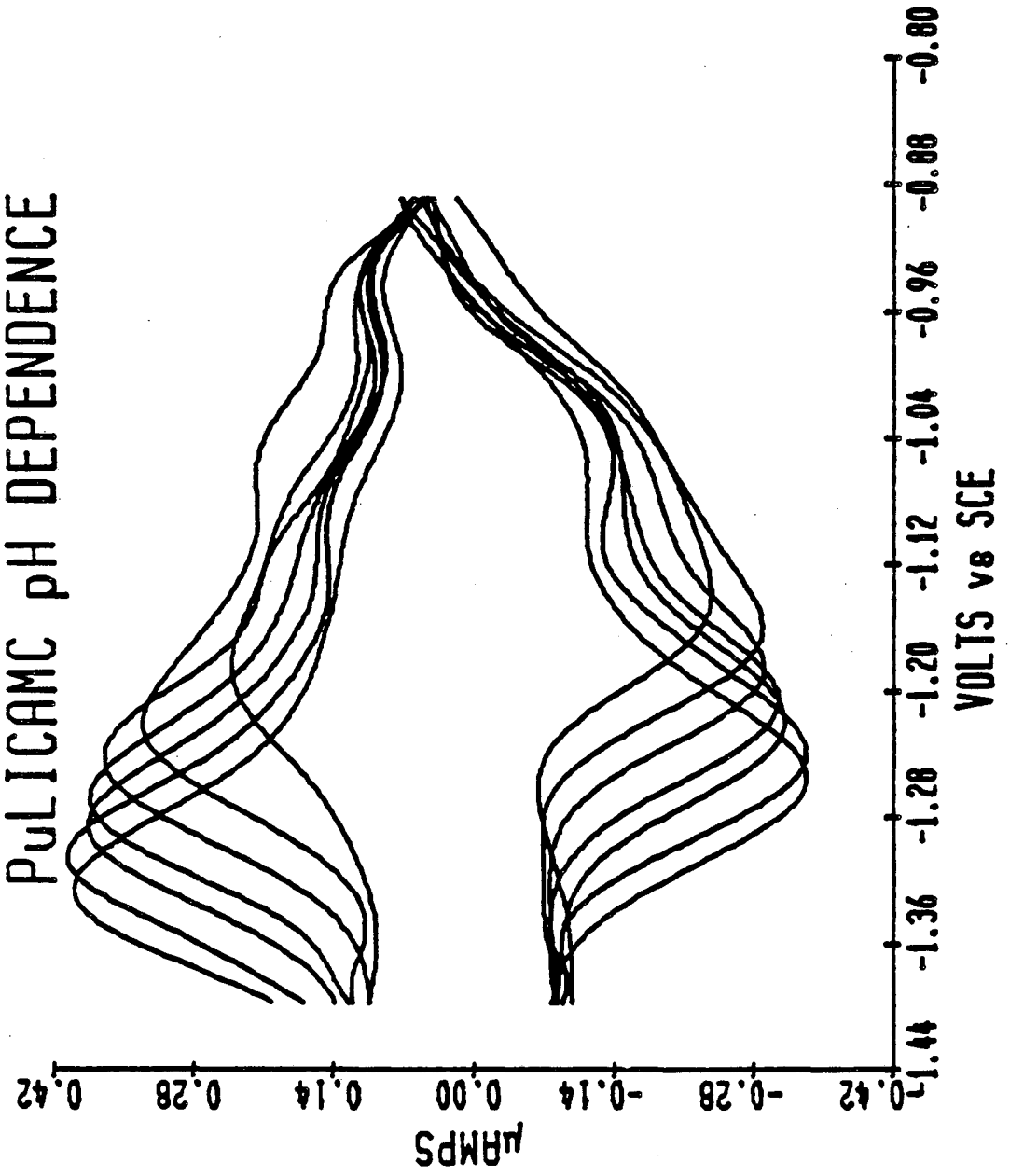
PuLICAMC pH DEPENDENCE
μAMPS
0.42
0.28
0.14
0.00
-0.14
-0.28
-0.42
VOLTS vs SCE
-1.44
-1.36
-1.28
-1.20
-1.12
-1.04
-0.96
-0.88
-0.80

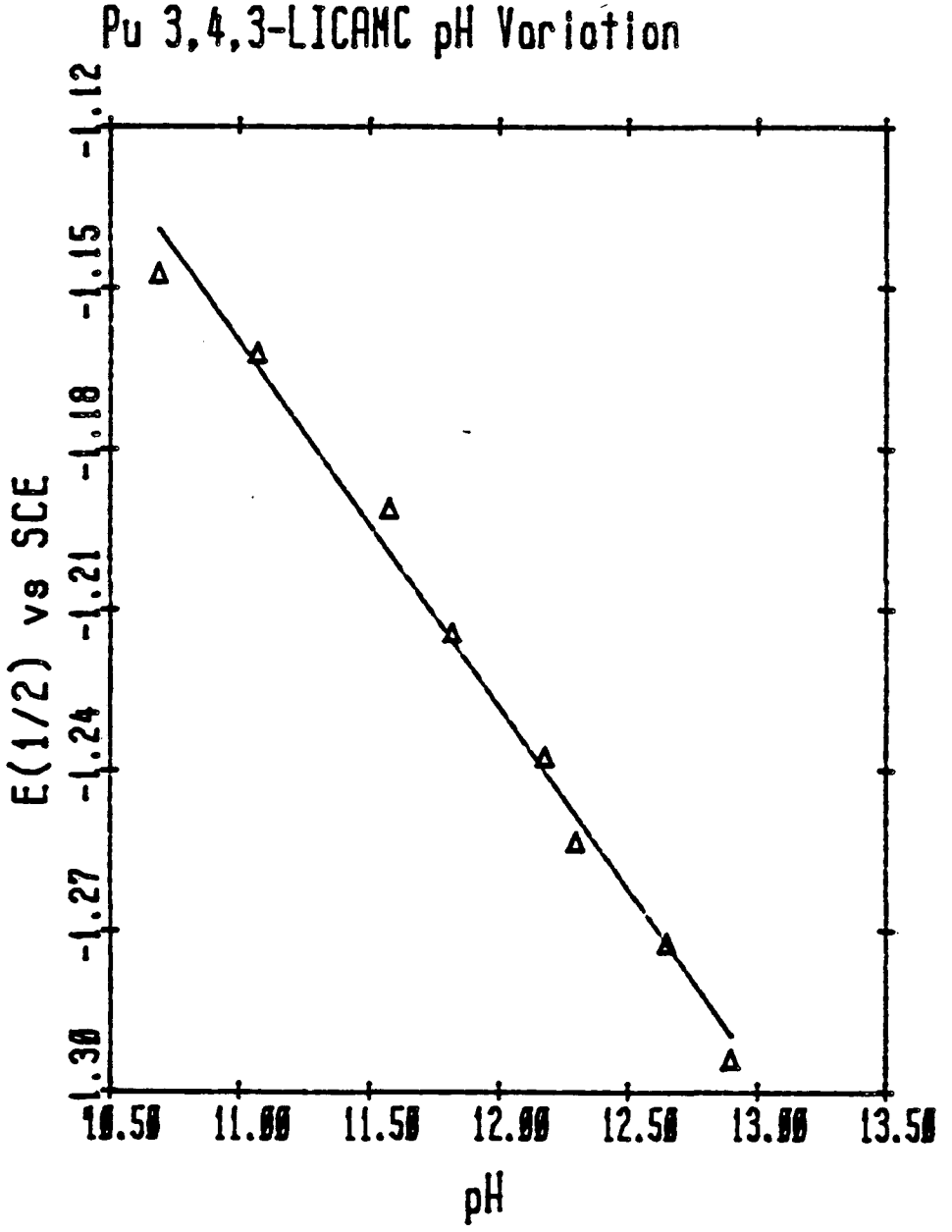
Pu 3,4,3-LICAMC pH Variation
E(1/2) vs SCE
-1.12
-1.15
-1.18
-1.21
-1.24
-1.27
-1.30
10.50
11.00
11.50
12.00
12.50
13.00
13.50
pH

XBL 833-8711

SUMMARY OF PU-CATECHOYLAMIDE COMPLEXATION

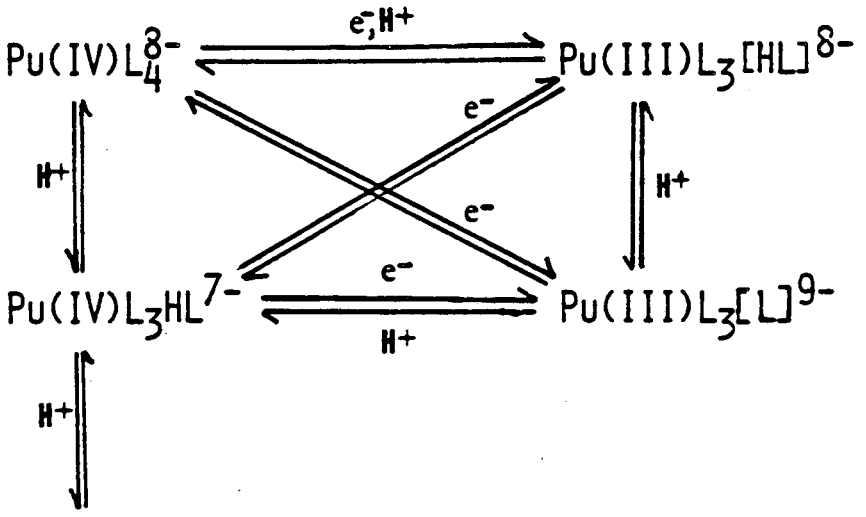

L = BOUND LIGAND ARM [L] = FREE LIGAND ARM

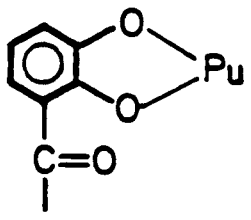

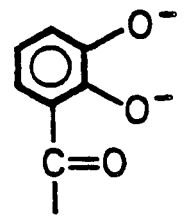

CHAPTER V

Complexation of Americium by Catecholate Ligands

The previous chapter was concerned with the nature of complexation of plutonium(IV) and plutonium(III) with catecholate ligands. These studies were prompted by test results which indicated that synthetic catechoylamide ligands were effective *in vivo* sequestering agents for Pu(IV).[1,2] Likewise, the study of americium-catecholate complexation was prompted by the puzzling results of *in vivo* experiments in mice and dogs on americium removal by 3,4,3-LICAMS and 3,4,3-LICAMC (*vide infra*).[3]

Earlier (Chapter II) the specificity of 3,4,3-LICAMS for metal ions of high charge to ionic radius ratios was demonstrated by thermodynamic measurements.[4] Most biologically significant metal ions are divalent ions and this study did not investigate the stability of catecholates with trivalent ions that have smaller charge to ionic radius ratios than Fe(III). Therefore, a study of lanthanide(III) catecholate complexes in solution was begun and continues.[5] The

trivalent lanthanides have been used extensively as models for trivalent actinides, since size variations between homologs of the two rows are small.[6] In particular, studies with catecholate ligands have concentrated on complexation by Eu(III), the homolog of Am(III).

Originally it was thought that complexation of Am(III) in vivo by catecholate ligands would not be of suffcient stability to remove Am(III) from test animals. Surprisingly, dogs injected with americium(III), followed 30 minutes later by injections of 3,4,3-LICAMS or 3,4,3-LICAMC, excreted 34% and 29%, respectively, of the Am after seven days. (Controls excreted 11%).[3] The calcium, trisodium salt of diethylenetriaminepentaacetic acid ($CaNa_3DTPA$), the current therapeutic chelating agent for Am, is much more efficient at sequestering Am under similar conditions (83% excreted).

The plasma clearance curves for americium-treated dogs following injection of the catecholate ligand are particularly unusual (Figure 5.1).[3] These curves indicate that the dogs injected with the catechol ligand increase and retain the amount of Am in the plasma. What is more, the slope of the lines following injection of LICAMS or LICAMC were similar to the slope of plasma clearance curves for untreated dogs injected with Pu(IV). The conclusion reached was that the injected catecholate induced the americium to circulate as a very stable transferrin complex, just as plutonium(IV) circulates. Such protein complexes are not filtered out of the plasma and even though Am(III) is known to form complexes with transferrin; they are of limited stability, just as for the lanthanide(III) ions.[7,8] (See the decrease in concentration for the "untreated" clearance curve.) The

increase of Am in the plasma following injection of catecholate ligand can be then attributed to the dynamic equilibrium that exists between extra-cellular fluid and the circulation, i.e., the Am can get in the plasma, but once in, it forms a very stable complex with transferrin and does not exit.

One possible explanation is that the catecholate ligand is facilitating oxidation of Am(III) to Am(IV) and promoting the formation of a very stable transferrin complex. The previous chapter discussed the ability of catechol to stabilize higher oxidation states of cerium and plutonium, as indicated by negative shifts of the (IV)/(III) reduction potential of 1.91 to 2.16 volts for 3,4,3-LICAMS and 3,4,3-LICAMC (Table I of Chapter IV). However, the Am(IV)/(III) reduction couple is very high and requires an extraordinary stabilization of Am(IV) to give a complex stable in aqueous solution. Many workers have given estimates for the Am(IV)/(III) reduction potential and they range between +2.0 to +2.9 V versus NHE.[9-13] Thus, stabilization of the Am(IV) oxidation state in vivo would require a shift in potential at least below +0.8 volts upon complexation of the catecholate ligand, providing that oxygen be the oxidant.

Before any electrochemical experiments on americium solutions were attempted it was necessary to study the electrochemistry of the catecholate ligands themselves. Of course, catechol will oxidize to the semiquinone and then the quinone however, this oxidation occurs at more positive potentials for catecholate ligands with electron-withdrawing groups on the ring,[14] such as the sulfonate and carbonyl groups present in 3,4,3-LICAMS. In addition, the

effectiveness of a relatively new electrode, reticulated vitreous carbon (RVC)[15] was to be assessed to operate in the potential range studied (-0.3 to +1.0 V vs. NHE). RVC is actually a by-product of glassy carbon, another commonly used electrode material. It is an inexpensive, mechanically very stable material with a large surface area, as it is essentially porous carbon. In neutral aqueous solution it has a range of -1.0 to +1.0 V versus NHE, but the reductive region is severely limited under the basic conditions employed for these experiments.

This chapter includes the study of the electrochemistry of catechol, 4-nitrocatechol, tiron, 3,4,3-LICAMS, and 3,4,3-LICAMC on reticulated vitreous carbon in 0.1 M KOH. The complexation of americium by 3,4,3-LICAMS and 3,4,3-LICAMC is also studied at various pH values.

I wish to express special thanks to Bob Silva and Heino Nitsche of Lawrence Berkeley Laboratory for making these experiments possible.

Experimental

Reagents. Chapter IV details the source and purification of the monocatecholate ligands used. The syntheses of 3,4,3-LICAMS and 3,4,3-LICAMC are found elsewhere.[2,16]

The americium, primarily ^{243}Am, was obtained through the Department of Energy's National Heavy Element Production Program at Oak Ridge. Initial purification was made via cation-exchange chromatography using ammonium alpha-hydroxyisobutyrate (0.4 M, pH 4.05, room temperature) as eluant.[17] The column was a 10 cm long by

0.5 cm diameter bed of Dowex 50X12 cation exchange resin from Biorad. Resin particle size was approximately 50 μm diameter. This column is used for interactinide separations but also gives some elemental purity. Before use, a final purification via cation exchange chromatography by using HCl as eluant was made to remove remaining contaminants, e.g., butyrate, silica, inorganic salts, Fe, etc.[18] The americium fraction from the first column was made 0.1 M in HCl and loaded onto a 11 cm long by 0.5 cm diameter Dowex 50X8 cation exchange resin bed. Resin particle size was 50 μm diameter. The column was washed with 3 column volumes of 0.1 M HCl and 3 column volumes of 3 M HCl to elute contaminants. The Am(III) was then eluted with 6 M HCl. Spark emission spectroscopy[19] and α-particle energy analysis verified sample purity. The concentration of Am(III) was determined by α-particle radiometry ([Am(III)] = 4.02 mM ± 0.3). The stock solution was stored in a test tube encased by lead.

Electrochemical and Spectral Measurements. A new glove box was prepared for electrochemical work with ^{243}Am. Holes were drilled for cables to the potentiostat and to the pH meter.

Electrochemical measurements were performed with the microcomputer-controlled system described in Chapter IV. All measurements were done with the IBM EC225 potentiostat using only differential pulse voltammetry.

The cell was a reduced volume cell (5 mL) from Princeton Applied Research (PAR). The electrodes used were a saturated calomel electrode as reference, a Pt wire as auxilliary electrode, and reticulated vitreous carbon as the working electrode. The RVC

electrode was made by punching out a piece of RVC with a cork borer, mounting it in pyrex tubing with a Pt wire from the RVC to the alligator clamp of the potentiostat cable, and securing the RVC to the pyrex tubing with 5-minute epoxy.

All measurements were performed at room temperature at 1.0 M ionic strength (0.9 M KCl/0.1 M KOH) in total volumes of 5.0 mL under argon. Typical ligand concentrations were about 1 mM, while americium concentrations were usually 0.1 mM.

Spectral measurements of the Am solutions were done on a Cary 17 spectrophotometer at slow scan rates (0.1 nm/second) and narrow slit widths, resulting in 0.2 nm resolution.

Results and Discussion

Ligand Electrochemistry. Although the oxidation of catechol has been studied by polarography and chronopotentiometry on graphite electrodes at pH 5 indicating reversible behavior and a two electron oxidation to the quinone at about +0.55 V versus NHE,[20-22] there is little in the literature concerning catechol electrochemistry in basic solutions under conditions where one or both phenolic oxygens are deprotonated. Earlier work by Kvalnes[14] and also by Fieser[23] relied on determination of the reduction potential of various o-benzoquinones in acidic alcohol/H_2O mixtures by use of potentiometry.

It is well established that electron-withdrawing groups present on the catechol ring will increase the stability of the reduced species toward oxidation. In fact, both Kvalnes and Fieser studied the effects of ring substituents on the reduction potential of

o-benzoquinone.[14,23]

Figure 5.2 illustrates the differential pulse voltammograms of catechol, tiron, and 4-nitrocatechol on an RVC electrode in 0.1 M KOH and 0.9 M KCl. The potentials are listed in Table I. The irreversible behavior observed at high pH values is not unusual since the oxidized product of catechol is known to be unstable.[23] This gives rise to much smaller currents for the reduction waves. The value obtained for the $E_{\frac{1}{2}}$ of catechol (+0.095 vs. NHE) is in excellent agreement with the value obtained by Ball and Chen at pH 12-13 in aqueous media by titration with ferricyanide (+0.052 to +0.092V vs. NHE).[24] As one would expect, the potential of all catechol derivatives is extremely pH dependent. The peak width at half height for catechol, tiron, and 4-nitrocatechol indicates that oxidation is a one electron process. This does not make sense if we are considering the formation of the o-quinone as the final product. Ball and Chen also observed a peculiarity in their measurements at high pH, namely a one-electron process. The reasons for this are not understood.[24]

Comparison of the relative reduction potentials of tiron, 4-nitrocatechol, and catechol in Table I reveals the anticipated trend; the nitro group of 4-nitrocatechol stabilizes the catechol ring toward oxidation by combined resonance and inductive effects.

The differential pulse voltammograms of 3,4,3-LICAMS and 3,4,3-LICAMC are illustrated in Figure 5.3 with $E_{\frac{1}{2}}$ values for the ligands in Table I. The oxidation of these ligands is very complex, although a yellow color is observed around the electrode at potentials

more positive than +0.34 for 3,4,3-LICAMS and +0.23 for 3,4,3-LICAMC (vs. SCE). This yellow color is common to oxidized catechols. The currents become very large at potentials more positive than those shown in Figure 5.3. A "prewave" for 3,4,3-LICAMC can be seen at about -0.10 V; it is not known whether this is attributable to catechol oxidation.

The most unusual aspect of Table I is that the 3,4,3-LICAMS and 3,4,3-LICAMC reduction potential is more positive than that of 4-nitrocatechol. This is not to be expected considering their relative pKa values (Table I).

The oxidation of all catechols studied has one common characteristic: huge currents. Concentrations of ligand ranged from about 1 mM for the tetracatecholates to about 4 mM for the monocatecholates with currents ranging from 35 to 270 μA. Of course, a direct comparison of currents is not possible due to variation in electrode surface area in the RVC electrode, but nonetheless, typical currents for the cerium and plutonium-catecholate complexes at similar concentrations were 10-fold less. Thus, the chances of seeing the Am(IV)/(III)-catecholate couple should it be near the oxidation wave of the catechol are slim.

Americium Catecholate Complexation. The negative shift in the metal ion potential observed for Pu(IV)/(III)-catecholate and Ce(IV)/(III)-catecholate were greatest for the tetracatecholates 3,4,3-LICAMS and 3,4,3-LICAMC. It was decided that these ligands were to be the first investigated with americium for this reason. Addition of Am(III) (≈0.1 mM) to a solution of 3,4,3-LICAMS or 3,4,3-LICAMC

(≈1 mM) at pH 13 resulted in no precipitate formation. Since Am(III) will form a hydroxide precipitate at this pH without catecholate ligand,[25] it was assumed that complexation by catechol was occurring. Also, the 3,4,3-LICAMS solution, normally pale yellow, turned lime-green upon addition of Am(III).

Differential pulse voltammetry of Am(3,4,3-LICAMS) and Am(3,4,3-LICAMC) from -0.4 to +0.7 V vs. SCE at slow scan rates (1.5 mV/second) showed only electrochemistry associated with the ligand. Holding the potential at positive values overnight to promote formation of an Am(IV)-catecholate complex at the electrode surface and subsequent stripping of the electrode gave no new peaks due to an Am(IV)/(III)-catecholate couple. It seems that, providing the negative shifts in the (IV)/(III) potential seen for plutonium and cerium are similar for americium, the free metal ion potential for Am(IV)/(III) must be at least +2.6 V vs. NHE. The Am(IV)/(III)-catecholate potential is probably more positive than the reduction potential for the free ligand, so it is not observable. This estimate of +2.6 volts versus NHE for the Am(IV)/(III) reduction potential is in agreement with a recent estimate by Hobart, et. al.[12] They used their measured value of the Am(IV)/(III)-carbonate potential to estimate the Am(IV)/(III) free ion reduction potential from known potential shifts of plutonium and cerium.

Upon lowering the pH a precipitate is formed in both the Am(3,4,3-LICAMS) (pH 10.0) and the Am(3,4,3-LICAMC) (pH 10.4) case. This is presumably due to some oligomerization process which occurs, although this is unclear. Results of tracer gel chromatography

experiments indicate that 3,4,3-LICAMS forms a complex with Am at pH 7.4 of higher molecular weight than the Pu complex.[3]

One method by which to determine whether or not an Am(III)-catecholate complex is formed is by visible spectroscopy. Free Am(III) has a large, sharp absorbance at 503 nm in acidic media due to a transition assigned as $^7F_0 \rightarrow {}^5L_6$ as well as a broad band at 812 nm due to a $^7F_0 \rightarrow {}^5F_6$ transition.[26] Upon complexation of Am(III) by various ligands these bands are known to shift and change in intensity. Figure 5.4 illustrates the spectral changes observed in the 503 nm band upon complexation by 3,4,3-LICAMS and 3,4,3-LICAMC. The spectrum of free Am(III) is of a diluted sample of stock Am(III), included for comparison (in HCl, pH 2). The sloping baseline in the Am- tetracatecholate spectra is due to partial oxidation of the ligand. Although the ligand solutions were prepared under argon and rigorously degassed, the transfer procedure into the cuvette causes a limited exposure to air and consequent partial oxidation of the free ligand. Nonetheless, the shift in the 503 nm band observed is conclusive evidence of complexation of Am(III) by 3,4,3-LICAMS and 3,4,3-LICAMC. Table II contains a summary of spectral characteristics.

It is noteworthy that the spectrum of Am(III) with 3,4,3-LICAMS and with 3,4,3-LICAMC are significantly different. This is indicative of a different type of bonding of the two tetracatecholates with Am(III). Although it is impossible to determine the identity of the coordinating groups, the 3,4,3-LICAMC ligand does possess carboxylate groups capable of coordinating Am(III). Polycarboxylateamines are

known to bind Am(III) with high affinity.[27]

The results of these experiments indicate that americium is probably not present as Am(IV) in vivo. Indeed, it proves that 3,4,3-LICAMS and 3,4,3-LICAMC form complexes with Am(III) of undetermined stoichiometry and stability. Titrations of Eu(III) with 3,4,3-LICAMS indicates that a complex is formed whereby 1.5 catechol arms bind Eu(III) at pH 5.5. At higher pH values, some hydroxide also appears to be involved in coordination and the titrations proceed slowly.[5] It would not be unreasonable to believe that the Am(III)(3,4,3-LICAMS) complex is similar.

Recently it has been established that monocatecholates can act as the necessary synergistic anion required in the binding of Fe(III) to transferrin, although the catecholates are not thermodynamically favored over the natural synergistic anion carbonate.[28] This does however establish the existence of ternary catechol-Fe(III)-transferrin complexes. One possible explanation for the unusual plasma clearance curves of the Am(3,4,3-LICAMS) and Am(3,4,3-LICAMC) is the existence of a ternary complex of tetracatecholate-Am-transferrin. Although such a ternary complex could never exist with Fe(III)(3,4,3-LICAMS) (because the 3,4,3-LICAMS would remove the Fe(III) from transferrin (Chapter III)), the Am(III)(3,4,3-LICAMS) complex may be of insufficient stability to remove Am(III) from transferrin and actually may facilitate formation of an Am(III)-transferrin complex by acting as a synergistic anion. Experiments with Eu(III)-transferrin could determine if this hypothesis were true.

Summary

Spectroscopic results indicate that the tetracatecholates, 3,4,3-LICAMS and 3,4,3-LICAMC, complex Am(III). The Am(IV)/(III)-catecholate couple (where catecholate=3,4,3-LICAMS or 3,4,3-LICAMC) is not observed, but may not be observable due to the large currents associated with ligand oxidation. However, within the potential range where ligand oxidation does not occur, these experiments indicate that the reduction potential of free Am(IV)/(III) is probably $\geq$ +2.6 V vs. NHE or higher.

Proof of the complexation of americium in the trivalent oxidation state by 3,4,3-LICAMS and 3,4,3-LICAMC eliminates the possibility of tetracatecholates stabilizing Am(IV) in vivo. An alternative explanation of the plasma clearance curves of Am(3,4,3-LICAMS) or Am(3,4,3-LICAMC) is the possible formation of a ternary catecholate-Am-transferrin complex.

REFERENCES

1. Durbin, P.W.; Jones, E.S.; Raymond, K.N.; Weitl, F.L.. Rad. Res. (1980), 81, 170.

2. Weitl, F.L.; Raymond, K.N.; Durbin, P.W., J. Med. Chem. (1981), 24, 203.

3. Lloyd, R.D.; Bruenger, F.W.; Atherton, D.R.; Jones, C.W.; Taylor, G.N.; Stevens, W.; Mays, C.W.; Durbin, P.W.; Jeung, N.; Jones, E.S.; Kappel, M.J.; Raymond, K.N.; Weitl, F.L., manuscript in preparation.

4. Kappel, M.J.; Raymond. K.N., Inorg. Chem. (1982), 21, 3437.

5. Zhu, Daohong; Kappel, M.J.; Raymond, K.N., manuscript in preparation.

6. Shannon, R.D., Acta Crystallogr. A32 (1976), Section 5, 751.

7. Durbin, P.W., "Handbook of Experimental Pharmacology, Vol. 36, Uranium, Plutonium, Transplutonic Elements" Springer-Verlag: Berlin (T973), 739.

8. Luk, C.K., Biochemistry (1971), 10, 2838.

9. Morss, L.R.; Fuger, J., J. Inorg. Nucl. Chem. (1981), 43, 2059.

10. Cunningham, B.B., Ann. Rev. Nucl. Sci. (1964), 14, 323.

11. Nugent, L.J.; Baybarz, R.D.; Burnett, J.L.; Ryan, J.L., J. Phys. Chem. (1973), 77, 1528.

12. Hobart, D.E.; Samhoun, K.; Peterson, J.R., Radiochimica Acta (1982), 31, 139.

13. Penneman, R.A.; Coleman, J.S.; Keenan, T.K., J. Inorg. Nucl. Chem. (1961), 17, 138.

14. Kvalnes, D.E., J. Am. Chem. Soc. (1934), 56, 2487.

15. Wang, J., Electrochimica Acta (1981), 26, 1721.

16. Weitl, F.L.; Raymond, K.N., J. Am. Chem. Soc. (1980), 102, 2289.

17. Choppin, G.R.; Harvey, B.G.; Thompson, S.G., Inorg. Chem. (1956), 2, 66.

18. Diamond, R.M.; Street, K.; Seaborg, G.T., J. Am. Chem. Soc. (1954), 76, 1461.

19. Conway, J.G.; Moore, M.F., Anal. Chem. (1952), 24, 463.

20. Elving, P.J.; Krivis, A.F., Anal. Chem. (1958), 30, 1648.

21. Gaylor, V.F.; Conrad, A.L.; Landerl, J.H., Anal. Chem. (1957), 29, 224.

22. Elving, P.J.; Krivis, A.F., Anal. Chem. (1958), 30, 1645.

23. Conant, J.B.; Fieser, L.F., J. Am. Chem. Soc. (1924), 46, 1858.

24. Ball, E.G.; Chen, T., J. Biol. Chem. (1933), 102, 691.

25. Schulz, W., "The Chemistry of Americium;" ERDA Critical Review Series (1976), ERDA Technical Information Center TID-26971, p. 50.

26. Shiloh, M.; Givon, M.; Marcus, Y., J. Inorg. Nucl. Chem. (1969), 31, 1807.

27. Site, A.D.; Baybarz, R.D., J. Inorg. Nucl. Chem. (1969), 31, 2201.

28. Loomis, L., personal communication.

29. Avdeef, A.; Sofen, S.R.; Bregante, T.L.; Raymond, K.N., J. Am. Chem. Soc. (1978), 100, 5362.

Table I. Half-Wave Potentials of Catecholate Ligands[a]

Ligand	$E_{1/2}$ vs. SCE	$E_{1/2}$ vs. NHE	pKa_2[b]
Catechol	-0.148 V	+0.095 V	9.2[c]
4-nitrocatechol	+0.080 V	+0.322 V	6.7[c]
Tiron	+0.026 V	+0.268 V	7.7[c]
3,4,3-LICAMS	+0.337 V	+0.579 V	7.2[d]
3,4,3-LICAMC	+0.229 V	+0.471 V	~8

[a]Determined at room temperature, μ = 1.0 M at pH 13.

[b] $Ka_2 = \frac{[H^+][HL]}{[H_2L]}$, for 3,4,3-LICAMS and 3,4,3-LICAMC pKa_2 is the dissociation of the phenolic oxygen ortho to the carbonyl.

[c]Ref 29.

[d]Ref 4.

Table II. Summary of Am(III) Spectra

	Band I[a] nm	Band II[b] nm
Free Am(III)	503(450)	812(77)
Am(III)(3,4,3-LICAMS)	507(822) 516(97) 523(24)	815(80)
Am(III)(3,4,3-LICAMC)	508(482) 520(59) 526(28)	830(126)

[a]Sharp band and satellites. Extinction coefficients in units of M^{-1} cm^{-1} are in parentheses.

[b]Broad band. Extinction coefficients in units of $M^{-1}cm^{-1}$ are in parentheses.

Figure Captions for Chapter V

Figure 5.1. ^{241}Am in plasma of young adult beagles injected with 30 μmole/kg of ligand 30 minutes after nuclide administration (first 3 hours).

Figure 5.2. Differential pulse voltammograms of catechol, 4-nitrocatechol, and tiron. [ligand] = 3 - 4 mM.

Figure 5.3. Differential pulse voltammograms of 3,4,3-LICAMS and 3,4,3-LICAMC. [ligand] = 1 mM.

Figure 5.4. Visible spectra of free Am(III) (0.20 mM, pH 2), Am(3,4,3-LICAMS) (0.12 mM, pH 13), Am(3,4,3-LICAMC) (0.12 mM, pH 13).

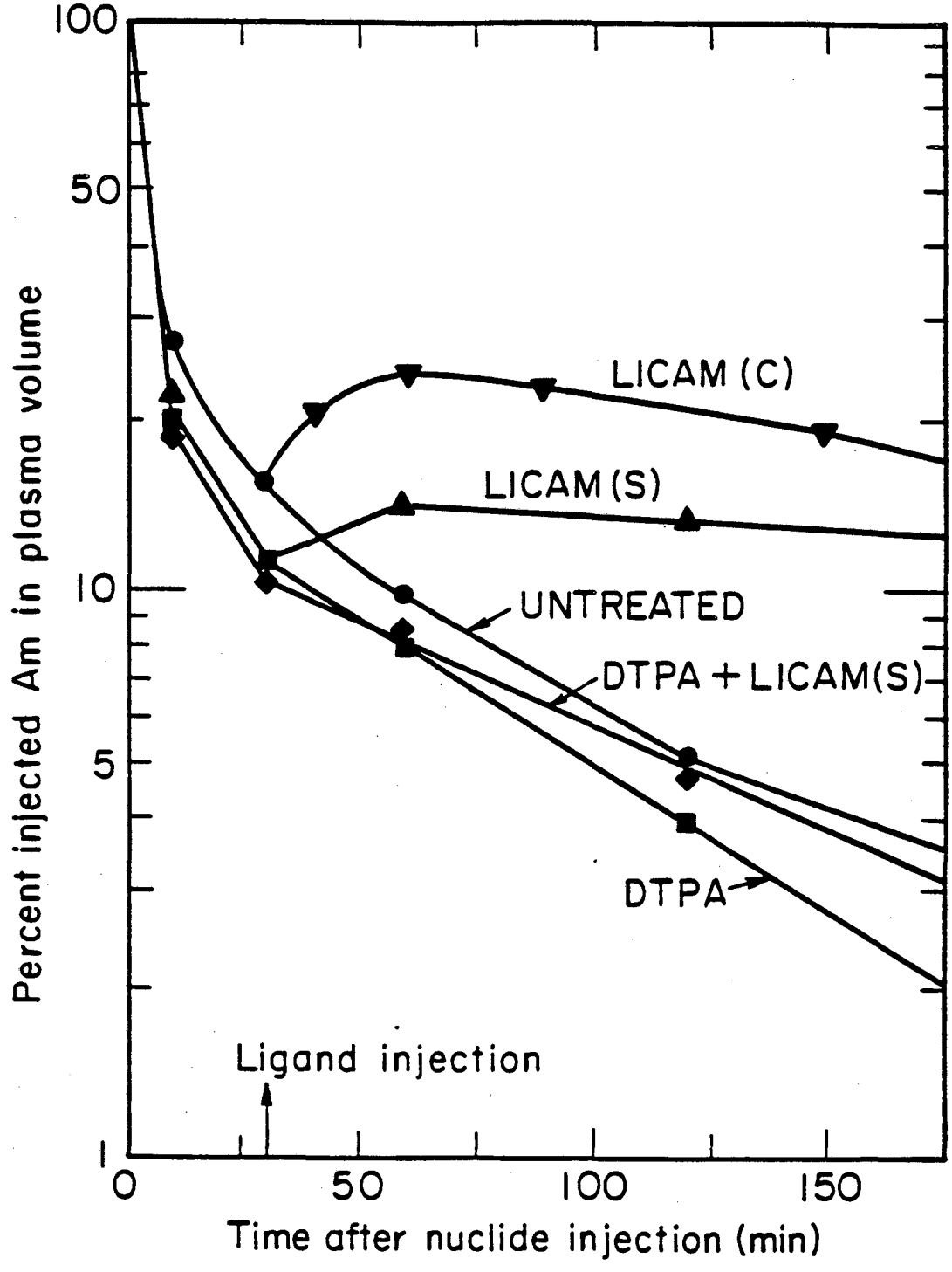
100
50
10
5
1
0
50
100
150
Percent injected Am in plasma volume
Time after nuclide injection (min)
LICAM (C)
LICAM (S)
UNTREATED
DTPA + LICAM(S)
DTPA
Ligand injection

XBL834-3695

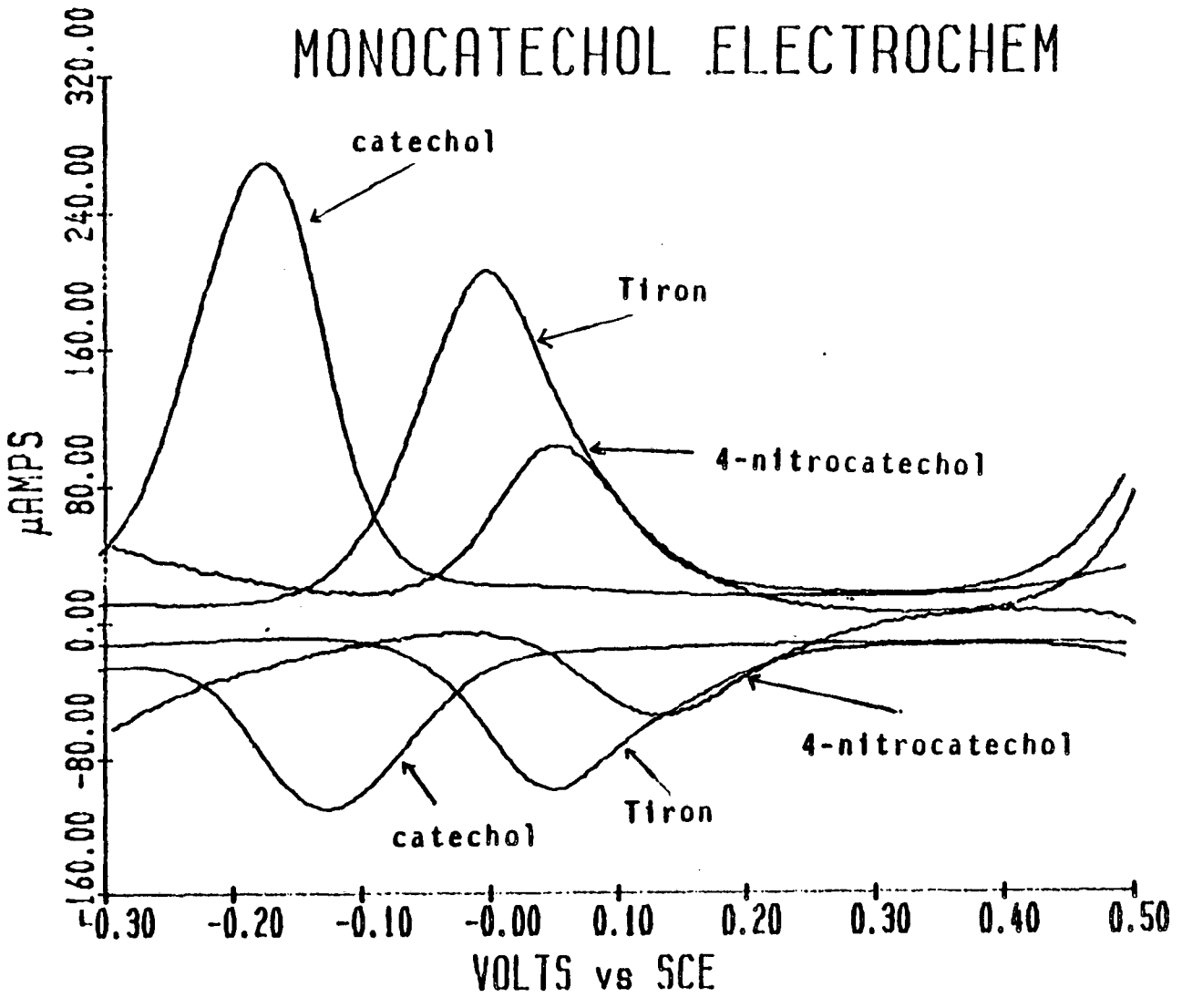
MONOCATECHOL ELECTROCHEM
catechol
Tiron
4-nitrocatechol
4-nitrocatechol
Tiron
catechol
μAMPS
320.00
240.00
160.00
80.00
0.00
-80.00
-160.00
-0.30
-0.20
-0.10
-0.00
0.10
0.20
0.30
0.40
0.50
VOLTS vs SCE

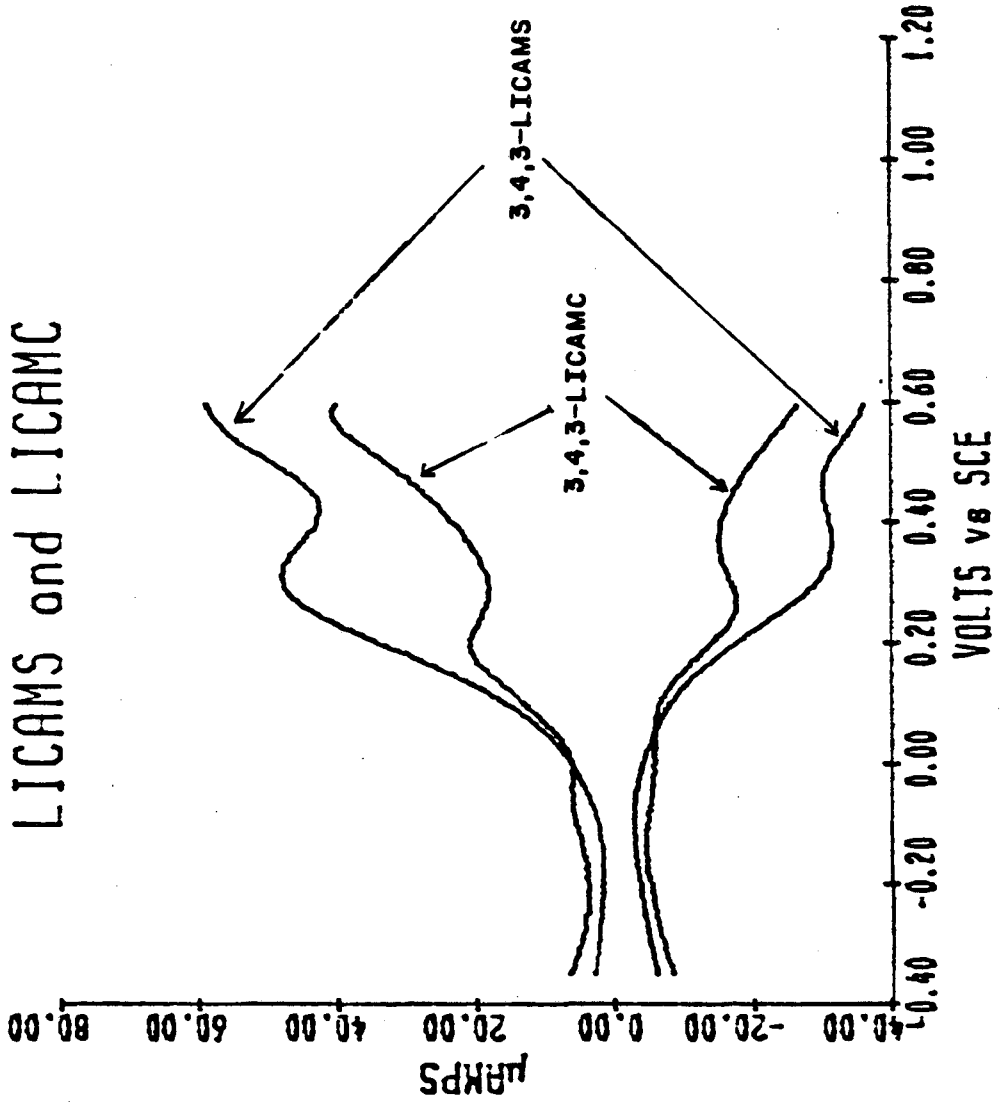
LICAMS and LICAMC
3,4,3-LICAMS
3,4,3-LICAMC
μAMPS
80.00
60.00
40.00
20.00
0.00
-20.00
-40.00
-0.40
-0.20
0.00
0.20
0.40
0.60
0.80
1.00
1.20
VOLTS vs SCE

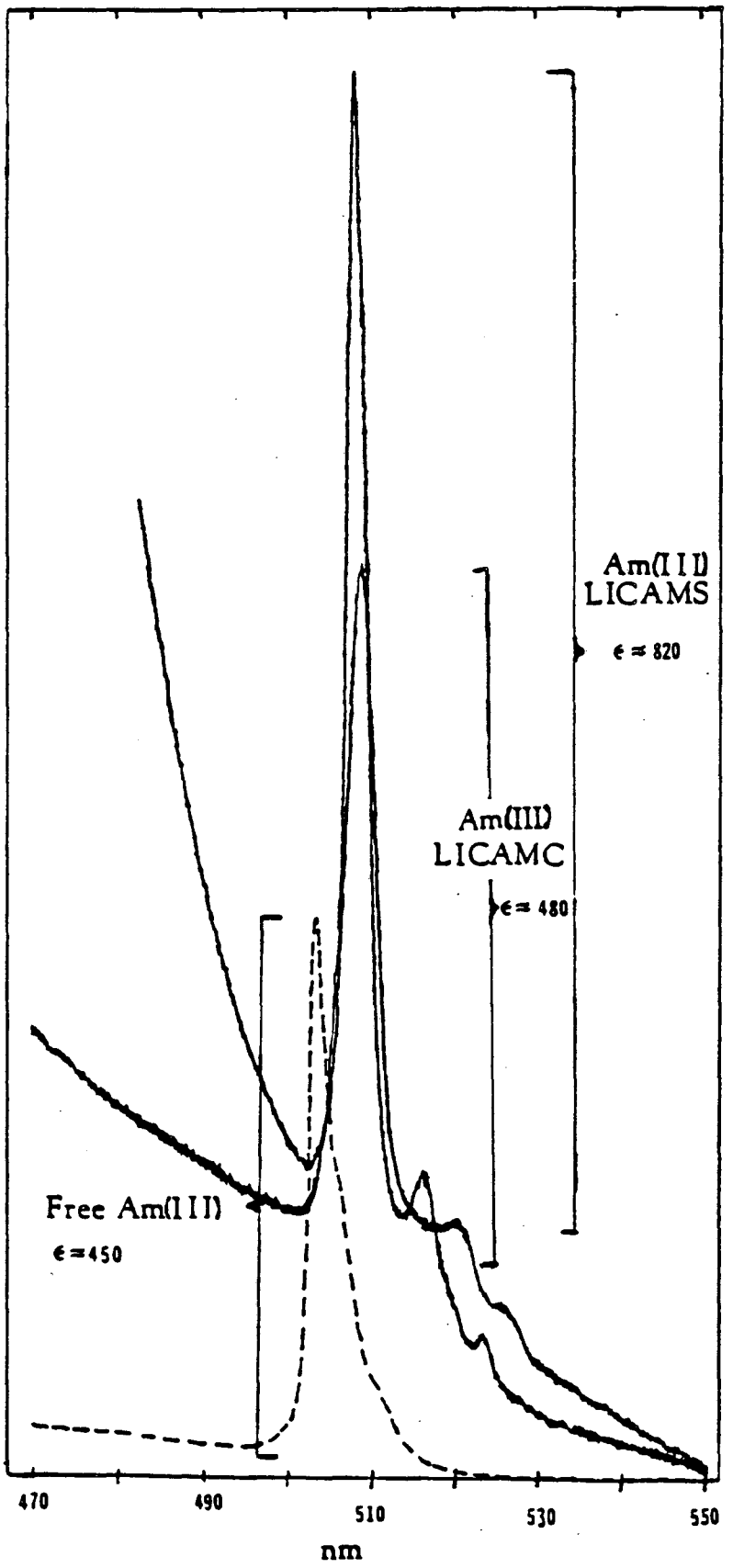
Am(III)
LICAMS
ε = 820
Am(III)
LICAMC
ε = 480
Free Am(III)
ε = 450
470
490
510
530
550
nm

APPENDIX

This supplement is provided to document the procedures by which the program BETA operates. BETA is a model-dependent non-linear least squares program used for the refinement of stability constants. Since Chapters II and III of this thesis depend largely on results obtained from BETA, it is appropriate that it be reviewed here. The term "model-dependent" implies that the identity of the species in solution must be known at least in part before attempting refinement of titration data. In addition, estimates of the formation constants to be refined must be made.

There are two main features of this program:

(1) A standard non-linear least squares program (ORGLS)[1] is used to refine stability constants based on differences in observed and calculated pH values.

(2) Calculated pH values are generated by a user's subroutine (CALC) which minimizes the difference between the known and calculated analytical concentration of each reacting specie.

In this manner, the program actually executes an algorithm (analytical derivatives) to output the calculated parameter (point 2) within a larger least squares framework (point 1).

SUBROUTINE CALC

The basic theory for development of the algorithm used (analytical derivatives) is presented in great detail elsewhere[2,3] and these references should be consulted before refinements are attempted. Subroutine CALC varies the initial estimates for free ligand, free metal, and free hydrogen with the given β values until

$$\left(Y_{T_{obs}} - Y_{T_{calc}}\right) \Big/ Y_{T_{obs}} < 10^{-3} \qquad (1)$$

where $Y_{T_{obs}}$ is the total known analytical concentration of each reacting specie and $Y_{T_{calc}}$ is the total calculated concentration of each reacting specie. When this criteria is met, the subroutine puts out a value for pH^{calc}.

Subroutine CALC is entered with estimates for free specie concentrations based on the first pH data point that is input. To minimize iterations the final values for free specie concentrations for the first calculated point which meets the criteria in (1) is used for the second calculated point and so on. The ouput only shows iterations for the first point.

PROGRAM ORGLS

ORGLS is a multi-use program for non-linear least squares refinement which supplies provisions to insert subroutines of choice, such as subroutine CALC for stability constant refinement and/or appropriate weighting schemes. It can also be used for refining formation constants for spectral data when provided with the appropriate subroutine.[4]

The endnotes in Chapters II and III describing the basic matrix equations for non-linear least squares refinement are expanded here.

Non-linear least squares solves for changes in the parameters given a set of trial (estimated) parameters. In this way it is different than linear least squares which solves for the parameters themselves that give "best fit" for the observations. Briefly, for the linear case, given m observations and n parameters (m> n) where a_j are the parameters, x_{ij} are the variables, and y_i^c are the

calculated values

$$y_i^c = \sum_{j=1}^{n} a_j x_{ij} \quad \underline{or} \quad \underline{y}^c = \underline{X}\,\underline{a} \tag{2}$$

Provided a set of observations, y_i^o, the objective is to minimize the disagreement between y_i^o and y_i^c to get the best values for the parameters, a_j. This can be accomplished by defining a residual, R, as

$$R = \sum_{i=1}^{m} (y_i^c - y_i^o)^2 \quad \underline{or} \quad R = (\underline{X}\,\underline{a} - \underline{y}^o)^T(\underline{X}\,\underline{a} - \underline{y}^o) \tag{3}$$

$$R = \underline{a}^T\underline{X}^T\underline{X}\underline{a} - 2\underline{a}^T\underline{X}^T\underline{y}^o + \underline{y}^{oT}\underline{y}^o$$

Differentiation of which gives

$$\frac{\partial R}{\partial a_j} = 2\sum_{i=1}^{m} (y_i^c - y_i^o)\,\frac{\partial y_i^c}{\partial a_j} \quad \underline{or} \quad \frac{dR}{d\underline{a}} = 2\,\underline{X}^T\underline{X}\underline{a} - 2\underline{X}^T\underline{y}^o \tag{4}$$

When set equal to zero equation (4) gives a minimum for function (3) and hence a "best fit" for parameters, a_j. The proof for this is found elsewhere.[5] Rearrangement of (4) gives

$$\underline{X}^T\underline{X}\underline{a} = \underline{X}^T\underline{y}^o \tag{5}$$

Provided $X^TX = 0$, then

$$\underline{a} = (\underline{X}^T\underline{X})^{-1}\ \underline{X}^T\underline{y}^o \qquad (6)$$

This is the solution for the best fit of parameters, a_j, given a set of observations, y_i^o, at values of variables, x_{ij}, for a linear problem.

In the refinement of stability constants non-linear least squares seeks to find values for the parameters, $\ln \beta_j$,[6] based on a set of estimated β's. From these estimated constants and estimates of the free metal, free ligand and free hydrogen concentrations (variables), one can use the pH value calculated (pH^c) for every point on the titration curve which then can be compared to the observed pH (pH^o). This problem is non-linear due to the (generally) non-linear dependence on hydrogen ion concentration.

Given $pH_i^c = f(\ln \beta_o)$ where β_o=estimated β's and i = no. of observations, define a residual

$$R = \sum_i (pH_i^c - pH_i^o)^2.$$

This is an alternate definition of residual than that described in the endnotes of Chapters II and III. This R is called a minimum for a set of $\ln \beta_{new}$, so that

$$\ln \beta_{new} = \ln \beta_{old} + \Delta \ln \beta$$

The question arises on how to determine $\Delta \ln \beta$ to generate a set of $\ln \beta_{new}$. Writing a Taylor's series expansion

$$pH_i^c(\ln \beta) = pH_i^c(\ln \beta_o) + \sum_{j=1} \frac{\partial pH_i}{\partial \ln \beta_j} \Delta \ln \beta_j + \text{higher order terms} \qquad (7)$$

if one neglects the higher order terms the equation is linearized and can be written as

$$pH_i^c\ (\ln\ \beta) = pH_i^c(\ln\ \beta_o) + \sum_j D_{ij}\ \Delta \ln\ \beta_j$$

where D_{ij} are the set of derivatives $\left(\frac{\partial pH_i}{\partial \ln\ \beta_j}\right) \ln\ \beta_o$

The solution then is analogous to (6)

$$\Delta\ \ln\beta_j\ = (D_{ij}{}^T D_{ij})^{-1}\ D_{ij}{}^T(pH_i^c - pH_i^o).$$

This $\Delta \ln\ \beta_j$ is then added to $\ln\ \beta_{old}$ and another cycle with new β values begins. When shifts in $\ln\ \beta$ become small the approximation made in linearization of equation (7) becomes a fact.

The weighting factor for this program was developed due to the uncertainty in the observed pH values. The two components are the uncertainty in the precision of the pH meter (σ_{meter}) and the uncertainty in the precision of buret delivery (σ_{V_T}). The weighting scheme also seeks to emphasize the more accurate data from buffer regions and minimize the inaccurate pH readings from the steep inflections:

$$\sigma_i^2\ = \sigma_{meter}^2\ + (\partial pH/\partial V_T)_i^2\ \sigma_{V_T}^2$$

This weighting factor is included in the least squares analysis such that

$$R = \sum_i \frac{1}{\sigma_i^2}\ (pH_i^c - pH_i^o)^2$$

Then the final equation to determine the shift in $\ln \beta_j$ becomes

$$\Delta \ln \beta_j = (D_{ij}{}^T W_{ij} D_{ij})^{-1} D_{ij}{}^T W_{ij} (pH_i^C - pH_i^O)$$

where W_{ij} is a diagonal matrix of elements $1/\sigma_i^2$.

MATRIX INVERSION

BETA also possesses a straightforward method by which the matrix $D_{ij}{}^T D_{ij}$ is inverted. The algorithm used is called the Choleski inversion process[7] and it is not an iterative technique.

Given that the matrix to be inverted is

$$\underline{S} = (D_{ij}{}^T W_{ij} D_{ij}), \text{ where } \underline{S} \text{ is symmetric.}$$

Inversion of $\underline{S}$ gives

$$\underline{S}^{-1} = (\underline{L}\underline{L}^T)^{-1} = \underline{L}^{-1T}\underline{L}^{-1}$$

where $\underline{L}$ is a lower triangular matrix.

Thus, the inversion of a symmetric matrix ($\underline{S}$) can then be done in three steps:

(1) Factoring to form a lower triangular matrix; $\underline{L}$ (All elements of $\underline{L}$ can be obtained from $\underline{L}\underline{L}^T = \underline{S}$)

(2) Inverting $\underline{L}$; $\underline{L}^{-1}$

(3) Premultiplying the inverse matrix by the inverse triangular transpose matrix; $\underline{L}^{-1T}\underline{L}^{-1} = \underline{S}^{-1}$

If the matrix to be inverted is assymmetric (call it $\underline{A}$), then it is first premultiplied by its transpose ($\underline{A}^T\underline{A}$), thus making it symmetric.

The program then follows the three steps:

(1) $\underline{A}^T\underline{A} = \underline{S}$

(2) $(\underline{A}^T\underline{A})^{-1} = \underline{S}^{-1}$

(3) $(\underline{A}^T\underline{A})^{-1}\underline{A}^T = \underline{S}^{-1}\underline{A}^T = \underline{A}.^{-1}$

A writeup regarding the format of the input and output for program BETA is available.[8]

REFERENCES

1. ORGLS is a non-linear least squares program developed at Oak Ridge National Laboratory by William Busing and Henri Levy. ORNL-TM-271.

2. Avdeef, A.; Raymond, K., Inorg. Chem. (1979), 18, 1605.

3. Pecoraro, V., progress report of June, 1978.

4. Harris, W.R.; Raymond, K.N.; Weitl, F.L., J. Am. Chem. Soc. (1981), 103, 2667-2675.

5. Hamilton, W., "Statistics in Physical Science," Ronald Press: New York, 1964.

6. The formation constant β is written in terms of free metal, free ligand, and free hydrogen ion concentrations.

7. Rollett, J.S., ed., "Computing Methods in Crystallography," Pergamon Press: New York (1965), 19.

8. Pecoraro, V., writeup of BETA program.

TECHNICAL INFORMATION DEPARTMENT
LAWRENCE BERKELEY LABORATORY
UNIVERSITY OF CALIFORNIA
BERKELEY, CALIFORNIA 94720